

University of New Hampshire

University of New Hampshire Scholars' Repository

Doctoral Dissertations

Student Scholarship

Fall 2013

The identification and characterization of the interaction between Upf1 and PAB1 during nonsense-mediated decay & the identification of novel protein complexes associated with translation termination factor eRF1

Roy Richardson

Follow this and additional works at: <https://scholars.unh.edu/dissertation>

Recommended Citation

Richardson, Roy, "The identification and characterization of the interaction between Upf1 and PAB1 during nonsense-mediated decay & the identification of novel protein complexes associated with translation termination factor eRF1" (2013). *Doctoral Dissertations*. 750.
<https://scholars.unh.edu/dissertation/750>

This Dissertation is brought to you for free and open access by the Student Scholarship at University of New Hampshire Scholars' Repository. It has been accepted for inclusion in Doctoral Dissertations by an authorized administrator of University of New Hampshire Scholars' Repository. For more information, please contact Scholarly.Communication@unh.edu.

**THE IDENTIFICATION AND CHARACTERIZATION OF THE
INTERACTION BETWEEN UPF1 AND PAB1 DURING NONSENSE-
MEDIATED DECAY & THE IDENTIFICATION OF NOVEL PROTEIN
COMPLEXES ASSOCIATED WITH TRANSLATION TERMINATION
FACTOR ERF1**

BY

ROY RICHARDSON

BS, UMBC, 2006

DISSERTATION

Submitted to the University of New Hampshire

In Partial Fulfillment of the Requirements

For the Degree of

Doctor of Philosophy

in

Biochemistry

September 2013

UMI Number: 3575990

All rights reserved

INFORMATION TO ALL USERS

The quality of this reproduction is dependent upon the quality of the copy submitted.

In the unlikely event that the author did not send a complete manuscript and there are missing pages, these will be noted. Also, if material had to be removed, a note will indicate the deletion.

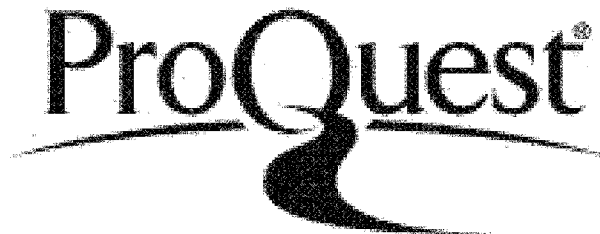


UMI 3575990

Published by ProQuest LLC 2013. Copyright in the Dissertation held by the Author.

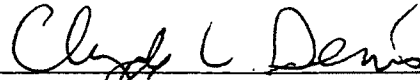
Microform Edition © ProQuest LLC.

All rights reserved. This work is protected against unauthorized copying under Title 17, United States Code.



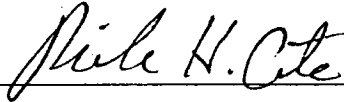
ProQuest LLC
789 East Eisenhower Parkway
P.O. Box 1346
Ann Arbor, MI 48106-1346

This dissertation has been examined and approved.

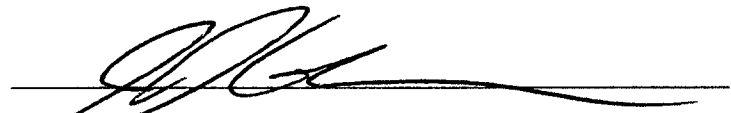


Dissertation Director, Clyde L. Denis, Professor of
Biochemistry, Molecular and Cellular Biology

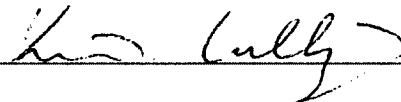
Thomas M. Laue, Professor of Biochemistry,
Molecular and Cellular Biology and Materials
Science



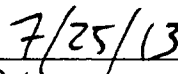
Richard H. Cote, Professor of Biochemistry,
Molecular and Cellular Biology



John J. Collins, Associate Professor of Genetics



Kevin Culligan, Research Assistant Professor of
Genetics



Date

DEDICATION

This thesis is dedicated to my parents and sister, who have always given their support and love. To April, who has always been a big sister to me. To all the aunts, uncles, grandparents, and cousins for their support and making sure I knew they were proud of me. To Gina and Joel for being there for our family and opening their home to us when we needed it the most. To all my Maryland friends for reminding me why I miss them whenever I visit and all of the wonderful friends I have met in New Hampshire for making this state feel like a second home. I could not have made it this far without all of you!

ACKNOWLEDGMENTS

I would like to thank my advisor, Dr. Clyde Denis for supporting, guiding, and educating me for all these years. Thank you to Dr. Tom Laue for the enthusiastic answers to all my questions and all the great conversations. Thanks to Dr. Rick Cote for providing me with all of the teaching opportunities to practice my craft. I would also like to thank the rest of my committee, Dr. Kevin Culligan and Dr. John Collins for their support and knowledge. I also thank all the fellow grad students from the lab throughout the years: Darren Lee, Chongxu Zhang, Xin Wang, Wen Xi, and Shiwa Park. Thank you all for passing on your knowledge and helping me with various tasks. Thanks to Dr. Yeuh-Chin Chiang for all of her expertise and assistance on my projects. Thank you to the Laue lab members who treated me like one of their own. I would also like to thank Laurie Westover for her relentless hard work ensuring that teaching labs ran smoothly and for all the times she let me use her equipment. Finally, I would like to thank NIH for providing funding for this research.

TABLE OF CONTENTS

DEDICATION.....	iii
ACKNOWLEDGEMENTS.....	iv
LIST OF TABLES.....	vii
LIST OF FIGURES.....	viii
ABSTRACT.....	x

CHAPTER	PAGE
GENERAL INTRODUCTION AND BACKGROUND.....	1
I. THE INTERACTION BETWEEN UPF1 AND PAB1 IS NOT REQUIRED FOR NONSENSE-MEDIATED DECAY, BUT DOES PLAY A ROLE IN THE SHIFT FROM DISTRIBUTIVE TO PROGRESSIVE DEADENYLATION.....	16
Introduction.....	16
Materials and Methods.....	17
Results.....	17
Discussion.....	20
II. THE IDENTIFICATION OF NOVEL COMPLEXES ASSOCIATED WITH TERMINATION FACTOR ERF1 USING ANALYTICAL ULTRACENTRIFUGATION WITH A FLUORESCENCE DETECTION SYSTEM.....	21
Introduction.....	21

Materials and Methods.....	22
Results.....	26
Discussion.....	48
GENERAL DISCUSSION.....	56
REFERENCES.....	60
APPENDIX I.....	66

LIST OF TABLES

NUMBER	PAGE
1- Yeast strains used.....	23
2- Average peak S position of each GFP-target sedimenting at that position.....	31
3- Change in abundance (AU-FDS or A230) of GFP fusion target after 10 minute Glucose deprivation.....	35
4- Change in abundance (FDS or A230) of GFP fusion target after 10 minute incubation with cycloheximide.....	38
5- Relative abundance of each protein at the identified peak positions.....	39

LIST OF FIGURES

NUMBER	PAGE
1- Eukaryotic pre-initiation complex formation and translation initiation.....	3
2- The translationally active yeast mRNP complex highlighting the closed loop structure interactions.....	4
3- Termination and peptide release via eRF1/eRF3.....	6
4- A simplified diagram of PAB1's domains.....	9
5- A typical profile of AU-A230 analysis of a Flag affinity pulldown of Flag-eRF1.....	27
6- AU-FDS analysis of eRF1 associated complexes using GFP fusions (eIF4E, eIF4G1, PAB1, RPS4B, and RPL7A).....	28
7- AU-FDS analysis of eRF1 associated complexes using GFP fusions (eIF2 α , eIF2 γ , eIF3b, and eRF3).....	29
8- Examples of GFP fusions that had low fluorescent signal compared to the control following AU-FDS analysis (eIF2B γ , eIF5, HRP1, and RPB1).....	30
9- Examples of GFP fusions that had low fluorescent signal compared to the control following AU-FDS analysis (SGN1, SSD1, and UPF1).....	31
10- AU-FDS analysis before and after 10 minute glucose deprivation.....	34
11- AU-FDS analysis before and after 10 minute cycloheximide treatment.....	37
12- GFP fusion targets that sediment below 28S shift sedimentation position between 200 and 500 scans (eIF4E and eIF4G1).....	43

13- GFP fusion targets that sediment below 28S shift sedimentation position between 200 and 500 scans (PAB1, RPS4B, and RPL7A).....	44
14- GFP fusion targets that sediment below 28S shift sedimentation position between 200 and 500 scans (eIF2 α , eIF2 γ , and eIF3b).....	45
15- AU-FDS analysis of eRF3 stress and dilution experiments.....	47

ABSTRACT

CHARACTERIZATION OF THE INTERACTION BETWEEN UPF1 AND PAB1 & THE IDENTIFICATION AND CHARACTERIZATION OF COMPLEXES ASSOCIATED WITH TRANSLATION TERMINATION FACTOR ERF1

By

Roy Richardson

University of New Hampshire, September 2013

There are still many protein interactions that occur during translation termination that are poorly understood. One of the important termination pathways still under investigation is nonsense-mediated decay (NMD), which rapidly degrades mRNAs that contain a premature stop codon (PTC). I identified that the interaction between Upf1, which is required for NMD, and PAB1 occurs via the RRM1 domain of PAB1 in the yeast *Saccharomyces cerevisiae*. Determining the role of this interaction during NMD was performed with pulse-chase assays using a *PGK1pG* mRNA. These assays revealed that the interaction between Upf1 and PAB1 is required for a shift from distributive to processive deadenylation, but is not required for decapping or general decay during NMD. These results also revealed that this interaction plays a role in the normal shift in deadenylation mode for non-PTC containing mRNAs from the relatively slow mode of distributive deadenylation to that of rapid processive deadenylation.

I also investigated the components of general termination complexes associated with the translation termination factor eRF1. This analysis was performed

using the novel technique of analytical ultracentrifugation with a fluorescence detection system (AU-FDS) on Flag-eRF1 affinity purified extracts. AU-FDS revealed that Flag-eRF1 associates with six distinct complexes that have S values of 20S, 28S, 39S, 57S, 77S, as well as complexes greater than 100S. All of these complexes contained the closed-loop components eIF4E, eIF4G1, and PAB1. However, stoichiometric analysis revealed that the complexes greater than 28S were comprised mostly of free ribosomal subunits associated with eRF1. Glucose deprivation and cycloheximide stress treatments revealed that these complexes are likely post-termination complexes rather than pre-initiation or translationally active complexes.

Additional observations from AU-FDS revealed a shifting behavior for the 20S complex during sedimentation, suggesting a shift in shape or composition during the experiment. Also, the abundance and sedimentation profile of eRF3 suggests that it forms a polymer-like structure consistent with a known eRF3 prion characteristic.

These analyses further reveal the interactions involved in the termination process. The application of AU-FDS continues to prove a useful tool for identifying novel protein complexes.

GENERAL INTRODUCTION AND BACKGROUND

Introduction

Deciphering the protein complexes and interactions during various stages of eukaryotic translation remains one of the major quests of current biology. These characterizations will inform all aspects of protein synthesis and regulation in cellular systems. This thesis aims to investigate two aspects of protein interactions during the termination stage of translation. The first is to investigate the interactions involved in the process of nonsense-mediated decay. In particular, these studies involved investigating the interaction between the proteins UPF1 and PAB1 and the role of this interaction during nonsense-mediated decay. The second focus is to explore the protein complexes that interact with the termination factor eRF1, and specifically, to utilize analytical ultracentrifugation with a fluorescence detection system to identify complexes associated with eRF1.

Eukaryotic Translation

Regulation of protein synthesis can occur by suppressing or stimulating many regulatory steps, including those of transcription or translation. Regulation of messenger RNAs (mRNAs) at the translational level can result in more rapid effects on protein levels than effects at the transcriptional level. There are four main stages of translation: initiation, elongation, termination, and ribosome recycling, each characterized by their individual mechanisms of regulation.

In the cytoplasm, mRNAs exist as a complex of mRNA and proteins called a messenger ribonucleoprotein (mRNP) complex. One of the most abundant mRNP complexes in the yeast *Saccharomyces cerevisiae* is the translationally active complex, but a number of such complexes exist (Richardson *et al.*, 2012; Mitchell *et al.*, 2013).

Translation Initiation

Translational initiation in the cytoplasm begins with the formation of the ternary complex, which consists of a Met-tRNA_i and initiation factor eIF2-GTP. The Met-tRNA_i interacts with the 40S subunit of the ribosome via the P site (Rabl *et al.*, 2011). The initiation factors eIF1, 1A, 3 and 5 also interact with the 40S subunit to form the 43S pre-initiation complex (Figure 1) (Asano *et al.*, 2000; Hinnebusch *et al.*, 2011). This complex can interact with the closed loop mRNP structure.

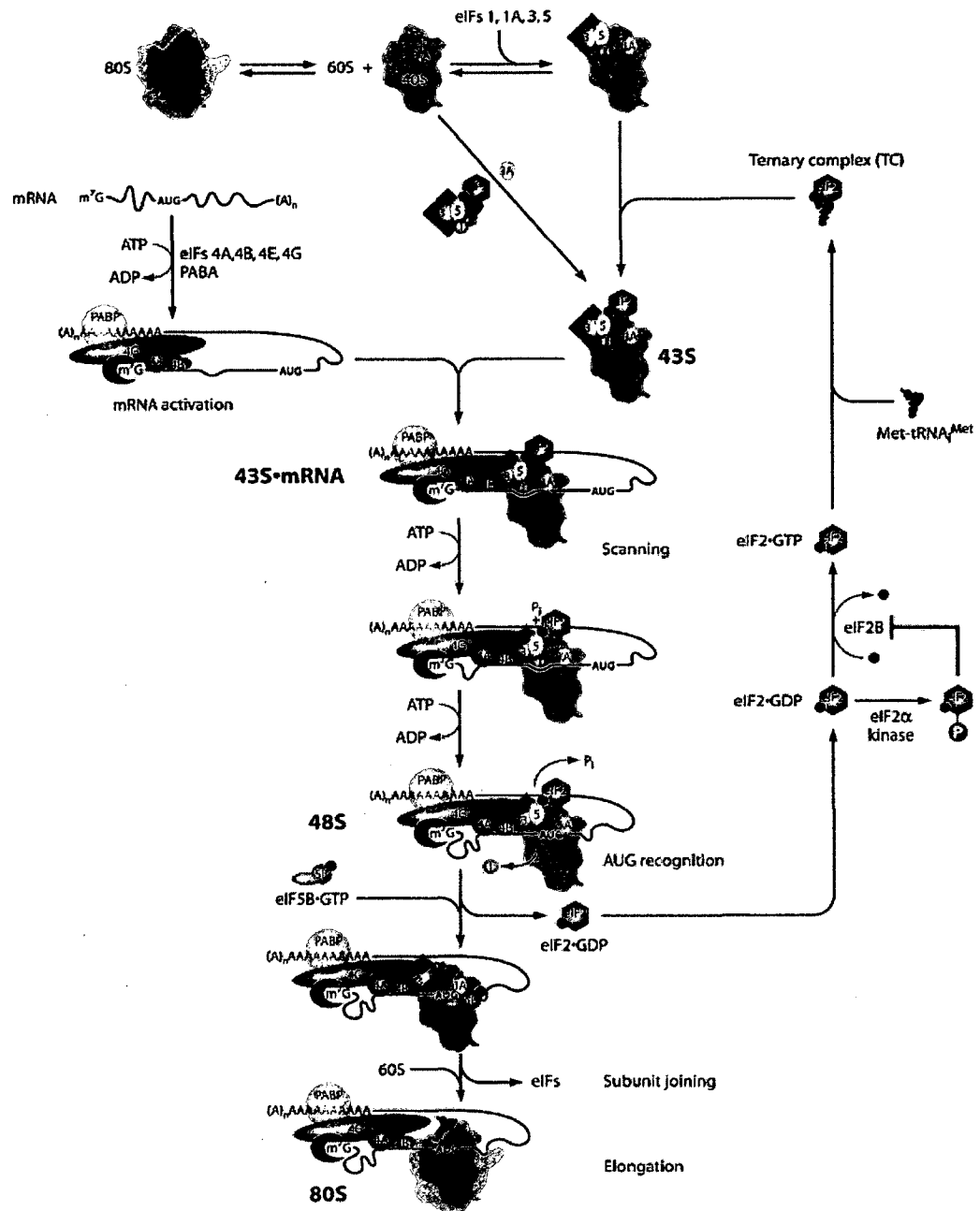


Figure 1: Eukaryotic pre-initiation complex formation and translation initiation. Hinnebusch, 2011

The core protein components of the closed loop mRNP complex are PAB1 (poly-A RNA binding protein), eIF4E (cap binding protein), and eIF4G (the bridging protein). PAB1 binds to the poly(A) tail of the mRNA (requiring about 25 adenosine residues per PAB1) and eIF4E binds the 5' cap with eIF4G interacting with both PAB1 and eIF4E, creating a closed loop structure (Figure 2) (Deo *et al.*, 1999). PAB1 must be on the poly(A) tail to interact with eIF4G (Wells *et al.*, 1998). This complex also contains the translation initiation factors eIF4A and eIF4B, which are required for the 43S complex to bind and begin scanning for the start codon.

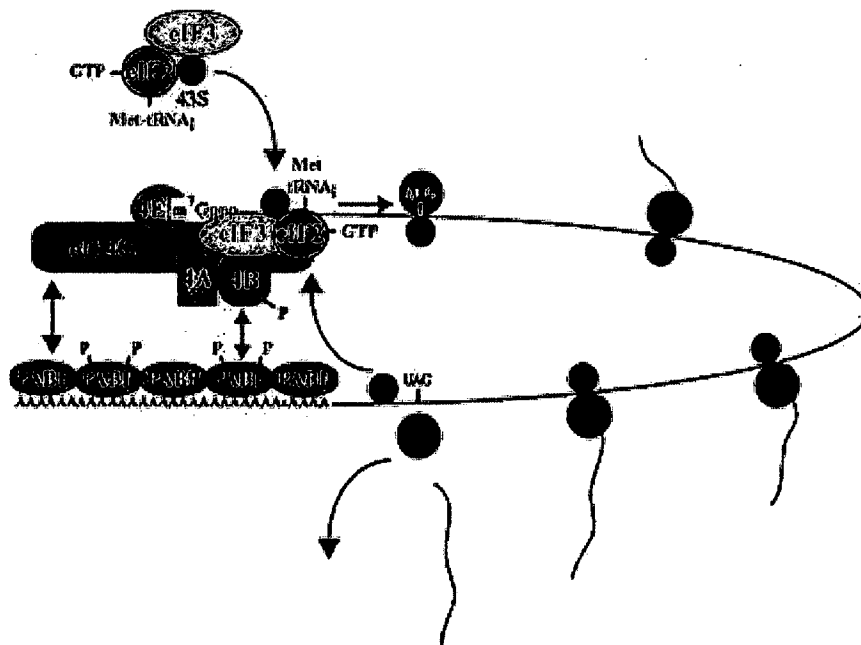


Figure 2: The translationally active yeast mRNP complex highlighting the closed loop structure interactions. Gallie, D, University of California, Riverside.

The 43S complex is aided in its interaction with the closed structure via the hydrolysis of ATP by eIF4A, thereby creating the 48S pre-initiation complex (Pisarev *et al.*, 2007a). The 48S complex travels along the 5' untranslated region (UTR), in a process known as the scanning mechanism, until it reaches and forms a stable base pairing with the AUG start codon (Hinnebusch AG, 2011). This process is assisted by the helicase activity of eIF4A (Spirin AS, 2009).

Once the Met-tRNA_i forms a stable pairing with the start codon the pre-initiation complex is joined by the 60S subunit of the ribosome following the hydrolysis of GTP by eIF2 via the GTPase activating initiation factor eIF5B (Pisarev *et al.*, 2007a). Once the 60S subunit joins the elongation stage of translation begins, and it is believed that following eIF2 GTP hydrolysis the initiation factor eIF2-GDP disassociates from the mRNP complex to form a new pre-initiation complex via the phosphorylation of eIF2-GDP by eIF2B.

Translation Termination

Translational termination occurs when the ribosome reaches a stop codon. At this point termination factor eRF1 interacts with the stop codon more tightly than any tRNA does at the A site (Conard *et al.*, 2012). The termination factor eRF3 then interacts with eRF1 and upon hydrolysis of GTP causes eRF1 to release the peptide chain, although the exact mechanism of this process is unknown (Figure 3) (For review, see Jackson *et al.*, 2012).

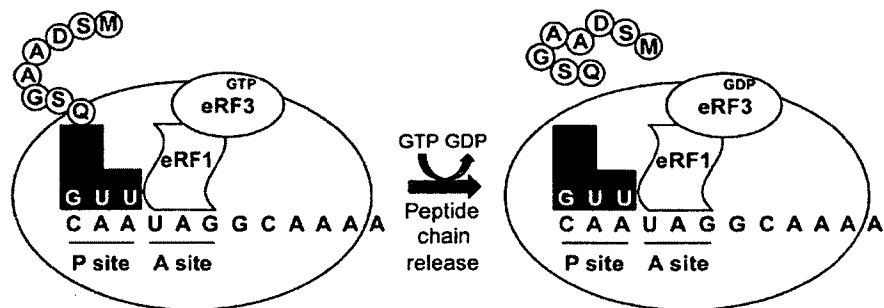


Figure 3: Termination and peptide release via eRF1/eRF3. Keeling & Bedwell, 2011.

After termination ribosome recycling can occur if the mRNP does not enter a degradation pathway. The separation of the ribosomal subunits by ribosomal recycling factors (RRFs) in conjunction with elongation factor G (EF-G) in prokaryotes does not have a conserved eukaryotic equivalent (Hirokawa *et al.*, 2005; Hirokawa *et al.*, 2006). The mechanism of ribosome recycling in eukaryotes is not understood, but it is dependent on the ATPase ABCE1 (Rli1 in yeast) (Pisarev *et al.*, 2010). It has also been determined that the initiation factor eIF3 is primarily responsible for splitting the post-termination subunits of the ribosome (Pisarev *et al.*, 2007b). Kinetic analysis suggests that the Rli1 dependency relies on an interaction with eRF1 and eRF3 (Shoemaker & Green, 2011).

Post Termination Degradation

The major degradation pathway of the mRNP complex requires the mRNA to be deadenylated by the cytoplasmic deadenylase, CCR4, after PAB1 has left the poly(A) tail (Denis and Chen, 2003). The DCP1/2 complex decaps the mRNA after it has been deadenylated to about 8 – 12 adenosine residues (Muhlrad and Parker, 1994). The mRNA is then degraded 5' to 3' by the exonuclease Xrn1p (Muhlrad and Parker, 1994). This

decay process occurs in P bodies (Sheth and Parker, 2003). A P body consists of mRNP aggregations along with proteins involved in mRNA decay and translational repression. If an mRNA contains a premature termination codon (PTC), it will also be targeted to a P body for degradation. However, in this case the mRNA is degraded much more rapidly than its wild type form to prevent the translation of a truncated protein. This degradation pathway is referred to as nonsense-mediated decay (NMD).

Translationally silent mRNPs in P bodies are not always degraded. Some silenced mRNPs, repressed under stress conditions, are reactivated and returned to polysomes when the stressor is removed (Brenques, Teixeira, and Parker, 2005). Complexes that are silenced due to specific stress conditions, such as glucose deprivation, aggregate in unique complexes called stress granules. Glucose deprived stress granules are known to contain eIF4E, eIF4G, PAB1, as well as mRNA and their formation is dependent on P body formation (Buchan, Muhrad, and Parker, 2008). Additional related types of stress granules are formed following robust heat shock (at 46°C). These latter stress granules contain the above stress granule components as well as the 40S ribosomal subunit and initiation factors such as eIF3 (Grousl *et al.*, 2009). These differences in stress granule composition have been related to different stages in blocking initiation by the different stress conditions (Wang *et al.*, 2012).

PAB1

The protein PAB1 plays an integral role in mRNP complex stability. PAB1 is a poly(A)-binding protein that has high affinity for poly adenosine residues but can also bind to AU mixed regions. It consists of four non-identical RNA recognition motif domains (RRMs), a proline rich loose coil region (P domain), and a C-terminal domain (Figure 4). Deletion of PAB1 is a lethal mutation in yeast (Wyers *et al.*, 2000). The domains RRM1 and RRM2 interact with poly(A) sequences tightly, however RRM3 and RRM4 can also interact with poly(A) sequences as well as possibly allowing for the interaction with U-rich sequences adjacent to the poly(A) tail (Deardorff and Sachs, 1997; Deo *et al.*, 1999; Mullin *et al.*, 2004; Sladic *et al.*, 2004). RRM1 has also been shown to interact with UPF1, causing a shift from distributive to processive deadenylation during NMD (Richardson *et al.*, 2012). RRM2 has been shown to be required for functionally interacting with eIF4G, strengthening the circular complex and being required for poly(A) tail-dependent translation (Kessler and Sachs, 1998). The P-domain is required for CCR4 deadenylation and along with the C domain interacts with eRF3 in yeast, which increases the efficiency of termination (Yao *et al.*, 2007; Cosson *et al.*, 2002; Richardson *et al.*, 2012).

PAB1 also regulates the length of the poly(A) tail. It assists in controlling tail length during mRNA synthesis as well as when deadenylation is initiated (Minvielle-Sebastia *et al.*, 1997; Brown *et al.*, 1998). An interaction between PAB1 and PAN2/PAN3 is required to initiate tail trimming (Brown *et al.*, 1996). To initiate mRNA degradation, PAB1 must leave the poly(A) tail before CCR4 can access the adenosine

residues and deadenylation can begin. RRM1 and the RRM4 domain have been shown to interact, forming a circular form of PAB1 itself that is believed to promote the dissociation of PAB1 from the poly(A) tail (Yao *et al.*, 2007).



Figure 4: A simplified diagram of PAB1's domains. The N terminal end is on the left side of the figure.

Nonsense-Mediated Decay

During NMD, decapping and deadenylation occur independently of one another (Cao and Parker, 2003). This means that the disassociation of PAB1 is not required for NMD since the mRNA can still be decapped and degraded 5' to 3' prior to deadenylation (Meaux, van Hoof, and Baker, 2008). Substrates for NMD are targeted by the RNA binding and RNA-dependent ATPase and helicase, UPF1. UPF1 is required for NMD and PTC containing mRNAs will have a half-life similar to their normal counterparts in a $\Delta upf1$ strain (Leeds *et al.*, 1991; Cao and Parker, 2003). UPF1 interacts with UPF2 and UPF3 with UPF2 linking UPF1 and UPF3, creating a surveillance complex (He, Brown, and Jacobson, 1997). UPF2 and UPF3 are also present in P bodies and mutating either of these has similar effects as mutating UPF1, although each has their own role in NMD (He, Brown, and Jacobson, 1997). UPF1 has been shown to aggregate in P bodies in $\Delta dcp1$, $\Delta dcp2$, $\Delta epf2$, $\Delta upf3$, and $\Delta xrn1$ strains as well as when its ATPase activity is inhibited (Sheth and Parker, 2006).

UPF1 accumulates in P bodies when its ATPase activity is inhibited by two sequential point mutations, D⁵⁷²E⁵⁷³→A⁵⁷²A⁵⁷³ (Weng, Czaplinski, and Peltz, 1996). When this ATPase defective form of UPF1 (UPF1-AD) is over expressed it causes the accumulation of DCP2-GFP in P bodies, which does not occur with UPF1-wt overexpression. Overexpression of UPF1-AD also increases the abundance of a PTC containing PGK1 mRNA in P bodies compared to UPF1-wt, showing that the ATPase activity of UPF1 is not required for targeting NMD substrates to P bodies. These results indicate that UPF1-AD targets NMD substrates but does not trigger decapping (Sheth and Parker, 2006). This form of UPF1 may trigger the formation of a translationally silent mRNP complex that is ready for degradation upon ATP hydrolysis.

There is also a polar effect in NMD in which candidate mRNAs with earlier PTCs are degraded faster than those with a PTC later in the coding sequence (Cao and Parker, 2003). One model that explains this phenomenon suggests that a downstream sequence element (DSE) 3' of the PTC is used to distinguish a normal termination codon from a premature one (Zhang *et al.*, 1995). HRP1, for example, has been identified as a protein that interacts specifically to a DSE-containing mRNA as well as interacts with UPF1. Furthermore, a mutation that prevents HRP1 from interacting with UPF1 stabilizes NMD substrate mRNAs without affecting normal mRNAs (Gonzalez *et al.*, 2000). HRP1 is likely to be in the translationally silent mRNP complex, possibly signaling UPF1 to localize the mRNA in a P body for destruction. Two other candidate proteins involved in this process, both found in P bodies, and may be present in the silent mRNP complex are RBP1 and SBP1. SBP1 is an RNA binding protein that promotes decapping. RBP1 is

also an RNA binding protein and has been found to localize to P body complexes under stress conditions. SBP1 may be found in the translationally silent mRNP during glucose deprivation.

eRF1-Associated Complexes

One of the principal foci of this thesis was to determine the protein complexes in which eRF1 is involved. Mass spectrometric analysis and *in vitro* studies indicate that termination factors eRF1 and eRF3 interact with PAB1 as well as the P-site of the 80S ribosome (Richardson *et al.*, 2012; Cosson *et al.*, 2002; Taylor *et al.*, 2012). Although methods such as sucrose gradient analysis and chromatography can be used to determine the components and sizes of protein complexes, the low abundance and small size of complexes associated with eRF1 make such methods difficult. Based on the sensitivity and success of using analytical ultracentrifugation with a fluorescence detection system (AU-FDS) with a Flag-tagged bait and GFP-tagged target system to identify novel protein complexes that interact with RPL25A and PAB1, the AU-FDS method was ultimately used to identify novel complexes that associate with eRF1 (Wang *et al.*, 2012).

Analytical Ultracentrifugation

Analytical ultracentrifugation (AU) has been widely used for some time to determine the molecular weight (MW) of biological molecules (Cole *et al.*, 2008). AU relies on measuring the rate, or sedimentation velocity, of the target molecule as it travels through a solution. Using this information and the analytical software Sedfit AU, one can determine the sedimentation coefficient of the target molecule as long as the buffer

density, the viscosity, and amount of centrifugal force are known (Schuck, 2000). The sedimentation coefficient is formulated by the ratio of the sedimentary boundary to the centrifugal force and is represented by the Svedberg unit (S value) (Equation 1). The S value has units of time since it measures the rate of movement in solution where $1\text{S} = 10^{-13}\text{s}$. The mass, density, and shape of the target molecule all contribute to the S value for a given centrifugal force. S values are standardized to the sedimentation rate in water at 20°C ($S_{20,w}$). Conversion of the experimental S value to the standard is done by using a conversion equation, with the density and viscosity of the experimental buffer determined by the software Sednterp (Equation 2) (Laue *et al.*, 1992). The MW of the target can only be approximated since the shape of the target must be assumed (Equation 3). Targets that have a 2-3 length to width ratio have an S value that is 1.4-fold smaller than a spherical target of equal mass due to a change in the frictional coefficient.

$$S = \frac{v}{\omega^2 r} = \frac{M(1 - \bar{v}\rho)}{N_A f} = \frac{MD(1 - \bar{v}\rho)}{RT}$$

Equation 1: The Svedberg equation

$$S_{20,w} = S \left(\frac{(1 - \bar{v}\rho)_{20,w}}{(1 - \bar{v}\rho)_{T,b}} \right) \frac{\eta_{T,b}}{\eta_{20,w}}$$

Equation 2: Svedberg conversion equation, where $\bar{v} = v$ bar, $\rho =$ density, $\eta =$ viscosity

$$MW = (S_{20,w} * 3.16)^{3/2}$$

Equation 3: Molecular weight determination equation assuming a spherical globular shape.

There are many advantages to using AU analysis compared to other techniques to determine protein complex sizes such as that of sucrose gradient analysis or chromatography. AU can provide more accurate approximations of complex size than sucrose gradients by tracking a target molecule in real time as it moves through solution during centrifugation. Sucrose gradients can only provide a single snap shot of the position of the molecule whereas AU analysis takes a series of snap shots over time. Utilizing multiple scans as the target moves also provides higher resolution in size profiling than chromatography. Furthermore, AU can be performed in a biologically relevant buffer with much more flexibility in regards to the density and composition of the buffer solution, which allows for the characterization of the target in its native state. AU is also much more sensitive than sucrose gradient or chromatography techniques, requiring as little as 100 pM concentration of the target molecule for detection (Cole *et al.*, 2008). Importantly, AU does not require a secondary detection method to determine the presence or size of its targets, such as Western analysis, which is time consuming and is restricted to analysis of just fifteen or so slices across a sucrose gradient MW continuum. In contrast, AU analysis can analyze hundreds of slices across the MW continuum, providing an order of magnitude greater resolution compared to standard sucrose gradient or chromatographic analysis.

AU can also be used to track multiple targets in solutions, providing a size distribution of targets (Schuck *et al.*, 2002). The target molecules can be tracked using either an absorbance or fluorescence detection system (MacGregor *et al.*, 2004; Cole *et al.*, 2008). Complexes comprised of protein and nucleic acids can be identified at 230 nm

or 260 nm, respectively, using the absorbance detection system. AU-FDS can track a protein that has been fused with green fluorescent protein (GFP) and excited it at 488 nm (Cole *et al.*, 2008). Using a GFP-fused protein allows a specific protein to be identified using the FDS rather than tracking all proteins present using absorbance.

By using a Flag-tagged protein and using Flag-bead affinity purification in conjunction with an individual GFP tagged protein, protein complexes can be identified with AU-FDS (Wang *et al.*, 2012). Using a Flag-tagged PAB1 or RPL25A protein in conjunction with various mRNP components fused with GFP, a 77S complex was identified as the monosomal translating complex using AU-FDS (Wang *et al.*, 2012). This complex was repressed under various stress responses, and the interactions responsible for various stress granule formations under varying stress conditions were elucidated. Subsequent studies have verified the utility of AU-FDS analysis for studying translation complexes (Zhang *et al.*, 2013).

Thesis Project

The first part of my thesis project was to investigate the interaction between UPF1 and PAB1 and the role of this interaction on NMD. UPF1 was identified as one of many proteins found to interact with PAB1 by using mass spectrometry (Richardson *et al.*, 2012). The site of interaction was suggested to be the RRM1 domain of PAB1. Deletion analysis, immuno-precipitation, and western blotting was used to confirm this. Deadenylation assays further demonstrated that NMD can occur independently of PAB1 leaving the poly(A) tail and also revealed that the interaction between UPF1 and the

RRM1 domain of PAB1 plays a role in transitioning mRNA degradation from distributive to processive deadenylation under normal conditions.

For the second part of this thesis project I used Flag affinity purification using Flag-eRF1 as a bait to identify translation related complexes containing eRF1. AU-FDS analysis was performed on these Flag-purified complexes. A 77S complex different from the one identified previously by our lab was detected (Wang *et al.*, 2012). The 77S complex associated with eRF1 does not change in abundance in response to various stress conditions, unlike the 77S complex identified using Flag-PAB1 and RPL25A-Flag. A 39S and 57S complex was also visualized similar to previous analysis (Wang *et al.*, 2012; X. Wang pers. comm.). Importantly, previously unknown protein complexes in the 10S-30S regions were identified as well as monomer GFP-fused targets. The character and stoichiometry of all of these eRF1-containing complexes was determined. Moreover, analyses of increasing scan fits indicate that protein complexes in the 10S-30S regions represent a reaction boundary rather than a single sedimentation boundary. This is characterized by a shift in S position of the peaks in this region as the number of scans increases whereas peaks greater than 30S and less than 10S do not shift in position. This suggests that the complexes sedimenting in the 10S-30S regions are changing size as the sedimentation experiment proceeds. These peaks no longer shift after 500 scans indicating that the complexes in the peaks identified have reached equilibrium between different forms.

CHAPTER I

THE INTERACTION BETWEEN UPF1 AND PAB1 IS NOT REQUIRED FOR NONSENSE-MEDIATED DECAY, BUT DOES PLAY A ROLE IN THE SHIFT FROM DISTRIBUTIVE TO PROGRESSIVE DEADENYLATION

Introduction

The investigation of proteins that associate with PAB1 utilizing mass spectrometry revealed that the UPF1 was one of the proteins that associated with the RRM1 domain of PAB1 (Richardson *et al.*, 2012; see Appendix I). UPF1 is the core component of the mRNA surveillance complex (comprised of UPF1, UPF2, and UPF3), which initiates the rapid decay of mRNA containing premature termination codons (PTCs), known as nonsense-mediated decay (NMD) (Leeds *et al.*, 1991). Western blots utilizing Flag-PAB1 and HA-UPF1 verified that the interaction between the two proteins occurred via the RRM1 domain and not through the other domains of PAB1 (Richardson *et al.*, 2012; Appendix I). Deadenylation assays were performed to further investigate the role of the interaction between UPF1 and the RRM1 domain of PAB1 on mRNA decay. These assays revealed that the interaction between UPF1 and the RRM1 domain was required to shift deadenylation from a distributive to a processive mode but was not required for decapping or decay in general. In addition, the interaction between UPF1 and RRM1 was also shown to play a role in this shift in deadenylation mode for non-PTC containing mRNAs.

It would be expected that an interaction between the RRM1 domain and UPF1 would play an important physiological role in NMD. However, deletion of PAB1 does not prevent the process of UPF1-mediated NMD (Meaux *et al.*, 2008). UPF1-mediated decay involves both decapping and deadenylation occurring independent of one another, which are both accelerated, with decapping as the major pathway (Cao and Parker, 2003). The deletion of RRM1 in PAB1 has been shown to have no effect on decapping but was found to be necessary for deadenylation (Yao *et al.*, 2007; Lee *et al.*, 2010; Simon and Seraphin, 2007). Therefore, PAB1 possibly plays a role in the deadenylation process of NMD.

Materials and Methods (see Appendix I)

Results

Pulse-chase assays were performed to determine the role of the RRM1 domain on the NMD process. *GAL1-PGK1* mRNA that was either wt or contained a PTC at residue 319 was used. The PTC at residue 319 was previously shown to be an NMD candidate (Cao and Parker, 2003). The isogenic yeast strains containing Flag-PAB1 or Flag-PAB1- Δ RRM1 with *GAL1-PGK1pG* or *GAL1-PGK1pG-319* were grown in galactose and glucose free media. The *GAL1* promoter was briefly induced with galactose and subsequently shut off with glucose. Samples were taken over time after transcription was shut off and rapidly frozen prior to RNA purification. Northern blot analysis was performed on the RNA extractions to identify *PGK1* mRNA as a function of time.

Analysis of the PAB1 wild-type with wild-type *PGK1pG* mRNA showed a shift in distributive to processive deadenylation as the poly(A) tail reached a reduction point of about 10 A's (Appendix I, Figure 4A). This is also when the decapped fragment appears and becomes more abundant over time. The PTC containing *PGK1pG* mRNA displayed much more rapid decapping and deadenylation, as expected (Appendix I, Figure 4C; Cao and Parker, 2003). The deadenylated and decapped mRNA fragment appears immediately in much greater abundance than any time point in the wild-type *PGK1* analysis. Additionally, the band of deadenylating *PGK1pG-319* mRNAs is much broader from the initial time point, indicating that processive deadenylation is occurring more rapidly than with wild-type *PGK1pG*.

Analysis of the *PGK1pG* and *PGK1pG-319* mRNAs in a Δ RRM1 PAB1 strain compared to the wild-type PAB1 data revealed that deleting RRM1 blocked the deadenylation process for both mRNAs (Appendix I, Figures 4B & 4D). For wild-type *PGK1pG* no fragment appeared, which is consistent with deadenylation dependent decapping (Decker and Parker, 1993). For the *PGK1pG-319* mRNA, there is little apparent deadenylation. However, a decapped, but not deadenylated, fragment appeared very rapidly. This indicates that RRM1 is not required for the decapping of PTC containing mRNAs, but it is required for the acceleration of NMD deadenylation.

Since deleting RRM1 prevents PAB1 from leaving the poly(A) tail, its contact with UPF1 may not play a role in the deadenylation inhibition effect. To test this, the same pulse-chase assay experiments as described above were performed in an isogenic

Δupf1 background. For *PGK1pG* mRNA, deadenylation rates occurred at the same rate as previously observed (Appendix I, Figures 5A & 5B). However, the banding pattern was tight throughout the assay, indicating that a shift from distributive to processive deadenylation did not occur. This suggests that UPF1 plays a role in the switch from distributive to processive deadenylation under normal conditions, a process which requires the removal of PAB1 from the poly(A) tail (Tucker *et al.*, 2002, Viswanathan *et al.*, 2003, Yao *et al.*, 2007). Also, fewer deadenylated fragments were seen, which is consistent with this observation.

For NMD with *Δupf1*, *PGK1pG-319* mRNA was deadenylated similarly to wild-type *PGK1* mRNA, since UPF1 is required for NMD deadenylation (Appendix I, Figures 5C & 5D). Little to no fragment was observed and a shift to processive deadenylation did not occur. *PGK1pG* and *PGK1pG-319* mRNA deadenylation was blocked by the deletion of RRM1 in the background strains, indicating that the RRM1 requirement for deadenylation is independent of UPF1. For more detailed results analysis, see Appendix I.

Discussion

We established that deletion of the RRM1 domain of PAB1 blocked NMD deadenylation but had no effect on the decapping step of NMD, which agrees with the results that indicate that PAB1 is not required for NMD (Meaux *et al.*, 2008). However, since this deletion blocks deadenylation in a $\Delta upf1$ background as well, it cannot be concluded that the interaction between RRM1 and UPF1 has a specific role in NMD.

Further analysis of the pulse-chase data revealed that the role for this interaction may be in the transition from distributive to processive deadenylation. This observation is supported by three observations. First, the deletion of UPF1 prevents a shift to processive deadenylation for PGK1 mRNA. Second, the removal of PAB1 from the poly(A) tail is required for this shift and deletion of RRM1 blocks PAB1 from leaving the mRNA (Yao *et al.*, 2007). Third, during NMD UPF1 is required for the observed rapid processive deadenylation. These observations support the model that UPF1 accelerates deadenylation during NMD via an interaction with RRM1 and accelerating the removal of PAB1 from the poly(A) tail. They also support a role for UPF1 in the transition from distributive to processive deadenylation in normal mRNA degradation. For a more detailed discussion, see Appendix I.

Chapter II

THE IDENTIFICATION OF NOVEL COMPLEXES ASSOCIATED WITH TERMINATION FACTOR eRF1 USING ANALYTICAL ULTRACENTRIFUGATION WITH A FLUORESCENCE DETECTION SYSTEM

Introduction

The use of AU-FDS to detect protein complexes with Flag-PAB1 identified a 77S monosomal complex (Wang *et al.*, 2012). Previous studies using this method showed that these complexes contained translation termination factor eRF3 (Zhang, 2011). The presence of eRF1 in complexes associated with Flag-PAB1 have also been observed (X. Wang & S. Park, pers. comm.). The intent of this project was to identify proteins that interact to form complexes with translation termination factor eRF1, the sedimentation values of the complexes associated with eRF1, and the general trends of glucose deprivation and cycloheximide treatment on these complexes. To identify the complexes associated with termination factor eRF1, AU-FDS analysis was performed on Flag-eRF1 purified complexes. AU-FDS analysis revealed the presence of six distinct complexes, which have S values of 20S, 28S, 39S, 57S, 77S, and complexes greater than 100S. The complexes greater than 100S are assumed to be polysomal material. AU-FDS analysis also revealed that the closed-loop components eIF4E, eIF4G1, and PAB1 as well as ribosomal proteins RPS4B and RPL7A, and translation initiation factors eIF2 α , eIF2 γ , and eIF3b interact with complexes containing eRF1.

Materials and Methods

Growth conditions and Flag pulldowns

The yeast strains used for this study can be found in Table 1. The GFP fusion proteins in these strains have been shown to be functional and not cause any apparent growth defects (Huh *et al.*, 2003). Yeast cell cultures were grown as previously described (Wang *et al.*, 2012) to mid-log phase (optical density at 600 nm of 0.8 – 1.2). For glucose deprivation, a 1L culture was divided in half and the cells in one fraction were resuspended in glucose free media and incubated for ten minutes while the other half remained incubating in glucose-containing media prior to cell harvesting. A similar procedure was performed for cycloheximide treatment, where half of a 1L culture was incubated with cycloheximide for ten minutes prior to harvesting cells. Flag-affinity pulldowns were performed as previously described (Wang *et al.*, 2012). Generally, 425 μL of eluent was collected, of which 300 μL were used for AU-FDS and 60 μL were diluted in 240 μL of lysis buffer lacking the yeast inhibitor cocktail (a 5-fold dilution) for AU absorbance analysis at 230 nm (AU-A₂₃₀). Samples analyzed by AU ranged in concentration from 0.1 – 0.3 mg/mL and control samples lacking Flag-eRF1 were in the 0.01 – 0.03 mg/mL range.

Name	Genotype
RP1950-RPS4B/TK41	<i>Mata ura3 leu2 his3 met15 RPS4B-GFP-[HIS3] TK41 [URA3-Flag-eRF1]</i>
RPL7A/TK41	Isogenic to RP1950 except <i>RPL7A-GFP-[HIS3]</i>
RP1946/TK41	Isogenic to RP1950 except <i>CDC33-GFP-[HIS3]</i>
RP1947/TK41	Isogenic to RP1950 except <i>TIF4631-GFP-[HIS3]</i>
RP2191/TK41	<i>Mata leu2-3,112 trp1 ura3-52 his4-539 cup1::LEU2/PGK1pG/MFA2pG PAB1-GFP(NEO)</i>
RP2522/TK41	Isogenic to RP1950 except <i>SUP35-GFP-[HIS3]</i>
RP2529/TK41	Isogenic to RP1950 except <i>HRP1-GFP-[HIS3]</i>
GRPB1/TK41	Isogenic to RP1950 except <i>RPB1-GFP-[HIS3]</i>
GUPF1/TK41	Isogenic to RP1950 except <i>UPF1-GFP-[HIS3]</i>
GSGN1/TK41	Isogenic to RP1950 except <i>SGN1-GFP-[HIS3]</i>
GSSD1/TK41	Isogenic to RP1950 except <i>SSD1-GFP-[HIS3]</i>
YMK880/TK41	<i>Mata ade2-1 his3-11,15 leu2-3,112, trp1-1 ura3-1 can1- 100 ADE2 GCD1-GFP:G418</i>
YMK882/TK41	Isogenic to YMK880 except <i>PRT1-GFP:G418</i>
YMK883/TK41	Isogenic to YMK880 except <i>SUI2-GFP:G418</i>
YMK1171/TK41	Isogenic to YMK880 except <i>TIF5-GFP:G418</i>
YMK1211/TK41	Isogenic to YMK880 except <i>GCDC11-GFP:G418</i>

Table 1: Yeast strains used

Analytical ultracentrifugation parameters

Samples were subjected to AU analysis as previously described by Wang *et al.* (2012) with the following exceptions. The AU experiments were performed at 20°C at a rotor speed of 25,000 rpm. For the control and stress experiments, AU-FDS was performed for 150-200 scans. For the peak shift experiments, AU-FDS was performed for 500-900 scans. AU-A₂₃₀ was performed for at least 125 scans. Parameters for data analysis using the software Sedfit were set as described by Wang *et al.* (2012), except

that the maximum S value was set to 150 and the resolution for the peak shift experiments was set to 200 data points.

Calculating absolute protein abundances in particular complexes

To assess the relative abundance of each target protein, AU-FDS and AU-A₂₃₀ were both run simultaneously with the Flag-affinity eluent. The x-coordinate values were first adjusted from experimental S values to the standard S_{20,w}. Using the program Sednterp, the conversion factor for the lysis buffer containing 10% glycerol was determined to be 1.51. All x-coordinates for AU-A₂₃₀ and AU-FDS analysis were multiplied by this factor prior to performing peak size determinations or abundance calculations.

The S value for each peak was determined by identifying the local maximum y-value and recording the associated x-coordinate. The abundance of each complex was determined by taking the integral of the peak seen in the AU analysis. The integral of a sedimentation peak is equal to its relative concentration since the function $c(S)$ represents $\frac{dc}{dS}$, the change in concentration over the change in sedimentation. Integration was simplified by taking a summation of the y-values for each peak and dividing it by the number of coordinates taken. The total number of coordinates can be set in the Sedfit parameters and the software equally separates the x-values of these coordinates. This allowed us to divide by the number of coordinates used rather than determining the total difference in x when making integral calculations. Comparison of FDS peaks can be

compared to A_{230} peaks provided the resolution used in Sedfit for both sets of data is the same.

After the abundance of each FDS and A_{230} peak was determined, the FDS values were divided by the A_{230} values of the corresponding peak. This was performed to calculate the fluorescence abundance relative to the total amount of protein and nucleic acid present at that peak. Absorbance at 230 nm detects protein/nucleic acid mixes with a 3:1 ratio favoring protein. This relative abundance value was then compared to a standard protein to calculate its abundance relative to the standard (see Table 5). The standard protein varied by complex and can be identified as the protein set to 100% abundance in Table 5 (either eIF4E, RPS4B, or RPL7A). This provides a way to determine the proportions of components at each peak observed. For glucose deprivation experiments, the percentage of the glucose-deprived peaks relative to the peaks from the culture in regular media was calculated. Cycloheximide treatment calculations were performed similarly, wherein the percentage of abundance of cycloheximide-treated peaks was compared to the normal growth condition. Glucose and cycloheximide treatment comparisons were calculated using either the FDS or the A_{230} rather than using the ratio of the two.

Results

Identifying proteins in complexes containing eRF1

Yeast strains containing the Flag-eRF1 plasmid versus strains lacking the plasmid were compared to identify proteins in Flag-eRF1 complexes. AU analysis using A_{230} absorbance optics was conducted, and typical results are shown in Figures 5A and B. Seven general complexes were detected: 15S, 20S, 28S, 39S, 57S, 77S, and complexes greater than 100S. Complexes greater than 100S are presumed to be polysomes (Wang *et al.*, 2012), whereas the 77S complexes migrated with the monosomal translation complex or the free 80S ribosome. The smaller complexes of 57S and 39S had been visualized previously using Flag-PAB1 as bait but had remained uncharacterized (Wang *et al.*, 2012). Their sizes and components however, had indicated they at least contained the 60S and 40S ribosomal subunits, respectively. The complexes smaller than 39S had also been visualized in much lower concentrations using Flag-PAB1 pulldowns but were uncharacterized. Material smaller than 10S were generally considered to be monomeric proteins and were not further analyzed.

Strains containing green fluorescent protein (GFP) fused to the C-terminal end of various known proteins involved in protein synthesis were subsequently used to identify proteins that associate with each of these Flag-eRF1 purified complexes. Single-step affinity purification of the Flag-eRF1 protein was conducted with Flag-agarose beads and was followed by AU-FDS analysis. Each GFP fusion protein was assayed to determine its presence in Flag-eRF1 complexes by comparison to the control AU-FDS analysis from extracts that lacked Flag-eRF1. The core protein components of the closed-loop structure

(eIF4E, eIF4G1, and PAB1) (see Figure 6, A-C) as well as RPS4B, RPL7A (Figure 6, D and E), eIF2 α , eIF2 γ , eIF3b, and eRF3 (Figure 7, A-D) were found to associate with Flag-eRF1 relative to the control. Proteins that did not exhibit much signal above the negative control signal included eIF2B γ , eIF5, HRP1, RPB1, SGN1, SSD1, and UPF1 (Figures 8 & 9). In addition, these proteins also displayed very low signal intensity ($c(S)$ below 0.05) as compared to the above proteins shown to be present in Flag-eRF1 complexes, which generally had a $c(S)$ signal intensity greater than 0.10. These proteins were not analyzed further.

The proteins identified to be in eRF1-specific complexes showed a number of novel complexes at 20S, 28S, 39S, and 57S as well as that of the previously identified 77S complex and polysomal material migrating at S values greater than 100S (Summarized in Table 2). These complexes correspond to those observed with AU-A₂₃₀ analysis.

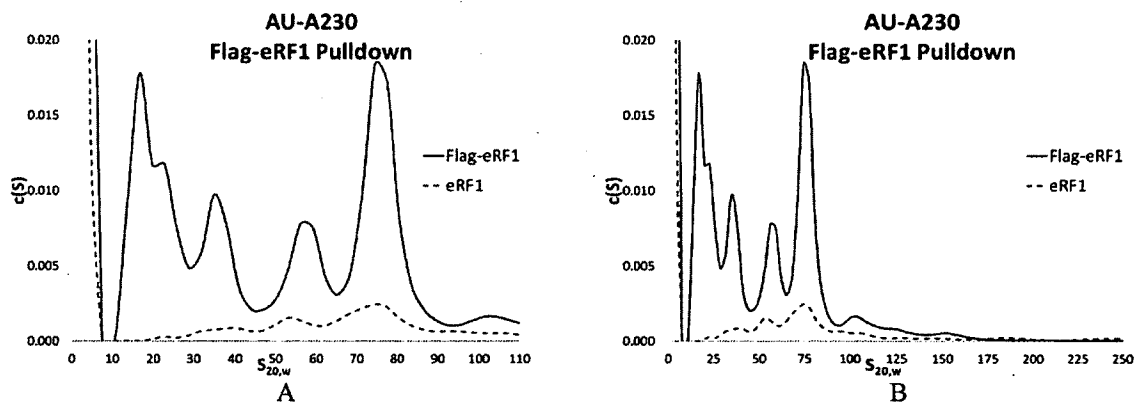


Figure 5: A typical profile of AU-A₂₃₀ analysis of a Flag affinity pulldown of Flag-eRF1 compared to the same strain lacking Flag-tagged eRF1. The two profiles show the profile range to a maximum of 110 S (A) and 250 S (B). The strain used for this figure was RP1947/TK41.

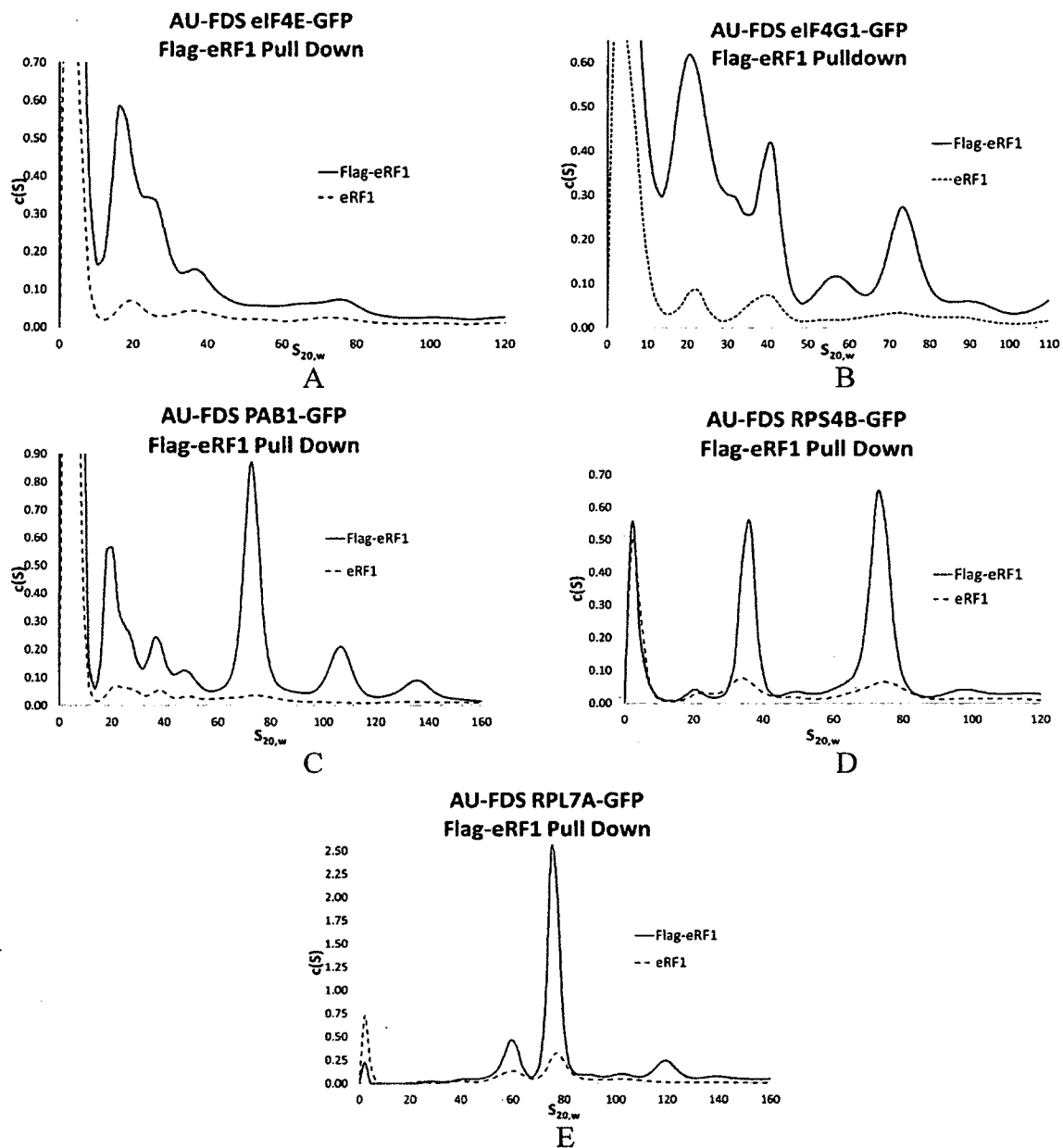


Figure 6: AU-FDS analysis of eRF1 associated complexes using GFP fusions. Each profile compares the same GFP-fusion strain with and without Flag-eRF1 after Flag purification. Flag control experiments were run at 25K rpm and analysis used 150-200 scans. The strains used for this figure were (A) RP1946/TK41 (eIF4E-GFP), (B) RP1947/TK41 (eIF4G1-GFP), (C) RP2191/TK41 (PAB1-GFP), (D) RPS4B/TK41 (RPS4B-GFP), (E) RPL7A/TK41 (RPL7A-GFP),

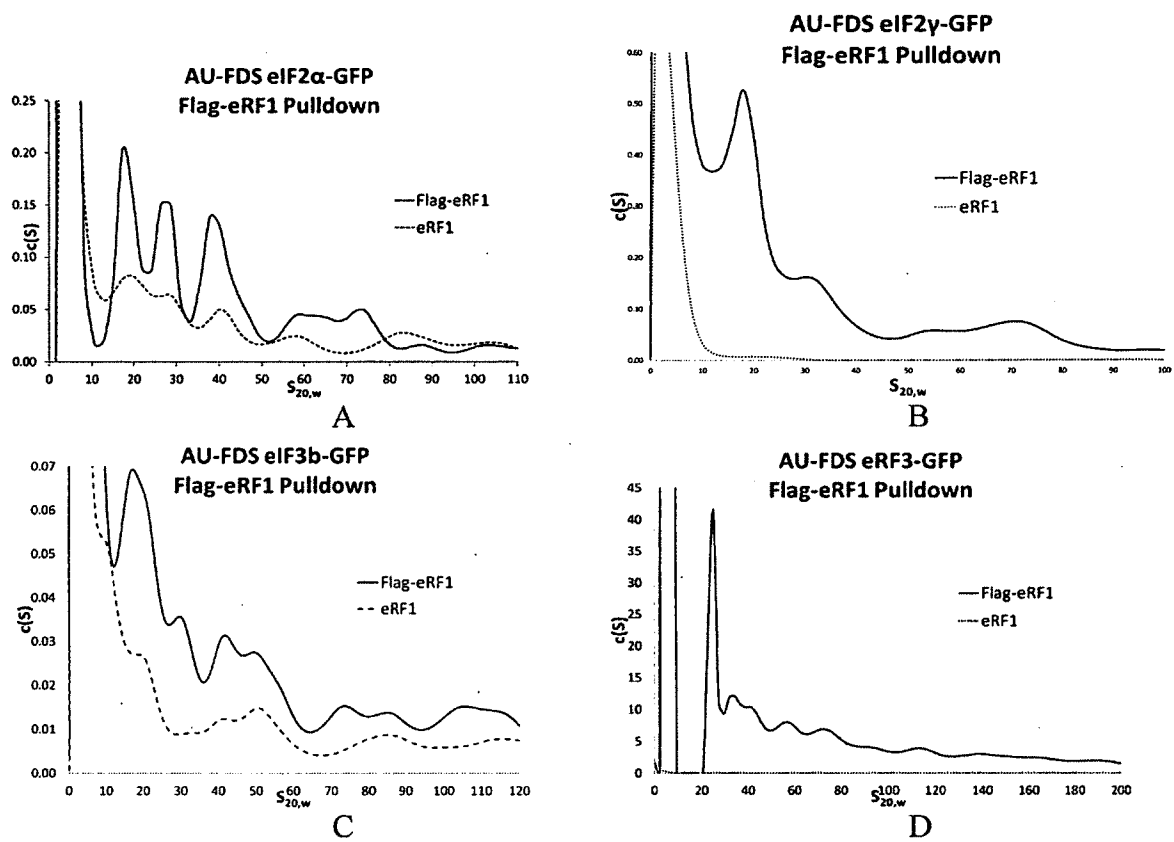


Figure 7: AU-FDS analysis of eRF1 associated complexes using GFP fusions. Each profile compares the same GFP-fusion strain with and without Flag-eRF1 after Flag purification. Flag control experiments were run at 25K rpm and analysis used 150-200 scans. The strains used for this figure were (A) YMK883/TK41 (eIF2 α -GFP), (B) YMK1211/TK41 (eIF2 γ -GFP), (C) YMK882/TK41 (eIF3b-GFP), (D) RP2522/TK41 (eRF3-GFP).

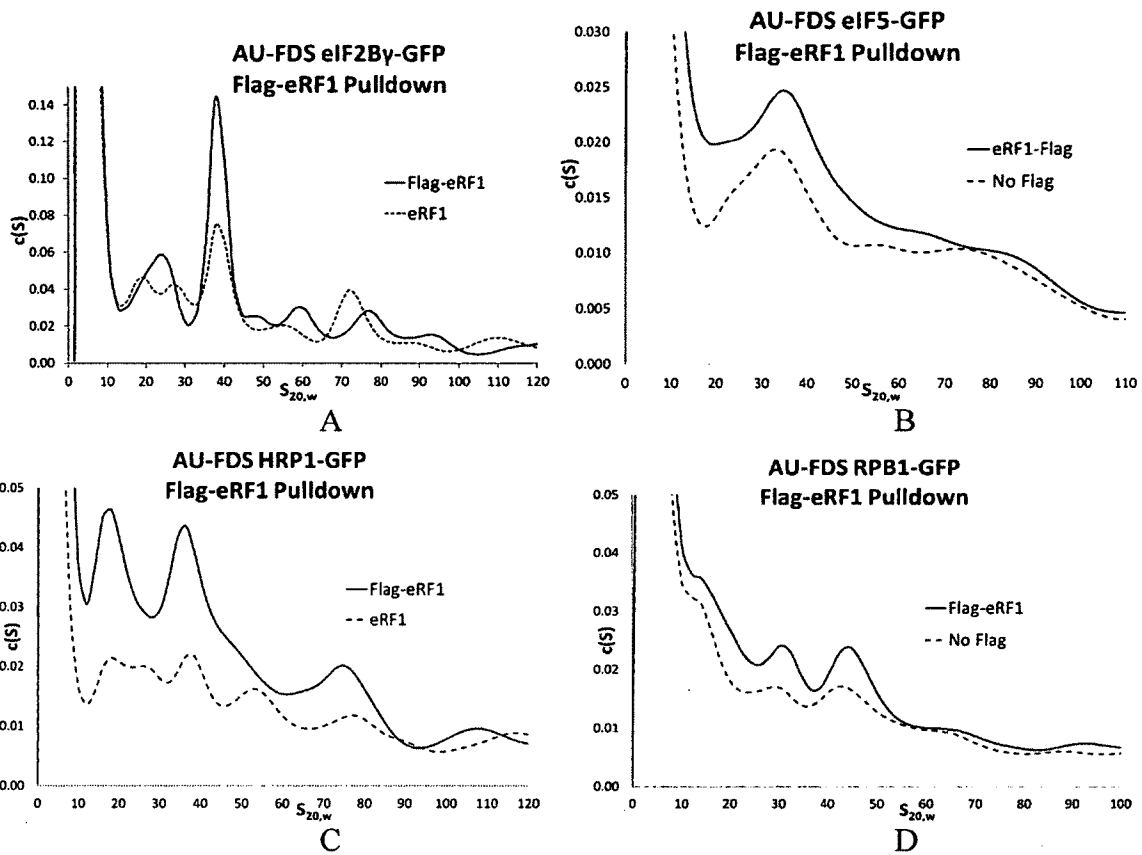


Figure 8: Examples of GFP fusions that had low fluorescence signal and did not exhibit much more signal compared to the control following AU-FDS analysis. These fusions were not analyzed further. Each profile compares the same strain with and without Flag-eRF1 after Flag purification. The strains used for this figure were (A) YMK880/TK41 (eIF2 β -GFP), (B) YMK1171/TK41 (eIF5-GFP), (C) RP2529/TK41 (HRP1-GFP), (D) GRPB1/TK41 (RPB1-GFP)

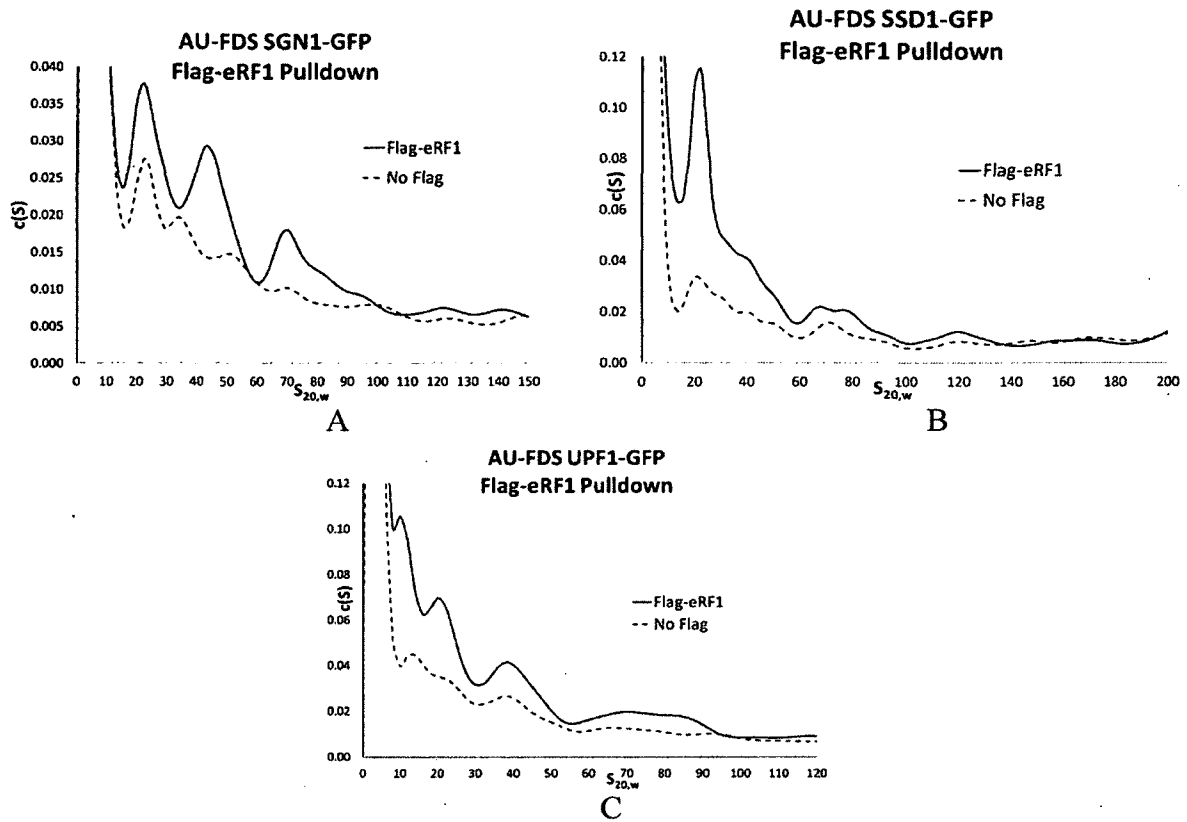


Figure 9: Examples of GFP fusions that had low fluorescence signal and did not exhibit much more signal compared to the control following AU-FDS analysis. These fusions were not analyzed further. Each profile compares the same strain with and without Flag-eRF1 after Flag purification. The strains used for this figure were (A) GSGN1/TK41 (SGN1-GFP), (B) GSSD1/TK41 (SSD1-GFP), (C) GUPF1/TK41 (UPF1-GFP)

Peak Name	Average AU-FDS S Position	Average AU-A ₂₃₀ S Position
15S	14.1 ± 0.561	15.9 ± 0.391
20S	20.1 ± 0.422	22.0 ± 0.443
28S	27.6 ± 0.291	25.6 ± 0.770
39S	38.8 ± 0.347	35.8 ± 0.294
57S	57.0 ± 0.573	57.2 ± 0.211
77S	74.4 ± 0.627	75.7 ± 0.365

Table 2: Average peak S position of each GFP-target sedimenting at that position. Error presented is standard error of the mean (SEM). GFP-fusions used to determine the S positions were 15S: eIF4E-GFP, eIF4G1-GFP, PAB1-GFP, eIF2 α -GFP, and eIF2 γ -GFP. 20S: The same fusions as 15S and eIF3b-GFP. 28S: The same fusions as 20S. 39S: The same fusions as 28S and RPS4B-GFP. 57S: The same fusions as 39S and RPL7A-GFP, but not eIF3b-GFP. 77S: The same fusions as 57S, but including eIF3b-GFP. All mentioned GFP fusions were used to determine each A₂₃₀ peak.

Effects of glucose depletion on Flag-eRF1 containing complexes

It has been previously shown that translational complexes run off of mRNA following the stress of glucose depletion (Ashe *et al.*, 2000; Wang *et al.*, 2012). For example, for Flag-PAB1 77S monosomal translation complexes, glucose depletion results in a reduction to 25% of the abundance seen under normal glucose growth conditions (Wang *et al.*, 2012). Therefore, we used the effect of glucose removal to determine which of the Flag-eRF1 complexes were translationally active. As shown in Figure 10E, the AU-A₂₃₀ profile indicates that only the polysomal material (greater than 100S) displayed a reduction in abundance following glucose depletion.

Similar analyses were conducted for individual GFP-tagged translation proteins (Figure 10 A-D, PAB1, eIF4G1, RPS4B, and RPL7A, respectively). The effect of glucose deprivation on the abundance of each protein in each complex is summarized in Table 3. The polysomal material following glucose deprivation decreased to 25% for the ribosomal proteins and about 50% for eIF4G1 indicating these were eRF1-containing translationally active complexes. PAB1 did not show a large decrease in abundance at the polysomal position, but further repeats are necessary to confirm this.

In contrast to the polysomal material, the 77S complex did not show a significant change following glucose deprivation. This suggests that these complexes containing PAB1 and eIF4G1 are already translationally stalled and therefore cannot run-off the mRNA. However, the RPS4B and RPL7A containing complexes could be translationally stalled complexes or free 80S ribosome whose abundance is insensitive to glucose

deprivation (Wang *et al.*, 2012). In addition, the A_{230} profile of the peaks observed below 77S showed little change or possibly increased in abundance in response to glucose deprivation, as previously seen (Wang *et al.*, 2012). An increase in abundance following glucose deprivation would be consistent with the complexes forming post-runoff and during termination of translation.

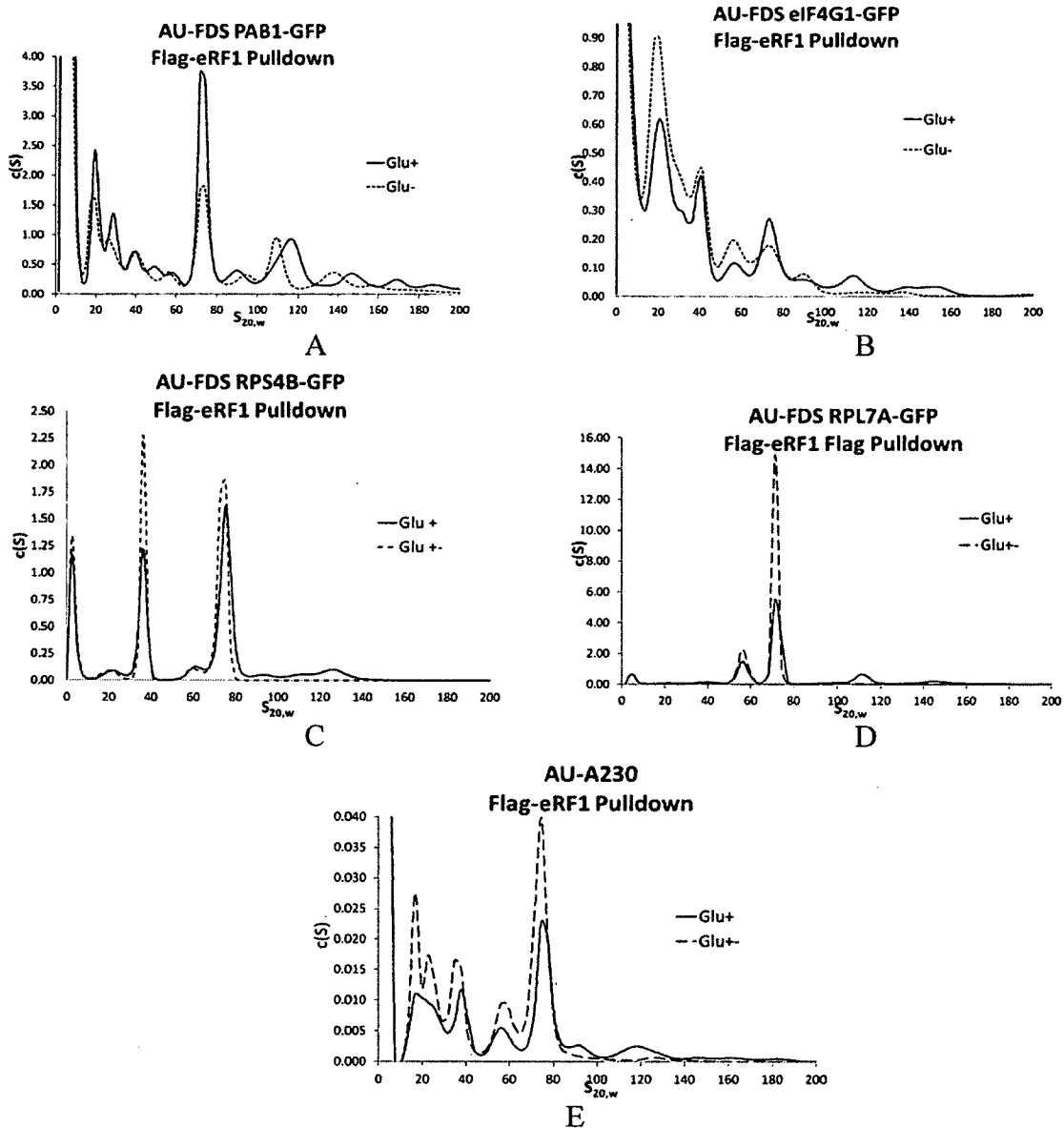


Figure 10: AU-FDS analysis was performed at 25,000 rpm for 150-200 scans. Samples run were prepared from the same culture before and after 10 minute glucose depletion and each pair was run on the same day. Strains used for this figure were (A) RP2191/TK41 (PAB1-GFP), (B) RP1947/TK41 (eIF4G1-GFP), (C) RPS4B/TK41 (RPS4B-GFP), (D) RPL7A/TK41 (RPL7A-GFP), (E) RPL7A/TK41 (RPL7A-GFP)

Target	20S	28S	39S	57S	77S	100-200S
eIF4G1	131 ± 14	145 ± 6.2	110 ± 16	163 ± 7.9	74 ± 15	45 ± 11
PAB1	96	74	151	94	63	72
RPS4B	N/A	N/A	137 ± 1.1	49 ± 37	113 ± 12	28 ± 18
RPL7A	N/A	N/A	N/A	140	178	13
A230	169 ± 7.8	92 ± 39	102 ± 9.1	135 ± 17	123 ± 14	78 ± 24

Table 3: Change in abundance (AU-FDS or A₂₃₀) of GFP fusion target after 10 minute glucose deprivation. Values are presented as percent of the abundance before glucose depletion.

Effects of cycloheximide treatment on Flag-eRF1 containing complexes

It has been previously shown that cycloheximide prevents the translational complex from leaving the mRNA (Wang *et al.*, 2012). This is because cycloheximide inhibits the translocation step of the ribosome during elongation. Cycloheximide treatment was performed to determine if the complexes smaller than 77S were pre-initiation complexes. While cycloheximide inhibits translation, transcription is not inhibited. If the smaller complexes were pre-initiation complexes, we might expect that their abundances would increase after cycloheximide treatment. However, there was no large increase in abundance seen in complexes smaller than 77S. Most abundances were similar or decreased after treatment (Table 4). This result is consistent with the model that the majority of the eRF1-containing complexes are termination complexes that fail to form if elongation is blocked.

Polysomal material associated with Flag-PAB1 was previously shown to be stabilized by cycloheximide, causing an increase by about 2-fold of the polysomal material. This indicates that these polysomal complexes were translationally active

elongating complexes (Wang *et al.*, 2012). However, the majority of polysomal material associated with Flag-eRF1 remained at a relatively similar abundance if not actually decreasing in abundance following cycloheximide treatment. Again, this is consistent with the model that these polysomal complexes containing eRF1 are termination complexes and fail to form if elongation is blocked.

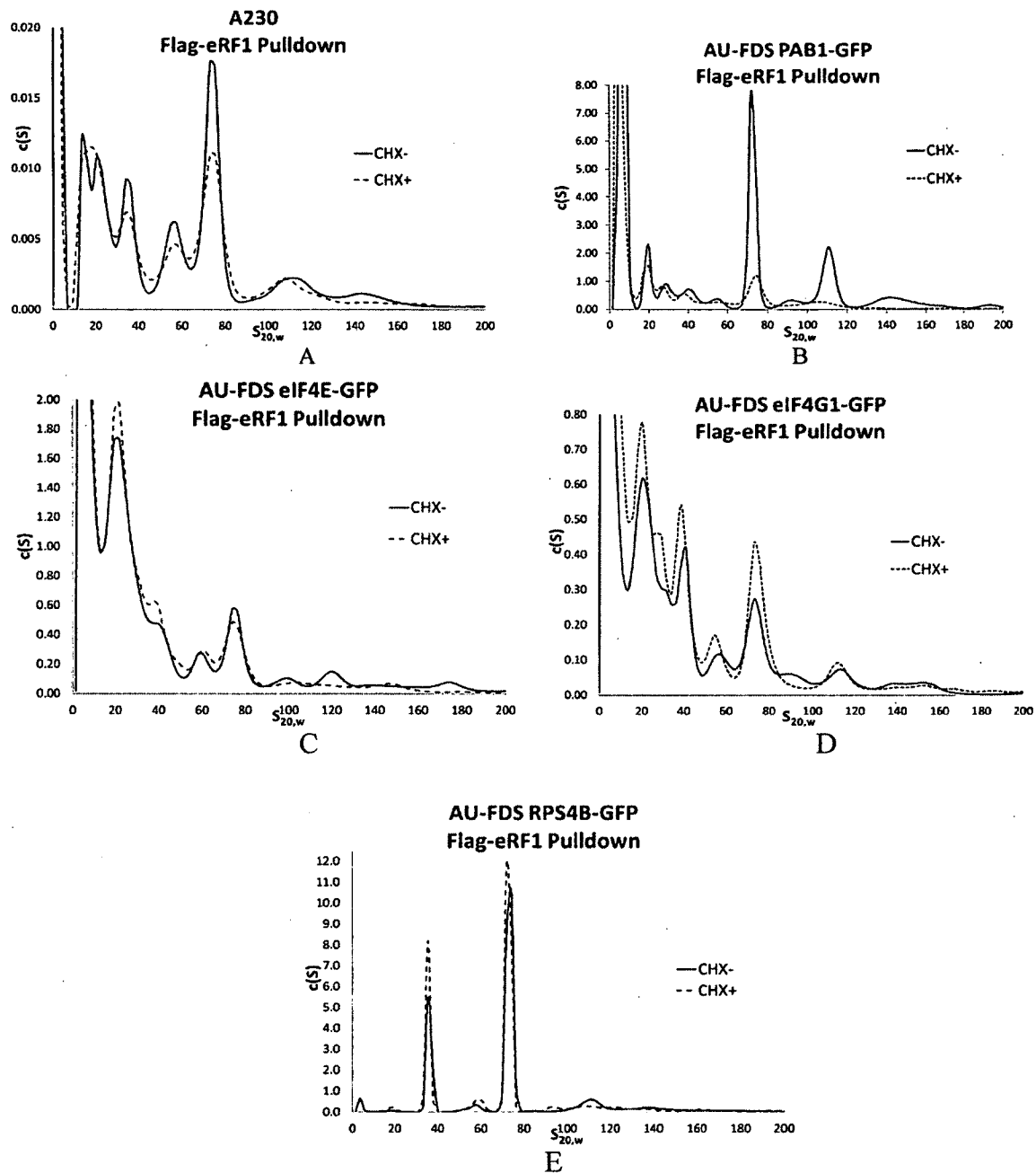


Figure 11: AU-FDS analysis was performed at 25,000 rpm for 150-200 scans. The samples run were prepared from the same culture before and after 10 minute cycloheximide treatment and each pair was run on the same day. Strains used for this figure were (A) RP1946/TK41 (eIF4E-GFP), (B) RP2191/TK41 (PAB1-GFP), (C) RP1946/TK41 (eIF4E-GFP), (D) RP1947/TK41 (eIF4G1-GFP), (E) RPS4B/TK41 (RPS4B-GFP)

Target	20S	28S	39S	57S	77S	100-200S
eIF4E	113 ± 5.9	N/A*	97 ± 31	113 ± 7.6	101 ± 3.4	60 ± 2.7
eIF4G1	127	124	123	122	141	104
PAB1	114	80	87	103	34	21
RPS4B	N/A	N/A	109 ± 16	89 ± 47	96 ± 22	80 ± 4.0
A230	97 ± 6.1	131 ± 6.9	103 ± 7.5	106 ± 9.9	87 ± 11	77 ± 15

Table 4: Change in abundance (FDS or A₂₃₀) of GFP fusion target after 10 minute incubation with cycloheximide. Values are presented as percent of the abundance before cycloheximide treatment. The eIF4E cycloheximide experiments were performed before the complex shift phenomenon was observed. The number of scans used for the eIF4E analysis did not allow for the clear determination of the 28S peak abundance.

Determining the stoichiometry of translation components in each complex

In order to absolutely determine the particular abundance of a protein in a particular complex, the ratio of the abundance of a protein was determined by AU-FDS and compared to the total protein in that particular peak using AU-A₂₃₀ analysis (see Materials and Methods section). The values provided in Table 5 were calculated from experiments where AU-A₂₃₀ was run simultaneously with AU-FDS.

Protein	20S	28S	39S	57S	77S
eIF4E	100%	100%	22 ± 2.8	13 ± 0.82	13 ± 0.81
eIF4G1	46 ± 1.6	46 ± 2.4	15 ± 2.9	8.4 ± 1.9	7.1 ± 1.2
PAB1	40 ± 9.9	49 ± 1.7	19 ± 3.3	9.0 ± 0.40	10 ± 3.3
eIF2 γ	212 ± 78	106 ± 37	22 ± 4.9	11 ± 1.2	8.0 ± 1.3
eIF2 α	34 ± 1.8	35 ± 1.8	5.0 ± 0.61	2.6 ± 1.3	0.85 ± 0.34
eIF3b	45 ± 0.55	29 ± 9.5	16 ± 0.21	N/A	N/A
RPS4B	N/A	N/A	100%	13 ± 3.1	100%
RPL7A	N/A	N/A	N/A	100%	117 ± 18
eRF3	6500 ± 340	2700 ± 500	N/A	950 ± 150	800 ± 280

Table 5: Relative abundance of each protein at the identified peak positions. The abundances at 20S and 28S were compared to the abundance of eIF4E. The abundances at 39S and 77S were compared to the abundance of RPS4B. The abundances at 57S were compared to the abundance of RPL7A. Values presented are percentage of abundance of the target protein compared to the different standard proteins. Error presented is SEM.

The 77S complex associated with Flag-eRF1 mostly contained the large and small ribosomal subunit proteins RPL7A and RPS4B, respectively (approximately 85% assuming separate pools of free ribosome and ribosomes with translationally stalled monosomal complexes that contained eIF4E, eIF4G1, and PAB1, see below). This complex did not have a major response to stressors as previously characterized, indicating that the majority of complexes at the 77S position behave like free 80S ribosome (Wang *et al.*, 2012). The rest of the complexes which contain the closed-loop proteins (13% based on eIF4E abundance) must also have an 80S ribosome and mRNA associated with them. We assume mRNA is present in these complexes because eIF4E binds the mRNA cap and PAB1 binds the poly(A) tail. However, these complexes may not all be translationally active because glucose depletion did not reduce the abundance

of these components to the degree observed for translationally active complexes containing Flag-PAB1 (Wang *et al.*, 2012).

The 57S complex associated with Flag-eRF1 is mostly comprised of the large ribosomal subunit protein RPL7A. Based on different pools of complexes as described for the 77S complex, these ribosomal subunit complexes comprise approximately 85% of these complexes. Translation termination factor eRF1 has been shown to interact with the 60S subunit of the ribosome and may be associating with free 60S subunits (Taylor *et al.*, 2012). It appears that the remainder of these complexes (13% based on eIF4E abundance) have similar abundances of the closed-loop proteins in addition to the small ribosomal subunit protein RPS4B. These complexes may be post-termination complexes which contain the small subunit still bound to the mRNA. It has been shown that eRF1 will remain associated with the small subunit on the ribosome following ribosome subunit separation by eIF3 (Pisarev *et al.*, 2010). Another possibility is that there is a pool of complexes which contain the closed-loop proteins as well as full ribosome, but have undergone a conformational change causing a shift in peak position. It is unlikely that this peak consists of mRNP complexes that have undergone ribosome separation during the affinity purification. Previous studies have found that active dissociation of translational complexes does not occur during the affinity purification process (Wang *et al.*, 2012).

The 39S Flag-eRF1 associated complex consists primarily of the small ribosomal subunit protein RPS4B. It is possible this pool of complexes mostly contains free 40S

subunit associated with eRF1, since eRF1 has known sites of interaction with the 40S subunit (Taylor *et al.*, 2010). The remainder of this pool of complexes may simply be the closed-loop proteins associated with mRNA, which still have a 40S subunit bound to them.

All of the Flag-eRF1 associating complexes migrating at 28S contain eIF4E and approximately half contain PAB1. These factors require mRNA to be present for this type of association. This pool likely contains various complexes with mRNA and different proportions of the various closed-loop proteins, each complex with eIF4E still associated. It is likely that the 28S complex is related to the 20S complex since they have similar abundances of each target protein. The shifting position of the 20S complex during sedimentation may be either due to an unwinding effect of this complex, resulting in a conformational shape change of the complex or a change in composition (see below). For more detailed interpretations of the complexes associated with Flag-eRF1, see the discussion section.

Shifting S value for the 20S complex

An additional observation that was made was that increasing the number of scans taken with the AU-FDS analysis resulted in a shift in the S value of peaks in the 10S-20S range for eIF4E, eIF4G1, PAB1, eIF2 α , and eIF2 γ without a change in total abundance (Figures 12A and C, 13A, 14A and C). The shift in this region in contrast to the fixed position of the 1S peak and peaks larger than 20S are indicative of a reaction boundary rather than a sedimentation boundary. In other words, this shift is consistent with a change in composition of the complex or a pressure effect on the complex during

sedimentation. The shift appears when comparing scans ranging from 200 to 500. The shift ceases after 500 scans (Figures 12B and D, 14B and D) indicating that the change in forms have reached equilibrium at later times. As sedimentation occurs, the pools of complexes at 20S becomes more distinct. In contrast, the initiation factor eIF3b does not show this shifting behavior for its peaks (Figure 14E). However, initiation factor eIF2 γ behaved similarly to the closed-loop components. Its 18S complex (Figure 14C) at a low number of scans migrated and settled into peaks at 17S and 12S after a high number of scans (Figure 14D). This shifting behavior could be due to either a change in composition or a change in shape of the complexes.

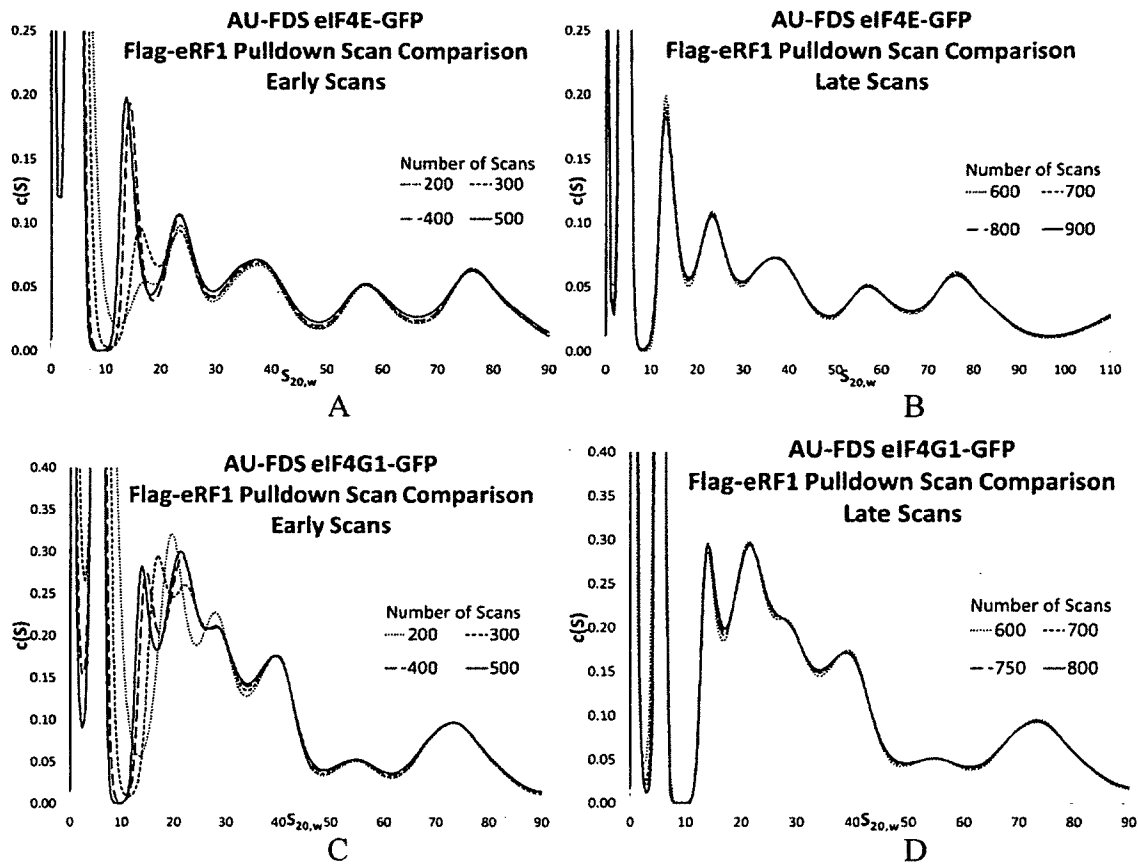


Figure 12: GFP fusion targets that sediment below 28S shift sedimentation position between 200 and 500 scans. Targets that sediment above 30S do not show this shifting pattern. Samples were run at 25,000 rpm. Strains used for this figure were (A,B) RP1946/TK41 (eIF4E-GFP), (C,D) RP1947/TK41 (eIF4G1-GFP)

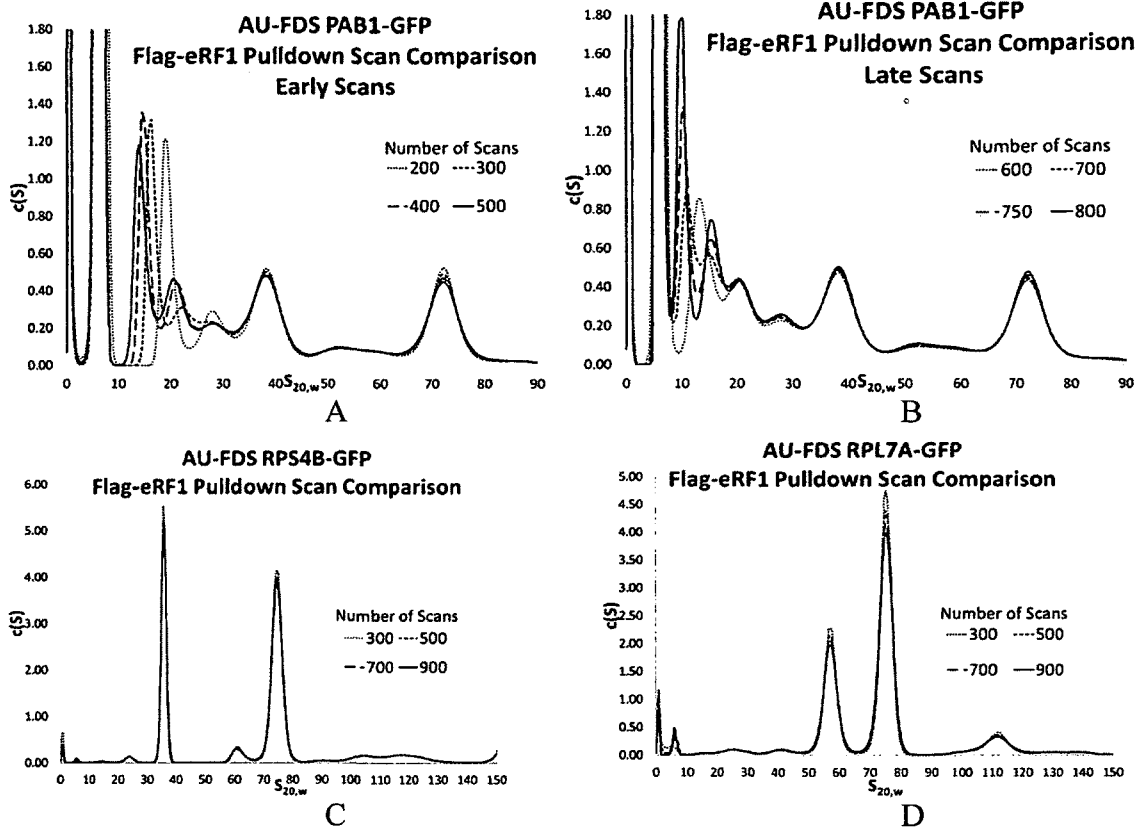


Figure 13: GFP fusion targets that sediment below 28S shift sedimentation position between 200 and 500 scans. Targets that sediment above 30S do not show this shifting pattern. Samples were run at 25,000 rpm. Strains used for this figure were (A,B) RP2191/TK41 (PAB1-GFP), (C) RPS4B/TK41 (RPS4B-GFP), (D) RPL7A/TK41 (RPL7A-GFP)

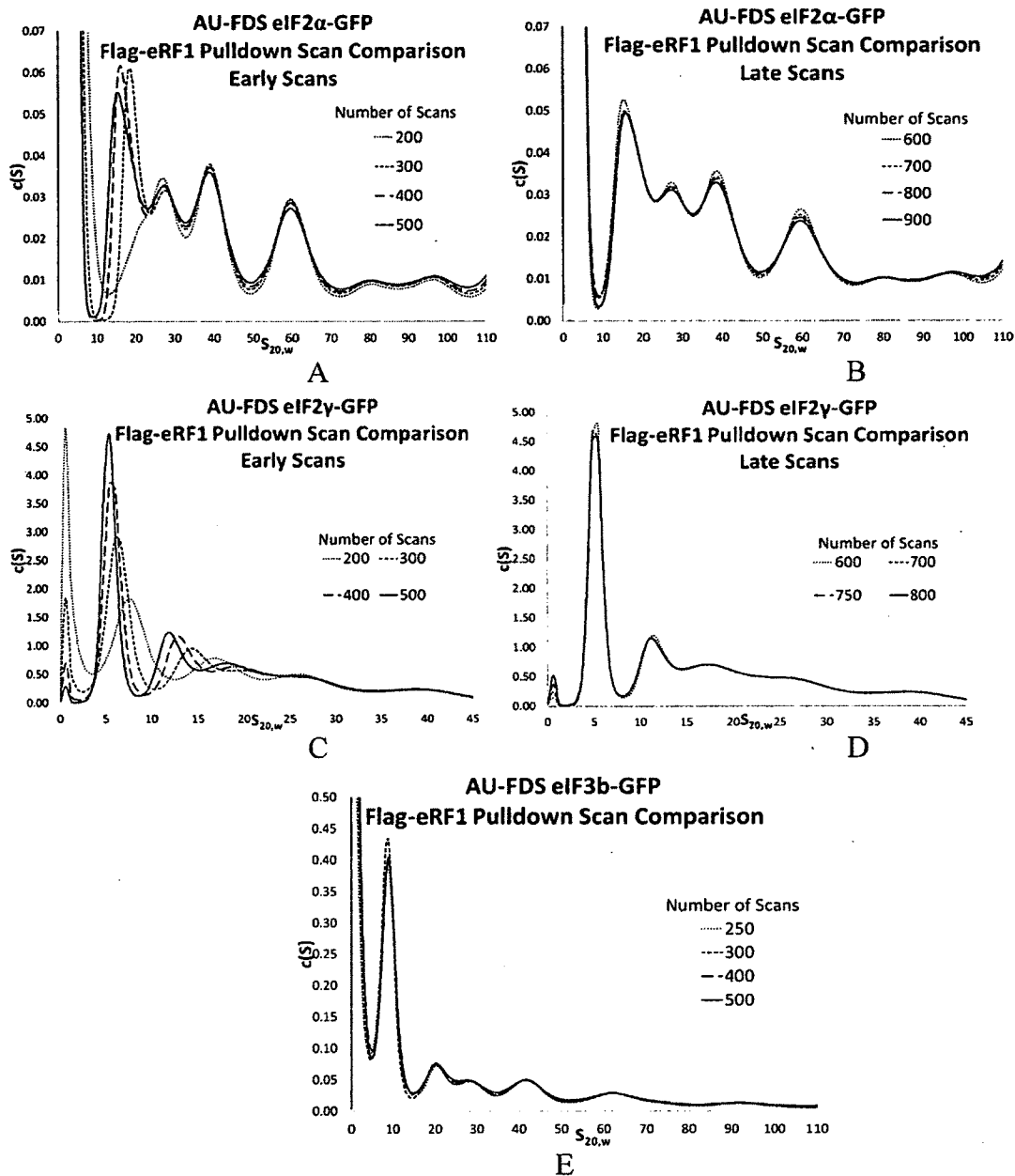


Figure 14: GFP fusion targets that sediment below 28S shift sedimentation position between 200 and 500 scans. Targets that sediment above 30S do not show this shifting pattern. Initiation factor eIF3b does not exhibit the shift below 28S. Samples were run at 25,000 rpm. Strains used for this figure were (A, B) YMK883/TK41 (eIF2 α -GFP), (C, D) YMK1211/TK41 (eIF2 γ -GFP), (E) YMK882/TK41 (eIF3b-GFP).

The abundance of termination factor eRF3 suggests a possible prion effect

Termination factors eRF1 and eRF3 have been shown to interact with each other using various biochemical methods (Stansfield *et al.*, 1995; Krogan *et al.*, 2006; Collins *et al.*, 2007). Using AU-FDS, eRF3-GFP was identified as present in Flag-eRF1 pulldowns (Figure 7D). However, the abundance of eRF3 present in eRF1 associated complexes was found to be much greater than any other eRF1-interacting protein (Figure 7D). Major peaks for eRF3 appear at 19S and 23S followed by a high abundance signal with less distinct peaks into the 100S region. The abundance throughout the eRF3 profile is also unaffected by glucose deprivation or cycloheximide treatment (Figure 15A). The estimated eRF3 abundance in 77S, 57S, 28S, and 20S regions is many fold higher than the observed abundances of the ribosomal proteins associated with eRF1 complexes (see Figures 6D and E, and 7C). These observations suggest that there are multiple copies eRF3 molecules in each complex. The abundances of eRF3-GFP in the more clearly defined peaks (Figure 7D) were found to be 8 to 60-fold greater than the ribosomal proteins or eIF4E (Table 5). Since it has been found that eRF3 can act like a prion factor in yeast, creating a barrel shaped polymer, eRF3 self-aggregation could explain the increased abundances that are observed (Namy *et al.*, 2008).

AU-FDS experiments with a dilution series of eRF3-GFP were subsequently conducted to determine if the putative aggregated eRF3 was acting as if it formed a micelle structure. If there is an equilibrium between a monomer and a micelle structure, then decreasing the concentration of the complex prior to AU-FDS analysis would favor disassociation and movement of the peaks to a smaller S value. Using a series of dilutions

of eRF3-GFP sample following a Flag-eRF1 pulldown, no difference was found in the movement or abundance of the 18S and 28S peaks (Figure 15B). These results do not support a micelle model for eRF3 in these complexes.

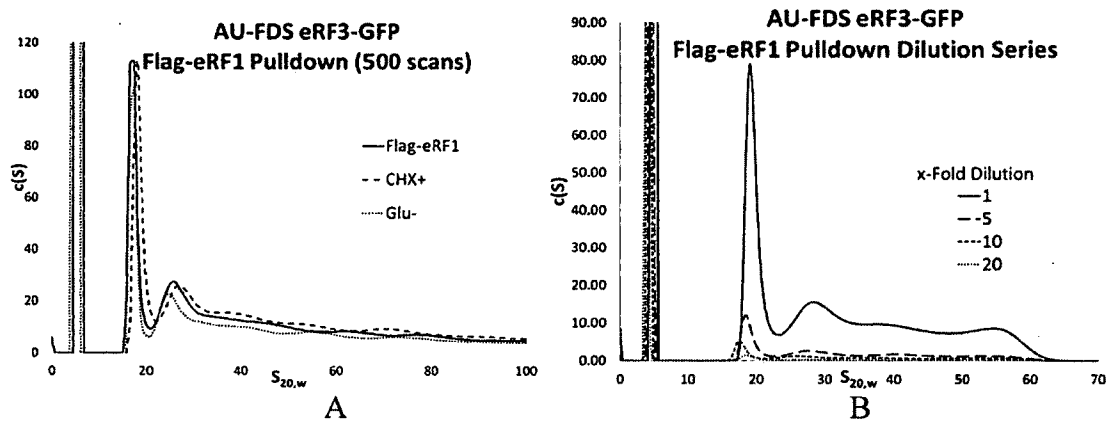


Figure 15: AU-FDS was performed at 25K rpm. (A) The same culture was used to perform ten minute glucose deprivation and ten minute cycloheximide treatment. (B) The same elution sample was used to create each dilution in the series. The strain used for this figure was RP2522/TK41 (eRF3-GFP).

Discussion

In this thesis I used AU-FDS to in seek the identity and characteristics of protein complexes involved in protein translation. By immunoprecipitating translation termination factor Flag-eRF1 in conjunction with various protein targets previously identified with mRNP complexes my studies revealed several complexes that migrate at sedimentation values previously unseen or uncharacterized. Overall, these eRF1 complexes may represent termination complexes. There are several pieces of evidence to support this. First, the complexes contain both eRF1 and eRF3, key elements for translation termination. Secondly, general insensitivity of the 77S complex containing closed-loop component eIF4G1 to glucose deprivation treatment suggests that this complex is probably not translationally active. Third, cycloheximide treatment, blocking the translocation elongation step, did not increase the abundance of these complexes, which is consistent with their formation after elongation. Fourth, complexes smaller than 28S do not increase after cycloheximide treatment, suggesting they are not newly transcribed pre-initiation complexes.

The 77S complex

The 77S complex identified with Flag-eRF1 contains components similar to the monosomal translating complex previously identified by our lab (Wang *et al.*, 2012). These components are the small and large ribosomal subunit proteins RPS4B and RPL7A, respectively, and the closed-loop components eIF4E, eIF4G1, and PAB1. However, this 77S complex has different characteristics compared to the monosomal translating complex. First, it does not respond in the same manner as the previously

identified complex to stress conditions. Glucose depletion causes runoff in translation of a majority of translationally active mRNP complexes. The relative insensitivity of the Flag-eRF1 77S complex to glucose deprivation indicates that the complex associated with eRF1 might already be translationally stalled or that the majority of the Flag-eRF1 77S complexes are actually free 80S ribosome, which are known to be insensitive to the effects of glucose deprivation.

The relative abundance of the mRNP closed-loop complex components relative to the ribosomal proteins RPS4B and RPL7A indicate that the majority of complexes migrating at 77S are actually free 80S ribosomes (approximately 85%). This is indicated by the relatively low abundance of eIF4E, eIF4G1, and PAB1 relative to the ribosomal proteins. The smaller pool of 77S mRNP complexes contains similar amounts of the core components eIF4E, eIF4G1, and PAB1. Interestingly, eIF2 γ is also present in a similar abundance in this complex as the closed-loop complex components. The presence of eIF2 may be part of the role eRF1 plays in its suggested involvement in ribosome recycling (Shoemaker & Green, 2011).

The abundance of the 77S complex containing the closed-loop components was relatively insensitive to glucose deprivation, which is unlike the reduction of the 77S monosomal complex by glucose deprivation previously observed (Wang *et al.*, 2012). Therefore, it is unlikely that the eRF1 containing complexes at 77S with closed-loop components consists of both monosomal complexes as well as stalled complexes, but rather a combination of free 80S ribosome and stalled complexes. Crystal structures of

mammalian free 80S ribosome combined with eRF1-eRF3-GMPPNP *in vitro* revealed that eRF1 interacts with the intersubunit space of the 80S ribosome (Taylor *et al.*, 2012). The affinity of the eRF1/eRF3 complex for the 80S ribosome could explain the presence of the free ribosomes in the 77S complex pool.

The 57S Complex

The 57S complex associated with eRF1 is mostly comprised of the large subunit of the ribosome as indicated by the abundance of RPL7A relative to closed-loop components. This may be a product of the splitting of the free 80S ribosome seen in the 77S complex. The initiation factor eIF3b can dissociate the 80S ribosome by itself and was observed to associate with eRF1 complexes (Figure 14E) (Pisarev *et al.*, 2010). However, this dissociation most likely occurred prior to lysing the cells since degradation of translation complexes has not been observed during the affinity purification process (Wang *et al.*, 2012). If this were true, then the large portion of 60S ribosome subunit comprising the 57S peak must be directly interacting with eRF1. Crystal structures of mammalian free 80S ribosome with eRF1-eRF3-GMPPNP have revealed that eRF1 interacts with the 60S subunit *in vitro* (Taylor *et al.*, 2012). This interaction could explain the presence of the high abundance of RPL7A in the 57S complex.

The remaining pool of 57S complexes contained closed loop components consisting of similar levels of the components that are found in the 77S peak. Interestingly, this smaller pool of mRNP complexes also contains a similar abundance of RPS4B as the core mRNP components. Two models could explain the presence of

RPS4B. The first is that RPS4B and RPL7A are present together, although that would lead one to an expected much larger S value. The smaller S value of 57S may be explained by a “dumbbell” effect, wherein the 60S subunit of the ribosome is in the process of terminating at the 5’ end while a 40S subunit is beginning a new round of translation at the 3’ end. Having such large components at either end of the mRNA would create a very elongated shape. Sedimenting targets that are 2-3 times longer than their width have an S value shift of approximately 1.4-fold that of the expected mass assuming a spherical shape. This elongation factor agrees well with the S value seen at 57S versus 77S. Again, the presence of eIF2 may suggest a new round of translation is beginning in this smaller pool of complexes.

The second model is that RPS4B is only associated with mRNA containing the closed-loop components, since they are present in similar abundance. In this case, this 40S-mRNA-closed-loop component 57S complex would be most similar to the predicted splitting apart of the translating ribosome following termination.

The 39S Complex

The 39S complex associated with eRF1 contains the small subunit of the ribosome but no large ribosomal subunit. Once again, there is a smaller pool of complexes that contain similar amounts of the closed-loop mRNP components. In addition, the initiation factor eIF3b also appears here with a similar abundance as compared to the closed-loop components. A possible model for the presence of both eIF2 and eIF3b would be that this smaller pool of complexes is actually in the process of

initiation following termination. This complex might be similar to the 48S initiation complex. After peptide release, eRF1 remains bound to the ribosome until it is split by eIF3 (Pisarev *et al.*, 2010). Also, eRF1 has been proposed to remain attached to the 40S ribosome post-termination until the mRNA is released by eIF1 and eIF3j (Pisarev *et al.*, 2007b) and some eRF1 and eRF3 is known to be present on translation initiation complexes (Amrani *et al.*, 2008). Perhaps the association between eIF3b and eRF1 is indicative of eRF1's ability to assist in recycling of the ribosome for additional rounds of translation following termination prior to degradation. The abundance of the 39S complex was insensitive to cycloheximide treatment. Since transcription continues during cycloheximide treatment, one would expect new mRNA to form more pre-initiation complexes. However, if the eRF1-associated 39S complex forms after translation termination and is not the result of new mRNA forming the 48S complex, then blocking elongation with cycloheximide would not cause an increase in the 39S complex, which is what was observed.

The 28S Complex

Assuming a spherical shape, the predicted size of a 28S complex is 832 kDa. The sum of the mass of the average yeast mRNA (600kDa) plus eIF4E, eIF4G1, PAB1, eRF1, and GFP gives a total of 871 kDa. We assume all of the complexes in the 28S peak contain the cap binding protein eIF4E. The assumption is based on the stoichiometric estimations seen in Table 5. However, not all of the complexes in this region appear to contain the other closed-loop complex proteins typically associated with mRNP formation. PAB1 and eIF4G1 have roughly half of the abundance as compared to eIF4E.

The relative abundance of these components suggest that there are likely multiple pools of complexes at 28S comprised of various closed-loop elements with each containing eIF4E. The above calculated mass of 871 kDa would be 807 kDa if lacking PAB1 and 764 kDa if lacking eIF4G1, which would have approximate S values of 27.4S and 26.4S, respectively.

The size of this complex and the presence of eIF4E strongly suggests that there is mRNA present in these complexes. Perhaps the portion of complexes that do not contain eIF4G1 or PAB1 are termination products awaiting degradation. The complexes that would contain all of the closed-loop components (if all of the components are found together and not in separate pools) also have similar abundances of the initiation factors eIF2 and eIF3. This suggests that these may be complexes preparing for a new round of translation.

The 20S Complex

The components of the 20S complex are present at levels similar to that of the 28S complex. Given this fact, we would expect them to have a similar MW. However, the approximate mass of a spherical 20S complex would be 502 kDa. The discrepancy could be explained by an elongated form of the 28S complex. A 2-3 ratio of length to width elongated form of a 28S sized complex would run at approximately 20S (a 1.4-fold difference).

The 20S peak is one of the peaks that shift during the sedimentation experiment and its initial position is closer to the 28S peak and shifts to a lower position before settling at 20S. This indicates that it is either losing components or undergoing a shape change. If this is the 28S complex losing components, then the components lost are not one of the core components, since their abundance does not change relative to the 28S. The lost components would, therefore, be proteins not targeted during these experiments. Proteins that may be worth targeting to investigate the possibility of composition change include Rli1, Dbp5, and Itt1. Each of these proteins has been indicated to interact with eRF1 and have importance in the regulation of translation termination (Shoemaker & Green, 2011; Gross *et al.*, 2007; Urakov *et al.*, 2001). Alternatively, the 20S complex may change shape during the AU-FDS experiment. This could occur if the 20S complex begins to unravel with time and assume a more elongated shape and therefore have a lower S value. However, this shape change would have likely reached equilibrium prior to centrifugation. This change may also be caused by a pressure effect during centrifugation. This would be caused by a change in pressure in the centrifuge cell as complexes are sedimenting.

Complexes smaller than 20S

In addition to the five peaks mentioned above, some of the targets were seen at smaller S values. Each GFP component analyzed displayed a peak at an S value similar to the one estimated for the MW of its monomer plus the MW of the GFP they were fused with, ranging from 4.4 - 9.0S. These values are well below the expected value of the GFP-fused monomer plus eRF1, indicating that the monomer has dissociated from an

eRF1 associated complex at some point during the affinity pulldown. PAB1 was present in a complex at 10S that increased in abundance as sedimentation occurred. The 10S peak correlates well with the MW of a dimer of PAB1-GFP (which is 150 kDa), suggesting that PAB1 is self-associating during the sedimentation experiment and subsequently splitting into a monomer form.

Closed-loop components

The relative abundance of the closed-loop components in the complexes larger than 28S suggest that only a small portion of the complexes associated with eRF1 contain closed-loop mRNPs with ribosomes attached. It appears that eRF1 is associating with or remains associated with ribosomal subunits post-termination. The shift in abundance of the various closed-loop structure proteins during stress also indicates that the pool of mRNP complexes that are associated with ribosomal subunits are in the process of termination. The relative abundances of the closed-loop components in the 28S and 20S complexes suggests that the majority of these complexes are in various states of decomposition. However, the presence of eIF2 and eIF3 in these smaller complexes suggest that some of these complexes may be involved in re-initiation. The cycloheximide effects on these small complexes suggest that the eIF2 and eIF3 associations are not a result of new mRNA being prepared for translation initiation.

GENERAL DISCUSSION

In Chapter 1, analysis of the interaction between UPF1 and PAB1 revealed that the RRM1 deletion prevented deadenylation but not decapping in UPF1-mediated NMD. Additionally, deleting UPF1 prevented a shift from distributive to processive deadenylation. This result suggests that UPF1 is the long sought after factor that controls normal acceleration of deadenylation, a process critical to all mRNA degradation. The presence of the RRM1 domain of PAB1 was required for UPF1 effects, but whether this is critical for this newly identified function of UPF1 remains to be clarified.

In Chapter 2, AU-FDS analysis revealed the presence of six distinct complexes that associate with Flag-eRF1. These complexes have S values of 20S, 28S, 39S, 57S, 77S, as well as complexes >100S. Analysis of the various components associating with Flag-eRF1 revealed that the closed-loop components of mRNP complexes (eIF4E, eIF4G1, and PAB1) are present in all of the complexes identified. Furthermore, small ribosomal protein RPS4B was identified in the 39S, 57S, 77S, and >100S complexes. Large ribosomal subunit protein RPL7A was identified in the 57S, 77S, and >100S complexes as well.

Stoichiometric analysis revealed that the 39S, 57S, and 77S complexes are mostly comprised of free ribosomal material, the remainder of the pool consisting of ribosomal associated closed-loop components. The smaller complexes at 28S and 20S all contained eIF4E with various mixtures of the other closed-loop components. These complexes also

contained a relatively similar abundance of eIF2 γ and eIF3b in comparison to the closed-loop components. The 20S complex revealed a peak shift behavior that is possibly the effect of either a loss of certain components during sedimentation or a change in shape of the complex.

The stress effects of glucose and cycloheximide revealed that these complexes are probably not translationally active. For the 77S complex, this is consistent with it being primarily comprised of the free 80S ribosome whose abundance is also unaffected by glucose deprivation (Wang *et al.*, 2012). Cycloheximide treatment did not cause an increase in abundance of the ribosome-free smaller complexes, suggesting that these complexes are not pre-initiation complexes transcribed after the addition of the cycloheximide but are rather post-termination complexes.

Further analyses of complexes associated with eRF1 need to be performed to further elucidate the roles of these complexes. Additional repeats of glucose deprivation must be performed to clarify the relative abundances of PAB1 and eIF4E in these complexes. In order to clarify if any of these complexes are initiation complexes forming after termination, experiments in which glucose is depleted and then restored for a short time should be performed. Such experiments will determine if there is an effect on the abundance of the initiation factors eIF3 and eIF2 in order to clarify the possibility that the smaller complexes are involved in re-initiation of terminating complexes. Finally, termination events can be looked at more directly by conducting 1 min heat shock experiments in which translational run-off and termination predominantly occur.

To further explore the results obtained with Flag-eRF1 complexes, the complexes and components obtained with Flag-eRF3 pull-down could be done. It would be expected that Flag-eRF3 complexes would be similar to those obtained with Flag-eRF1. Also, experiments adjusting the levels of Mg^{2+} in solution may provide interesting results as the concentration of Mg^{2+} has been shown to effect eRF1-eRF3 interactions as well as eRF1 interactions with post-termination complexes *in vitro* (Pisarev *et al.*, 2010).

These above types of experiments would help in clarifying whether the eRF1 complexes that I have detected are primarily termination complexes. Dissecting whether multiple types of complexes exist at each peak size (for example, 57S) may be more difficult to accomplish. Experiments in which other baits are used to detect 57S complexes, such as eIF4E-Flag, eRF3-Flag, or eIF4G1-Flag, may aid this process. Clearly, the large number of distinct complexes observed with eRF1 suggest that translation termination holds many secrets yet to be revealed.

Finally, my data suggests that eRF3 is forming multimers in a prion-like configuration and warrants further investigation. One way to approach this would be to determine if other known eRF3 prion-associated factors, such as SSA2, SSE1, and YDJ1, are present in the eRF1 complexes that I have detected. If these proteins were to be present, then that would strengthen the argument that at least under termination conditions eRF3 is forming multiple prion-like particles. Whether these particles have any specific role in termination remains to be determined. Since actively translating 77S

complexes purified with Flag-PAB1 have only very low levels of eRF3 (about 1% of the complexes contain eRF3), then it is possible that eRF3 prion-like assemblies do form only during termination.

REFERENCES CITED

Amrani N, Ghosh S, Mangus DA, Jacobson A., Translation factors promote the formation of two states of the closed-loop mRNP., *Nature*. 2008 Jun 26;453(7199):1276-80.

Asano K, Clayton J, Shalev A, Hinnebusch AG., A multifactor complex of eukaryotic initiation factors, eIF1, eIF2, eIF3, eIF5, and initiator tRNA(Met) is an important translation initiation intermediate in vivo, *Genes Dev*. (2000) Oct 1;14(19):2534-46.

Ashe MP, De Long SK, Sachs AB., Glucose depletion rapidly inhibits translation initiation in yeast., *Mol Biol Cell*. 2000 Mar;11(3):833-48.

Ausubel, F.M., Brent R., Kingston R.E., Moore, D.D., Seidman, J.G., Smith, J.A., and Struhl, K., *Current Protocols in Molecular Biology*, (1992), Vol. 2, 13.1-13.3

Bregues M, Parker R., Accumulation of polyadenylated mRNA, Pab1p, eIF4E, and eIF4G with P-bodies in *Saccharomyces cerevisiae*., *Mol Biol Cell*. (2007) Jul;18(7):2592-602.

Bregues M, Teixeira D, Parker R., Movement of eukaryotic mRNAs between polysomes and cytoplasmic processing bodies, *Science*. (2005) Oct 21;310(5747):486-9.

Brodsky, A.S., and Silver, P.A., Pre-mRNA processing factors are required for nuclear export., *RNA* 6, 1737-1749 (2000)

Brown CE, Tarun SZ Jr, Boeck R, Sachs AB., PAN3 encodes a subunit of the Pab1p-dependent poly(A) nuclease in *Saccharomyces cerevisiae*., *Mol Cell Biol*. (1996) Oct;16(10):5744-53.

Brown C E, Sachs A B., Poly(A) tail length control in *Saccharomyces cerevisiae* occurs by message-specific deadenylation., *Mol Cell Biol*. (1998);18:6548–6559.

Buchan, JR, Muhlrad, D, and Parker, R., P bodies promote stress granule assembly in *Saccharomyces cerevisiae*, *J Cell Biol*., (2008) Nov 3;183(3):441-55

Cao D, Parker R., Computational modeling and experimental analysis of nonsense-mediated decay in yeast, *Cell*. (2003) May 16;113(4):533-45.

Cole JL, Lary JW, P Moody T, Laue TM., Analytical ultracentrifugation: sedimentation velocity and sedimentation equilibrium., *Methods Cell Biol*. (2008);84:143-79.

Collins SR, Kemmeren P, Zhao XC, Greenblatt JF, Spencer F, Holstege FC, Weissman JS, Krogan NJ, Toward a comprehensive atlas of the physical interactome of *Saccharomyces cerevisiae*., *Mol. Cell Proteomics* Mar. 01, (2007); 6(3);439-50

Conard SE, Buckley J, Dang M, Bedwell GJ, Carter RL, Khass M, Bedwell DM., Identification of eRF1 residues that play critical and complementary roles in stop codon recognition., *RNA*. (2012) Jun;18(6):1210-21.

Cosson B, Couturier A, Chabelskaya S, Kiktev D, Inge-Vechtomov S, Philippe M, Zhouravleva G., Poly(A)-binding protein acts in translation termination via eukaryotic release factor 3 interaction and does not influence [PSI(+)] propagation., *Mol Cell Biol*. (2002) May;22(10):3301-15.

Deardorff JA, Sachs AB., Differential effects of aromatic and charged residue substitutions in the RNA binding domains of the yeast poly(A)-binding protein., *J Mol Biol*. (1997) May 30;269(1):67-81.

Decker CJ, Parker R., A turnover pathway for both stable and unstable mRNAs in yeast: evidence for a requirement for deadenylation., *Genes Dev*. (1993) Aug;7(8):1632-43.

Denis CL, Chen J., The CCR4-NOT complex plays diverse roles in mRNA metabolism, *Prog Nucleic Acid Res Mol Biol*. (2003);73:221-50. Review.

Deo RC, Bonanno JB, Sonenberg N, Burley SK., Recognition of polyadenylate RNA by the poly(A)-binding protein., *Cell*. (1999) Sep 17;98(6):835-45.

Gietz, R.D., Willems, A.R., Woods, R.A., Studies on the transformation of intact yeast cells by the LiAc/SS-DNA/PEG procedure, *Yeast*, (1995), Vol. 11;355-360.

Gonzalez, C., Ruiz-Echevarria, M.J., Vasudevan, S., Henry, M.F., Peltz, S.W., The yeast hnRNP-like protein HRP1/Nab4 marks a transcript for nonsense-mediated mRNA decay, *Mol Cell*, (2000);Vol. 5, 489-499

Gross T, Siepmann A, Sturm D, Windgassen M, Scarcelli JJ, Seedorf M, Cole CN, Krebber H, The DEAD-box RNA helicase Dbp5 functions in translation termination., *Science*; 646-9; 2007-02-02

Grousl T, Ivanov P, Frýdlová I, Vasicová P, Janda F, Vojtová J, Malínská K, Malcová I, Nováková L, Janosková D, Valásek L, Hasek J., Robust heat shock induces eIF2 α -phosphorylation-independent assembly of stress granules containing eIF3 and 40S ribosomal subunits in budding yeast, *Saccharomyces cerevisiae*., *J Cell Sci*. (2009) Jun 15;122(Pt 12):2078-88.

He, F., A. H. Brown, and A. Jacobson, UPF1p, Nmd2p, and UPF3p are interacting components of the yeast nonsense-mediated mRNA decay pathway. *Mol. Cell. Biol.* . (1997);17:1580-1594.

- Hinnebusch AG., Molecular mechanism of scanning and start codon selection in eukaryotes., *Microbiol Mol Biol Rev.* (2011) Sep;75(3):434-67
- Hirokawa G, Nijman RM, Raj VS, Kaji H, Igarashi K, Kaji A, The role of ribosome recycling factor in dissociation of 70S ribosomes into subunits, *RNA*, (2005) Aug; 11(8):1317-28.
- Hirokawa G, Demeshkina N, Iwakura N, Kaji H, Kaji A, The ribosome-recycling step: consensus or controversy?, *Trends Biochem Sci.* (2006) Mar; 31(3):143-9.
- Huh, W. K. *et al.* Global analysis of protein localization in budding yeast *Nature* (2003), 425, 686–691
- Jackson RJ, Hellen CU, Pestova TV, Termination and post-termination events in eukaryotic translation., *Adv Protein Chem Struct Biol.* (2012); 86():45-93.
- Keeling KM, Bedwell DM., Suppression of nonsense mutations as a therapeutic approach to treat genetic diseases., *Wiley Interdiscip Rev RNA.* (2011) Nov-Dec;2(6):837-52.
- Kessler SH, Sachs AB, RNA recognition motif 2 of yeast Pab1p is required for its functional interaction with eukaryotic translation initiation factor 4G. *Mol Cell Biol* (1998);18(1):51-7
- Klann, E & Dever, TE, Biochemical mechanisms for translational regulation in synaptic plasticity, *Nature Reviews Neuroscience* 5, 931-942 December (2004)
- Krogan NJ, Cagney G, Yu H, Zhong G, Guo X, Ignatchenko A, Li J, Pu S, Datta N, Tikuisis AP, Punna T, Peregrin-Alvarez JM, Shales M, Zhang X, Davey M, Robinson MD, Paccanaro A, Bray JE, Sheung A, Beattie B, Richards DP, Canadien V, Lalev A, Mena F, Wong P, Starostine A, Canete MM, Vlasblom J, Wu S, Orsi C, Collins SR, Chandran S, Haw R, Rilstone JJ, Gandi K, Thompson NJ, Musso G, St Onge P, Ghanny S, Lam MH, Butland G, Altaf-Ul AM, Kanaya S, Shilatifard A, O'Shea E, Weissman JS, Ingles CJ, Hughes TR, Parkinson J, Gerstein M, Wodak SJ, Emili A, Greenblatt JF, Global landscape of protein complexes in the yeast *Saccharomyces cerevisiae*., *Nature* Mar. 30, (2006); 440(7084):637-43
- Laue, T.M., Shah, B.D., Ridgeway, T.M., and Pelletier, S.L., Computer-aided interpretation of analytical sedimentation data for proteins., In *Analytical ultracentrifugation in biochemistry and polymer science* (eds. S.E. Harding et al.) pp. 90–125. The Royal Society of Chemistry, Cambridge, UK., (1992)
- Lee D, Ohn T, Chiang YC, Quigley G, Yao G, Liu Y, Denis CL., PUF3 acceleration of deadenylation in vivo can operate independently of CCR4 activity, possibly involving effects on the PAB1-mRNP structure., *J Mol Biol.* (2010) Jun 18;399(4):562-75.

- Leeds P, et al., The product of the yeast UPF1 gene is required for rapid turnover of mRNAs containing a premature translational termination codon. *Genes Dev* (1991);5(12A):2303-14
- MacGregor IK, Anderson AL, Laue TM., Fluorescence detection for the XLI analytical ultracentrifuge., *Biophys Chem.* (2004) Mar 1;108(1-3):165-85.
- Meaux S, van Hoof A, Baker KE., Nonsense-mediated mRNA decay in yeast does not require PAB1 or a poly(A) tail., *Mol Cell.* (2008) Jan 18;29(1):134-40.
- Minvielle-Sebastia L, Preker P J, Wiederkehr T, Strahm Y, Keller W., The major yeast poly(A)-binding protein is associated with cleavage factor IA and functions in premessenger RNA 3'-end formation., *Proc Natl Acad Sci USA.* (1997);94:7897-7902.
- Mitchell SF, Jain S, She M, Parker R., Global analysis of yeast mRNPs., *Nat Struct Mol Biol.* (2013) Jan;20(1):127-33.
- Muhrad D, Decker CJ, Parker R., Deadenylation of the unstable mRNA encoded by the yeast MFA2 gene leads to decapping followed by 5'-->3' digestion of the transcript, *Genes Dev.* (1994) Apr 1;8(7):855-66.
- Mullin C, Duning K, Barnekow A, Richter D, Kremerskothen J, Mohr E., Interaction of rat poly(A)-binding protein with poly(A)- and non-poly(A) sequences is preferentially mediated by RNA recognition motifs 3+4., *FEBS Lett.* (2004) Oct 22;576(3):437-41.
- Namy O, Galopier A, Martini C, Matsufuji S, Fabret C, Rousset JP., Epigenetic control of polyamines by the prion [PSI+]., *Nat Cell Biol.* (2008) Sep;10(9):1069-75.
- Parker R, Sheth U., P bodies and the control of mRNA translation and degradation., *Mol Cell.* (2007) Mar 9;25(5):635-46.
- Pisarev AV, Unbehaun A, Hellen CU, Pestova TV., Assembly and analysis of eukaryotic translation initiation complexes., *Methods Enzymol.* (2007a);430:147-77.
- Pisarev AV, Hellen CU, Pestova TV., Recycling of eukaryotic posttermination ribosomal complexes, *Cell.* (2007b) Oct 19;131(2):286-99.
- Pisarev AV, Skabkin MA, Pisareva VP, Skabkina OV, Rakotondrafara AM, Hentze MW, Hellen CU, Pestova TV, The role of ABCE1 in eukaryotic posttermination ribosomal recycling, *Mol Cell,* (2010) Jan 29; 37(2):196-210.
- Rabl J, Leibundgut M, Ataide SF, Haag A, Ban N., Crystal structure of the eukaryotic 40S ribosomal subunit in complex with initiation factor 1., *Science.* (2011) Feb 11;331(6018):730-6.

Richardson R, Denis CL, Zhang C, Nielsen ME, Chiang YC, Kierkegaard M, Wang X, Lee DJ, Andersen JS, Yao G., Mass spectrometric identification of proteins that interact through specific domains of the poly(A) binding protein., *Mol Genet Genomics*. (2012) Sep;287(9):711-30.

Schuck, P, Size distribution analysis of macromolecules by sedimentation velocity ultracentrifugation and Lamm equation modeling. *Biophysical Journal* 78:1606-1619 (2000)

Schuck, P., Perugini, M.S., Gonzales, N.R., Howlett, G.J., and Schubert, D., Size-distribution analysis of proteins by analytical ultracentrifugation: strategies and application to model systems, *Biophysical Journal* 82:1096-1111 (2002)

Sheth U, Parker R, Decapping and Decay of Messenger RNA Occur in Cytoplasmic Processing Bodies, *Science*. (2003) May 2;300(5620):805-8.

Sheth, U., Parker, R., Targeting of aberrant mRNAs to cytoplasmic processing bodies, *Cell* 125:1095-1109, (2006).

Shoemaker CJ, Green R., Kinetic analysis reveals the ordered coupling of translation termination and ribosome recycling in yeast, *Proc Natl Acad Sci U S A*. (2011) Dec 20;108(51):E1392-8

Simón E, Séraphin B., A specific role for the C-terminal region of the Poly(A)-binding protein in mRNA decay., *Nucleic Acids Res*. 2007;35(18):6017-28.

Sladic RT, Lagnado CA, Bagley CJ, Goodall GJ., Human PABP binds AU-rich RNA via RNA-binding domains 3 and 4., *Eur J Biochem*. (2004) Jan;271(2):450-7.

Spirin AS., How does a scanning ribosomal particle move along the 5'-untranslated region of eukaryotic mRNA? Brownian Ratchet model., *Biochemistry*. (2009) Nov 17;48(45):10688-92.

Stansfield I, Jones KM, Kushnirov VV, Dagkesamanskaya AR, Poznyakovski AI, Paushkin SV, Nierras CR, Cox BS, Ter-Avanesyan MD, Tuite MF, The products of the SUP45 (eRF1) and SUP35 genes interact to mediate translation termination in *Saccharomyces cerevisiae*., *EMBO J*. Sep. 01, 1995; 14(17):4365-73

Taylor D, Unbehaun A, Li W, Das S, Lei J, Liao HY, Grassucci RA, Pestova TV, Frank J., Cryo-EM structure of the mammalian eukaryotic release factor eRF1-eRF3-associated termination complex., *Proc Natl Acad Sci U S A*. (2012) Nov 6;109(45):18413-8.

Tucker M, Valencia-Sanchez MA, Staples RR, Chen J, Denis CL, Parker R., The transcription factor associated Ccr4 and Caf1 proteins are components of the major cytoplasmic mRNA deadenylase in *Saccharomyces cerevisiae*., *Cell*. 2001 Feb 9;104(3):377-86.

Urakov VN, Valouev IA, Lewitin EI, Paushkin SV, Kosorukov VS, Kushnirov VV, Smirnov VN, Ter-Avanesyan MD, Itt1p, a novel protein inhibiting translation termination in *Saccharomyces cerevisiae*., *BMC Mol. Biol.*; 9; (2001)-09-26

Viswanathan P, Chen J, Chiang YC, Denis CL., Identification of multiple RNA features that influence CCR4 deadenylation activity., *J Biol Chem.* 2003 Apr 25;278(17):14949-55. Epub 2003 Feb 17.

Wang X, Zhang C, Chiang YC, Toomey S, Power MP, Granoff ME, Richardson R, Xi W, Lee DJ, Chase S, Laue TM, Denis CL, Use of the novel technique of analytical ultracentrifugation with fluorescence detection system identifies a 77S monosomal translation complex, *Protein Sci.* (2012) Sep;21(9):1253-68.

Wells SE, Hillner PE, Vale RD, Sachs AB., Circularization of mRNA by eukaryotic translation initiation factors., *Mol Cell.* (1998) Jul;2(1):135-40.

Weng, Y, Czaplinski, K, and Peltz, SW, Identification and characterization of mutations in the UPF1 gene that affect nonsense suppression and the formation of the Upf protein complex but not mRNA turnover, *Mol Cell Biol.*, (1996) Oct;16(10):5491-506

Wyers F, Minet M, Dufour ME, Vo LT, Lacroute F., Deletion of the PAT1 gene affects translation initiation and suppresses a PAB1 gene deletion in yeast., *Mol Cell Biol.* (2000) May;20(10):3538-49.

Yao G, Chiang YC, Zhang C, Lee DJ, Laue TM, Denis CL., PAB1 self-association precludes its binding to poly(A), thereby accelerating CCR4 deadenylation in vivo., *Mol Cell Biol.* (2007) Sep;27(17):6243-53.

Zhang, S., M. J. Ruiz-Echevarria, Y. Quan, and S. W. Peltz, Identification and characterization of a sequence motif involved in nonsense-mediated mRNA decay. *Mol. Cell. Biol.* (1995);15:2231-2244.

Zhang C, Lee DJ, Chiang YC, Richardson R, Park S, Wang X, Laue TM, Denis CL., The RRM1 domain of the poly(A)-binding protein from *Saccharomyces cerevisiae* is critical to control of mRNA deadenylation., *Mol. Genet. Genomics.* (2013) Jun 21. [Epub ahead of print]

Zhouravleva G, Frolova L, Legoff X, Leguellec R, Ingevechtomov S, Kisselev L, Philippe M, Termination of translation in eukaryotes is governed by 2 interacting polypeptide-chain release factors, eRF1 and eRF3., *EMBO J* 14:4065– 4072 (1995)

APPENDIX I

Mass spectrometric identification of proteins that interact through specific domains of the poly(A) binding protein

Roy Richardson · Clyde L. Denis · Chongxu Zhang ·
Maria E. O. Nielsen · Yueh-Chin Chiang · Morten Kierkegaard ·
Xin Wang · Darren J. Lee · Jens S. Andersen · Gang Yao

Received: 20 June 2011 / Accepted: 10 July 2012 / Published online: 27 July 2012
© Springer-Verlag 2012

Abstract Poly(A) binding protein (PAB1) is involved in a number of RNA metabolic functions in eukaryotic cells and correspondingly is suggested to associate with a number of proteins. We have used mass spectrometric analysis to identify 55 non-ribosomal proteins that specifically interact with PAB1 from *Saccharomyces cerevisiae*. Because many of these factors may associate only indirectly with PAB1 by being components of the PAB1-mRNP structure, we additionally conducted mass spectrometric analyses on seven metabolically defined PAB1 deletion derivatives to delimit the interactions between these proteins and PAB1. These latter analyses identified 13 proteins whose associations with PAB1 were reduced by deleting one or another of PAB1's defined domains. Included in this list of 13 proteins were the translation initiation factors eIF4G1 and eIF4G2, translation termination factor eRF3, and PBP2, all of whose previously known direct interactions with specific PAB1 domains were either confirmed, delimited, or extended. The remaining nine proteins that interacted through a specific PAB1 domain were CBF5, SLF1, UPF1, CBC1, SSD1, NOP77,

yGR250c, NAB6, and GBP2. In further study, UPF1, involved in nonsense-mediated decay, was confirmed to interact with PAB1 through the RRM1 domain. We additionally established that while the RRM1 domain of PAB1 was required for UPF1-induced acceleration of deadenylation during nonsense-mediated decay, it was not required for the more critical step of acceleration of mRNA decapping. These results begin to identify the proteins most likely to interact with PAB1 and the domains of PAB1 through which these contacts are made.

Keywords PAB1 · Proteome · UPF1 · Nonsense-mediated decay · Protein domain interactions

Introduction

The poly(A) binding protein (PAB1 from *Saccharomyces cerevisiae* and PABPC from humans) binds the poly(A) tail of mRNA and functions at a number of steps involving RNA metabolism (Kuhn and Wahle 2004; Mangus et al. 2003). mRNA polyadenylation, export, translation, and turnover have all been shown to be affected by PAB1 (Kuhn and Wahle 2004; Mangus et al. 2003; Hosoda et al. 2006). The fact that PAB1 plays a number of roles in both the nucleus and the cytoplasm indicates that it may be in contact with multiple proteins and complexes and that these interactions may dictate its functions. Most importantly, PAB1 protein interactions may be continually changing as it regulates RNA metabolism in the cell.

Several whole organism proteomic analyses have been conducted to identify all the protein complexes within a yeast cell or involved in a given process (Gavin et al. 2002; Ho et al. 2002; Krogan et al. 2004; Staub et al. 2006). A summary of mass spectrometric analyses involving purified

Communicated by T. Ito.

R. Richardson and C. L. Denis contributed equally to this manuscript.

R. Richardson · C. L. Denis (✉) · C. Zhang · Y.-C. Chiang ·
X. Wang · D. J. Lee · G. Yao
Department of Molecular, Cellular, and Biomedical Sciences,
Rudman Hall, University of New Hampshire, Durham,
NH 03824, USA
e-mail: cldenis@unh.edu

M. E. O. Nielsen · M. Kierkegaard · J. S. Andersen
Department of Biochemistry and Molecular Biology,
University of Southern Denmark, Campusvej 55, Odense M,
DK 5230, Denmark

TAP-tagged proteins has identified 41 significant non-ribosomal protein interactions with PAB1 (Collins et al. 2007), and other studies have demonstrated additional putative PAB1 protein targets (SGD database). Yet, for the most part, the significance of these interactions has not been defined, nor has the domains of PAB1 important for these contacts been determined.

The PAB1 protein consists of six readily defined functional regions (Fig. 1). At its N-terminus are four RNA binding motifs (RRM domains). While RRM1 and RRM2 of PAB1 appear to bind most strongly to poly(A) (Kessler and Sachs 1998; Deardorff and Sachs 1997), RRM3 and RRM4 can also make critical contacts (Kessler and Sachs 1998; Deardorff and Sachs 1997; Deo et al. 1999) and may bind U-rich regions located adjacent to the poly(A) tail (Mullin et al. 2004; Sladic et al. 2004). Its C-terminal region comprises a penultimate proline-rich (P) domain and a terminal structured region (C), neither of which is critical for RNA binding (Kessler and Sachs 1998; Yao et al. 2007). Each RRM domain is comprised of four antiparallel β -strands (the RNA binding surface) that is backed by two α -helices (Deo et al. 1999).

A few of the protein contacts for each of these PAB1 domains have been defined through conventional biochemical analyses. For example, the C region of PAB1 binds the PAN2/3 deadenylase (Siddiqui et al. 2007; Mangus et al. 1998, 2004) that functions in poly(A) trimming. Whether this process takes place solely in the nucleus, upon export, or in the cytoplasm is still not clear (Brown et al. 1996; Brown and Sachs 1998; Kuhn and Wahle 2004). The translation

termination factor eRF3 also contacts the C-terminus (Hosoda et al. 2003), as do other proteins in mammalian systems (Kuhn and Wahle 2004; Mangus et al. 1998, 2004). The P domain is responsible for PAB1 self-association (Yao et al. 2007; Melo et al. 2003; Kuhn and Pieler 1996). RRM2, with the aid of RRM1, contacts eIF4G (Tarun and Sachs 1996), important in forming the closed-loop structure of mRNA (Kuhn and Wahle 2004). Some of the key residues for this interaction in RRM2 are 180–182 and 184–187, whose alterations in vitro block PAB1-eIF4G contacts and translation (Otero et al. 1999). The RRM1 and the P domain are most important to PAB1 for deadenylation by the major deadenylase CCR4-NOT (Yao et al. 2007; Lee et al. 2010). The RRM1 domain but not the P domain was also found to be most critical for PUF3-induced deadenylation (Lee et al. 2010). Both of these regions of PAB1 were also shown to be critical for PAB1 self-association (Yao et al. 2007). In contrast, deleting the RRM3 domain accelerated deadenylation by some unknown mechanism (Yao et al. 2007). Also, deletion of RRM4, but not other domains, has been shown to reduce mRNA transport to the cytoplasm (K. Weis, personal communication) (Brune et al. 2005; Simon and Seraphin 2007). Finally, in vivo protein synthesis analysis indicates that RRM1 and RRM2 are more critical to this process (Yao et al. 2007; Ohn et al. 2007) with the other domains having no or limited effect on in vivo translation (see Table 1 for a summary of known PAB1 domain contacts).

To expand on previous studies that used mass spectrometric techniques to detect proteins interacting with PAB1, we have included two control mass spectrometric

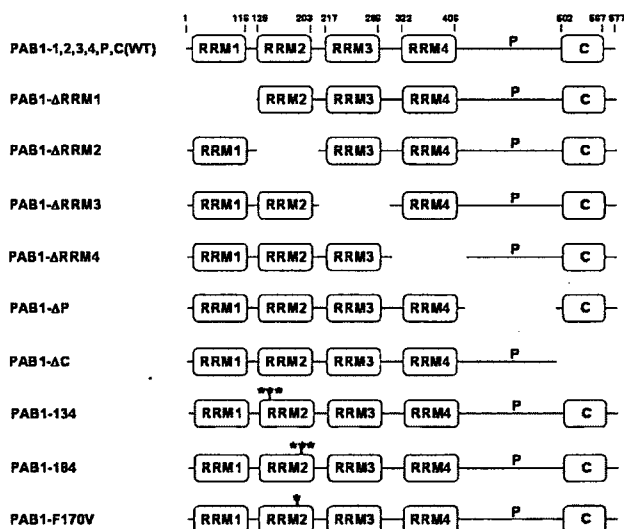


Fig. 1 PAB1 constructs as discussed in the manuscript. Residues for each domain are indicated at the top. PAB1-184 has residues 184DAL186 replaced with EKM, PAB1-180 has residues 180KE181 with ER (not shown in the figure), and PAB1-134 has 134HPD136 replaced with DKS (Otero et al. 1999)

Table 1 Summary of the proteins identified by MS as linked to specific PAB1 domains

PAB1 domain	Known role	Previous protein contact	Our MS identified PAB1 contacts
RRM1	Translation, deadenylation	eIF4G1, eIF4G2, PAB1	eIF4G1, eIF4G2, UPF1, GBP2, NAB6, SLF1, NOP77
RRM2	Translation, CCR4-NOT complex stability	eIF4G1, eIF4G2	eIF4G1, eIF4G2
RRM3	Deadenylation		SSD1
RRM4	mRNA export		CBC1
P	Deadenylation	PAB1, PBP1, PBP2	eRF3, CBC1, yGR250c
C	Translation termination, deadenylation	eRF3, PBP1, PBP2, PAN3	eRF3, PBP2

Summary of known roles of PAB1 domains, previous known contacts, and proteins we identified as co-purifying with specific PAB1 domains

experiments in our studies so as to eliminate many non-specific interactions that might have been detected. We also incorporated the analyses of PAB1 deletion derivatives to identify possible PAB1-specific domain interactions. We identified 55 proteins that associated with PAB1, the vast majority of which would be expected to be in the presence of PAB1 and mRNA due to their known roles in RNA metabolism. Using PAB1 deletion derivatives, we delimited this group of 55 proteins to 13 proteins that interacted with PAB1 dependent on one specific PAB1 domain or another. Four of the six previous known specific PAB1 domain interactors were found in this group of 13 proteins, confirming the validity of this approach. We extended this analysis by verifying that UPF1 did interact with PAB1 through the RRM1 domain. The RRM1 domain, in turn, while important for UPF1-induced deadenylation in nonsense-mediated decay (NMD), was not required for the more critical decapping step in NMD.

Materials and methods

Yeast strains and growth conditions

The parental yeast strain AS319/YC504 (*MAT α ura3 leu2 trp1 his3 pab1::HIS3 (YC504-Flag-PAB1-TRP1)*) was generally used for Flag pull-downs and mass spectrometric analyses. Different PAB1 variants, as indicated in Fig. 1 and the text, were swapped into this strain using standard genetic methods (Yao et al. 2007). The strain carrying the *cdc33-1* allele (AS1881/YC504) was isogenic to this strain. For one series of mass spectrometric analyses with the seven different deletion derivatives of PAB1, strain 1773-10 was used whose genotype was the same as AS319/YC504 and is 75 % congenic with AS319/YC504. For the control experiments AS319/YC360 was used (isogenic to strain AS319/YC504 except for carrying plasmid *YC360-PAB1-URA3* instead of plasmid *YC504*) (Yao et al. 2007). For the UPF1-PAB1 protein analysis, strain AS319/YC504 (PAB1-wt) or YC505 (PAB1- Δ RRM1) was transformed with plasmid pRS315 (*HA-UPF1-LEU2*) or pRP910 (*UPF1-LEU2*). Deadenylation assays were conducted in the *UPF1* background with strains AS319/YC504 and AS319/YC505 each transformed with plasmid pRP469 (*PGK1pG URA3*) or pRP1078 (*PGK1pG-319 URA3*) and in the *upf1* Δ background with strains RR27-1 (*Mata ura3 leu2 trp1 his3 pab1::his3::Neo upf1 Δ ::HIS3*) carrying the YC504, YC505, and *PGK1* plasmids as described for AS319.

Yeast strains were routinely grown on minimal medium supplemented with 2 % glucose and the appropriate amino acids (Yao et al. 2007). For the RNA pulse-chase experiments, the initial growth of cells was in medium containing 2 % sucrose.

Mass spectrometric analysis

Flag immunoprecipitated extracts were fractionated by SDS-PAGE prior to trypsin digestion of gel slices across the gel lane as described (Kristensen et al. 2008). Tandem mass spectrometry (LC MS/MS) was used for peptide and protein identification as previously described (Andersen et al. 2002; Gruhler et al. 2005).

Protein immunoprecipitations

Flag pull-down experiments conducted either for Western analysis or for mass spectrometric analysis were conducted as previously described (Liu et al. 1998; Yao et al. 2007). RNase A (0.1 mg/mL) treatment of extracts was conducted for 30 min prior to the treatment of the extracts with Flag beads. For Western analysis, 50 mL cultures were routinely used. For the mass spectrometric studies, 300 mL cultures were used. The HA immunoprecipitations were conducted in a manner similar to that described for the Flag immunoprecipitations.

RNA analysis

Pulse-chase analyses for the *GAL1-PGKpG* mRNA were conducted as previously described (Lee et al. 2010; Tucker et al. 2001; Cao and Parker 2003). Briefly, after growth of cells in non-inducing medium containing 2 % sucrose, the mRNA was induced for 10 min with 2 % galactose and the mRNA expression was shut off with 4 % glucose. At the time points indicated, the RNA was isolated and subjected to Northern analysis following polyacrylamide gel electrophoresis. The oligo(A) lengths were determined using the following standards: the length of the completely deadenylated *PGK1* poly(A) tail (dT sample), the length of the deadenylated *PGK1* fragment, and the length of the completely undeadenylated poly(A) tail at time zero based on other experiments using different *GAL1* poly(A) tail lengths as standards. All pulse-chase experiments were conducted at least in duplicate.

Results

Purification of proteins associating with PAB1 using Flag-PAB1 derivatives

Prior to conducting mass spectrometric studies on PAB1-associated proteins, we assessed whether proteins known to be associated with PAB1 could be co-purified using a PAB1 tagged at its N-terminus with the Flag peptide (Yao et al. 2007). Following purification of Flag-PAB1, both eIF4G1 and eIF4E were found to co-elute with PAB1

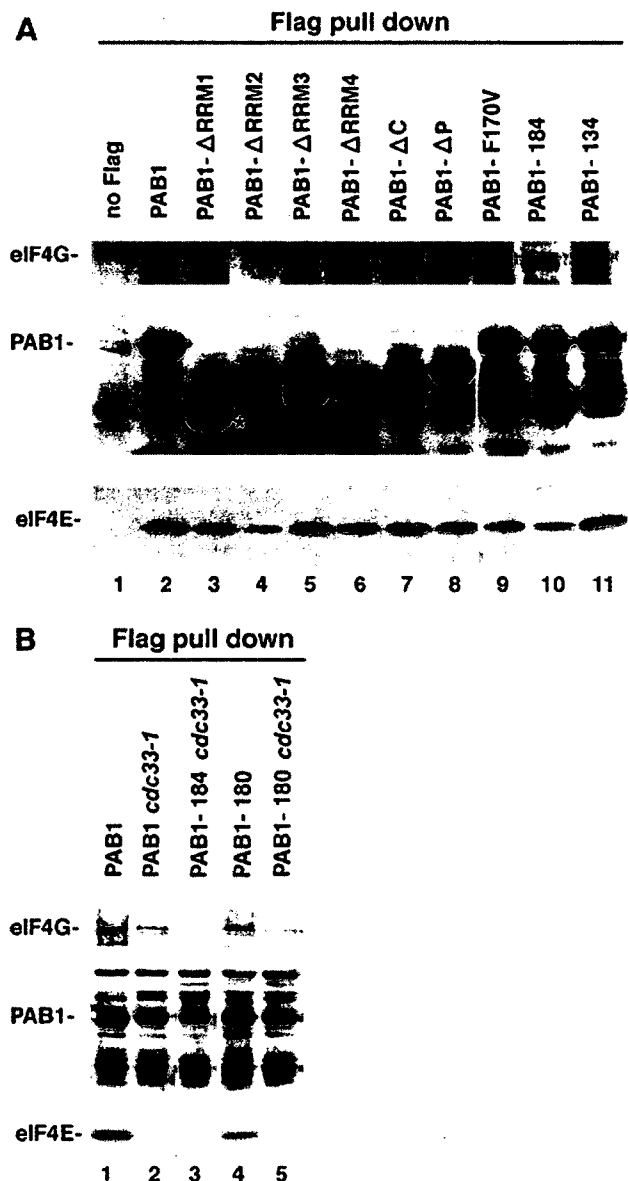


Fig. 2 PAB1 regions involved in binding eIF4G and eIF4E. Cell extracts from strains carrying only the Flag-PAB1 variants as indicated were bound to Flag beads, eluted with Flag peptide, and detected by western analysis using the antibodies as indicated in the figure. eIF4G refers to eIF4G1, as the antibody does not recognize eIF4G2. The asterisk in lane 3, left, refers to the PAB1- Δ RRM1 protein band. The major band above it is a non-specific species that binds to the Flag antibody. **a** All strains carried either a Flag-PAB1 derivative as indicated (lanes 2–11) or PAB1 alone (lane 1). **b** Flag-PAB1 derivatives were expressed in strains carrying either wild-type CDC33 (lanes 1 and 4) or *cdc33-1* (lanes 2, 3, and 5)

(Fig. 2a, lane 2). Removal of RRM2 from PAB1 diminished eIF4G1 co-elution and reduced eIF4E association (Fig. 2a, lane 4), as previously demonstrated using in vitro binding assays (Kessler and Sachs 1998). In addition, we showed that the PAB1-184 protein, carrying mutations in

amino acids 184–186 of RRM2 that fails to bind eIF4G in vitro (Otero et al. 1999), resulted in reduced eIF4G1 binding to PAB1 but did not eliminate it (Fig. 2a, lane 10). Similar results, albeit not as dramatic as observed for PAB1-184, were obtained for PAB1-180, which mutated residues 180,181 (Otero et al. 1999) (Fig. 2b, lane 4). In contrast, other point mutations in PAB1 such as PAB1-134 that affects an unknown translation process of PAB1 (Otero et al. 1999; Ohn et al. 2007) and PAB1-F170V that affects PAB1 binding to poly(A) (Deardorff and Sachs 1997; Yao et al. 2007) did not have any effect on eIF4E or eIF4G1 binding (Fig. 2a, lanes 11 and 9, respectively). These results indicate that our purifications of Flag-PAB1 are capable of recapitulating PAB1-specific interactions that have been studied previously. However, our analysis of interactions present in crude extracts between PAB1 and eIF4G1 was found to be more robust than those observed in vitro, suggesting that in vivo the contact between PAB1 and eIF4G1 is not stabilized by a simple single interaction.

Isolation of Flag-PAB1 from a strain carrying the *cdc33-1* allele (encoding an eIF4E protein that is defective for cap binding at 37 °C but that is stably expressed) (Altmann et al. 1989), reduced both the eIF4E and eIF4G1 association with PAB1 (Fig. 2b, lane 2). Combining *cdc33-1* with either PAB1-184 or PAB1-180 (Fig. 2b, lanes 3 or 4) severely interfered with eIF4G1 and eIF4E binding to PAB1. It should be mentioned that eIF4A was not found to be present in our Flag-PAB1 immunoprecipitations as assessed by Western analysis (not shown). This result is expected, as eIF4A from yeast is known to be transiently associated with the eIF4F complex that contains eIF4G and eIF4E (Neff and Sachs 1999; Von der Haar and McCarthy 2002; Pause et al. 1994; Yoder-Hill et al. 1993).

Rationale for using mass spectrometric analysis to identify PAB1-mRNP protein contacts to specific PAB1 domains

Our rationale for identifying the most likely bona fide protein contacts either with PAB1 or within the context of the PAB1-mRNP structure was as follows. While a number of proteins are known to associate with PAB1 through previous mass spectrometric experiments (Gavin et al. 2002; Ho et al. 2002), the specificity of proteins interacting with PAB1 or its domains could not be determined. We sought to significantly bypass this limitation by delimiting contacts to specific domains of PAB1, thereby identifying the specificity of these interactions suggestive of their directness. This analysis would begin to approximate the bona fide PAB1 proteome. The identification of specific domains of PAB1 used in these contacts also would allow internal verification of the validity of the approach since a few proteins have been shown to bind to specific PAB1 domains (Table 1).

Two types of control experiments (done at least in duplicate) were conducted to eliminate contaminating proteins from the list of proteins interacting with PAB1. The first was to conduct mass spectrometric analysis on Flag bead purified material from a strain with PAB1 without the Flag tag. The second was to conduct mass spectrometric analysis on Flag bead purified material extracted from strains carrying the Flag-PAB1 following an extensive RNase A treatment. RNase A treatment eliminates PAB1 binding to the poly(A) tail, allowing us to identify only those proteins that associated with PAB1 within the context of the PAB1-mRNP structure (Yao et al. 2007). Each control experiment was conducted with strains carrying either wild-type PAB1 (without the Flag tag) or with Flag-PAB1 (RNase A treatment) and compared with Flag-PAB1 (no RNase A treatment). The number of unique peptides detected for each protein present following the Flag pull down experiment rather than the number of total peptides detected was compared between these samples. Significant bias can be introduced with the counting of the total peptides due to the fact that certain peptides are more readily detected by mass spectrometric analysis than other peptides (Fleischer et al. 2006). Proteins that were not present in the control samples and which were present in the arbitrary cut-off of greater than 40 % of the experimental samples with Flag-PAB1 were considered to be likely PAB1-associated proteins. Table 2 lists these 44 proteins, the average number of unique peptides observed in each case, their protein abundance factor (PAF), and the most likely function related to PAB1. A PAF value represents the average number of unique peptides observed divided by the molecular weight of the protein ($10 \times$ kDa). The PAF value normalizes the number of unique peptides to the size of the protein, which, in turn, is proportional to the number of possible tryptic peptides that could be observed in the experiment (Fleischer et al. 2006). An additional nine proteins interacted with PAB1 in 40 % or less of the mass spectrometric experiments (Table 3). However, the PAF score for these proteins was uniformly at the lower end when compared with the list presented in Table 2, supporting our limiting the most likely PAB1 interacting proteins to those in Table 2.

Comparison of our identified PAB1 interactors with known PAB1 protein contacts

We judged that our analysis was detecting and identifying specific PAB1-mRNP contacts by three means. First, the summary of two different TAP mass spec analyses of the yeast proteome (Collins et al. 2007; Ho et al. 2002; Gavin et al. 2002) have identified 41 significant non-ribosomal protein contacts to PAB1. Of the top 12 proteins on this list, we identified 8 of these (eIF4G1, eIF4G2, CBC1, NAB6, NAB3, SGN1, GBP2, and CBF5).

Second, the direct interactions of PAB1 with other proteins have been studied by other biochemical procedures. Translation initiation factors eIF4G1 and eIF4G2 are known to contact PAB1 through its domains RRM1 and RRM2 (Tarun and Sachs 1996; Otero et al. 1999), eRF3, involved in translation termination, is known to contact PAB1 through its C domain (Gorgoni and Gray 2004), and PBP2 is known to contact PAB1 through either the P or C domain (Mangus et al. 1998). All four of these proteins were found in our group of 44 proteins associating with the PAB1-mRNP structure.

Third, our list of 44 proteins contains 38 proteins that would be expected to associate with the PAB1-mRNP complex. There are nine proteins involved in translation, three in mRNA decay, seven in RNA binding, three in mRNA transport, one in splicing, and another fifteen proteins in nucleolar and/or ribosomal biogenesis, all processes known to include PAB1 (Table 2) (Peng et al. 2003; Brune et al. 2005; Yao et al. 2007). Only six other proteins were identified that play no obvious roles related to that of PAB1.

Identification of proteins that interacted with specific PAB1 domains

Because the above list of 44 possible and known PAB1-associated proteins may contain proteins that are part of the PAB1-mRNP structure but are not dependent on binding PAB1 through any of its domains, we wished to further delimit this group by identifying those proteins that interacted through a specific PAB1 domain. To identify specific protein contacts to different domains of PAB1, mass spectrometric analysis was conducted on all the proteins that co-purified with each of seven Flag-PAB1 derivatives (PAB1, Δ RRM1, Δ RRM2, Δ RRM3, Δ RRM4, Δ P, Δ C; see Fig. 1). Each strain carried only the Flag-PAB1 derivative as indicated, for the genomic *PAB1* gene that had been deleted (Yao et al. 2007). Prior to mass spectrometric analysis, the resultant immunoprecipitations were shown to contain equivalent amounts of each PAB1 derivative as detected by Western analysis (data not shown). Each of these derivatives have been extensively characterized for effects on poly(A) binding, mRNA export, translation, deadenylation, and decapping (unpublished observation) (Yao et al. 2007; Brune et al. 2005; Dunn et al. 2005; Kessler and Sachs 1998; Simon and Seraphin 2007), and they do not result in severe growth defects. All PAB1 derivatives were assayed for general effects on in vivo protein synthesis (Yao et al. 2007; Ohn et al. 2007) and for effects on ribosomal and polysomal abundance. No specific effects on 80S ribosomal and polysomal abundance were observed with any of the PAB1 deletions (data not shown). In terms of global protein

Table 2 Proteins that associated with wild-type PAB1

Protein	Mol. wt. (kDa)	Unique peptides (Avg.)	PAF score	Function related to PAB1
UTP20	288	13	0.45	Nucleolar
URB1	204	2.6	0.13	Nucleolar
RRP5	194	50	2.6	Nucleolar
RPA190	188	10	0.53	Transcription
RLR1	185	15	0.81	THO complex
XRN1	176	40	2.3	mRNA degradation
SKI3	165	8.6	0.52	mRNA degradation
yLR419w	164	10	0.61	RNA helicase
RSE1	155	3.2	0.21	Splicing
CLU1	145	9.8	0.68	Translation initiation
SSD1	140	19	1.4	RNA binding
NAB6	127	11	0.87	RNA binding
YEF3	117	6.0	0.51	Translation
RRP12	114	13	1.1	Nucleolar
UPF1	110	14	1.3	mRNA degradation
eIF4G1	107	31	2.9	Translation initiation
MIS1	107	12	1.1	Mitochondrial
eIF4G2	104	13	1.2	Translation initiation
UBP3	102	3.0	0.29	Nucleolar
CBC1	99.7	14	1.4	RNA binding
NAB3	90.5	2.6	0.29	RNA binding
yGR250c	89.7	7.0	0.78	Translation
ENP2	82.0	2.1	0.26	Nucleolar
NOP77	78.1	7.0	0.90	Nucleolar
eRF3	76.9	12	1.5	Translation
yGR054w	71.8	5.6	0.78	Translation initiation
yIL055c	70.8	4.0	0.56	Unknown
KRI1	68.6	3.6	0.52	Nucleolar
AEP2	68.1	7.4	1.1	Mitochondrial
NUG1	57.8	3.8	0.68	Nucleolar
CBF5	55.2	8.4	1.5	Nucleolar
SLF1	50.9	5.0	0.98	Translation
HRB1	49.3	4.0	0.81	mRNA export
GBP2	49.0	8.4	1.7	mRNA export
PUB1	48.0	4.6	0.96	RNA binding
TMA46	46.3	3.2	0.69	Translation
PBP2	45.6	5.7	1.2	RNA binding
KRR1	37.4	3.8	1.0	Nucleolar
RLP7	36.7	2.7	0.74	Nucleolar
BRX1	33.7	2.6	0.77	Nucleolar
LHP1	32.2	5.3	1.6	Nucleolar
SGN1	30.0	4.6	1.5	RNA binding
NOP6	25.2	3.3	0.13	Nucleolar
MNP1	20.6	1.4	0.68	Mitochondrial

Average number of unique peptides identified by mass spectrometric analysis across all wild-type PAB1 pull-downs for proteins not present in the control experiments. Proteins in the list were identified in greater than 40 % of the mass spectrometric experiments (5–7). The PAF score is the average number of unique peptides divided by MW (kDa) \times 10. Protein names in bold were also present in greater than 40 % of the mass spectrometric pull-downs across all PAB1 deletion derivatives (Table 4). Nucleolar refers to proteins that are found in the nucleolus or play a role in rRNA biogenesis

Table 3 Proteins that associated with wild-type PAB1 in 40 % or less of the mass spectrometric experiments

Protein	Mol. wt. (kDa)	Unique peptides (Avg.)	PAF score	Function related to PAB1
RPB1	192	2.4	0.12	Transcription
TOP2	164	4.2	0.090	DNA metabolism
SKI2	147	2.2	0.15	mRNA degradation
RMD11	131	2.8	0.21	Unknown
MAK21	117	2.2	0.19	Nucleolar
PWP1	64	0.8	0.12	Nucleolar
AEP1	60	2.6	0.43	Unknown
PRP4	53	0.6	0.11	Splicing
NSR1	27	0.6	0.22	Nucleolar

Average number of unique peptides identified by mass spectrometric analysis across all wild-type PAB1 pull-downs for proteins not present in the control experiments. Proteins in the list were identified in 40 % or less of the mass spectrometric experiments. Other terms are defined in Table 2. Proteins yER138c, SOV1, and MRD1 were also identified in these mass spectrometric experiments, but since they were not identified in the wild-type pull-downs when the controls were conducted, they are not included in the list

synthesis, deleting either RRM1 or RRM2 had the most general effects: 28 % reduction by Δ RRM1 and 15 % by Δ RRM2, whereas the other deletions had insignificant effects. These effects by RRM1 and RRM2 deletions are, however, not overly severe, for in contrast, the *cdc33-1* (eIF4E) or *prt1-46* (eIF3b) alleles block translation by at least 70 % (Yao et al. 2007; Ohn et al. 2007). The RRM1 and P domains are known to be required for general and regulated deadenylation, and RRM3 restricts the deadenylation process (Yao et al. 2007; Lee et al. 2010; Simon and Seraphin 2007). Deletion of the RRM4 domain, but not other domains, also appears to play some role in mRNA export from the nucleus (Brune et al. 2005; Simon and Seraphin 2007) (see Table 1 for a summary of these previously known interactions).

Following our mass spectrometric analysis done in duplicate for each PAB1 derivative, the number of unique peptides of proteins associated with a particular PAB1 variant was determined. Only those proteins (not present in the control experiments described above) which were found to be associated with at least 1 derivative in both duplicate analyses and which were present in greater than 40 % of the total of 14 PAB1 derivative mass spectrometric analyses were considered as likely PAB1 interacting proteins. This group of 43 proteins overlapped significantly with the proteins identified only in the wild-type PAB1 Flag pull downs described above: 32 were present in both sets (Table 4). The 11 new proteins found to be associated with the majority of PAB1 deletion derivatives included 1 RNA binding protein involved in translation and mRNA degradation (SBP1), 2 proteins in mRNA splicing (RAI1, and SMB1), 3 nucleolar/RNA biogenesis proteins (MAK21, GAR1, and NHP2), 2 mitochondrial mRNA splicing proteins (CBP2 and MSS116), and 3 other proteins

(RMD11, MPD1, and an unknown protein). An additional eight proteins interacted in 40 % or less of the mass spectrometric experiments (Table 5) but were judged less likely to be associated with PAB1, as, again, their PAF scores were extremely low.

Of the 43 proteins that specifically co-immunoprecipitated with the various PAB1 deletion derivatives, the average number of unique peptides found for each PAB1 derivative was compared across the derivatives. Those PAB1-associated proteins that displayed twofold differences in peptide abundance (Table 6), as compared to wild-type PAB1, were initially judged as displaying possible specific contacts to one or another of the PAB1 domains. By this criterion, only 13 proteins were affected in their binding to one or another of the PAB1 domains (Table 6). Of these 13 proteins, we identified several proteins that previous biochemical studies have demonstrated or suggested to make specific contacts to one or another of the PAB1 domains. eIF4G1 and eIF4G2 are known to contact PAB1 through at least the RRM1 and RRM2 domains (Tarun and Sachs 1996; Otero et al. 1999) with RRM2 being most critical, which we have confirmed (Table 6). eRF3, involved in translation termination, is known to contact PAB1 through its C domain (Gorgoni and Gray 2004), an observation we confirmed and extended by indicating that the P region was also important to this contact. Finally, PBP2 is known to contact PAB1 through either the P or C domain (Mangus et al. 1998), and we established that it is the C region and not the P domain that was critical for this interaction. These correspondences and extensions indicated that the methodology we were using was consistent with published biochemical analyses. Importantly, these similarities indicate that the specific domain interactions we were observing for the other nine

Table 4 Proteins that interacted with PAB1 and its deletion derivatives

Protein	Mol. wt. (kDa)	Unique peptides (Avg.)	PAF score	Function related to PAB1
UTP20	288	5.7	0.2	Nucleolar
RRP5	194	41	2.1	Nucleolar
RPA190	188	4.1	0.22	Transcription
RLR1	185	12	0.68	THO complex
XRN1	176	46	2.6	mRNA degradation
SKI3	165	2.9	0.17	mRNA degradation
yLR419w	164	16	0.95	RNA helicase
RSE1	155	3.4	0.22	Splicing
SSD1	140	10	0.75	RNA binding
RRP12	138	5.3	0.38	Nucleolar
RMD11	131	2.4	0.18	Nitrogen regulation
NAB6	127	13	1.0	RNA binding
YEF3	117	1.8	0.15	Translation
MAK21	117	2.3	0.2	Nucleolar
UPF1	110	20	1.8	mRNA degradation
eIF4G1	107	38	3.6	Translation
MIS1	107	3.3	0.31	Mitochondrial
eIF4G2	104	17	1.7	Translation
CBC1	100	12	1.2	RNA binding
NAB3	90	2.1	0.23	RNA binding
yGR250c	90	6.4	0.72	Translation
NOP77	78	8.6	1.1	Nucleolar
eRF3	77	10	1.4	Translation
MSS116	77	3.6	0.48	Mitochondrial
CBP2	74	1.0	0.14	Mitochondrial splicing
yIL055c	71	5.3	0.75	Unknown
CBF5	55	3.4	0.62	Nucleolar
SLF1	51	4.7	0.93	Translation
GBP2	49	10	2.1	mRNA export
TMA46	46	1.3	0.28	Translation
PBP2	46	9.2	2.0	RNA binding
RAI1	45	1.3	0.29	Splicing
RLP7	37	2.1	0.56	Nucleolar
MPD1	37	1.2	0.33	Chaperone
BRX1	34	1.8	0.53	Nucleolar
SBP1	33	5.8	1.3	Translation

Table 4 continued

Protein	Mol. wt. (kDa)	Unique peptides (Avg.)	PAF score	Function related to PAB1
LHP1	32	5.9	1.8	Nucleolar
SGNI	29	6.4	2.2	RNA binding
NOP6	25	1.6	0.63	Nucleolar
SMB1	22	2.0	0.89	Splicing
GAR1	22	0.72	0.33	Nucleolar
NHP2	19	0.78	0.41	Nucleolar
Unknown	17	2.1	1.1	Unknown

Average number of unique peptides identified by mass spectrometric analysis across all PAB1 deletion derivative pull-downs for proteins not present in the control experiments. Proteins in the list were identified in greater than 40 % of the mass spectrometric experiments. The PAF score is the average number of unique peptides divided by MW (kDa) \times 10. Protein names in bold were also present in greater than 40 % of the mass spectrometric pull-downs across all wild-type PAB1 analyses (Table 2). The Unknown protein has accession number 7537305. Six additional proteins, BRR2, SNF2, PRP19, SOV1, MRD1, and NOP14, were present in greater than 40 % of the PAB1 deletion derivative mass spectrometric analyses but could not be compared to controls, as they were not detected in PAB1 wild-type pull-downs when the control experiments were conducted. These six proteins were, therefore, not included as part of the 43 proteins that are listed in the table

proteins (NAB6, UPF1, SSD1, CBC1, GBP2, CBF5, SLF1, NOP77, and yGR250c) were very likely to be valid. It should be noted that while NOP77 appears to interact through RRM1 of PAB1, there appears sufficient variability in all of its interactions with PAB1 deletion derivatives to place less confidence on this particular identification.

To further assess the importance of the differences we observed in the interactions of certain PAB1 deletion derivatives with the particular proteins listed in Table 6, we analyzed the intensities of specific peptide species that were co-immunoprecipitated with each PAB1 deletion derivative. Intensity refers to the number of times a particular peptide was detected in the mass spectrometric experiment. In this case, if a protein interacted through a particular PAB1 domain, then specific peptides of that protein should be decreased or absent for the mass spectrometric analysis conducted with that PAB1 deletion derivative when compared across all PAB1 deletion derivatives. By analyzing particular peptide species across the mass spectrometric data for the PAB1 deletion derivative pull downs, we would not be creating a bias in terms of the ability of the mass spectrometer to detect a particular peptide species. This analysis was, however, limited to only those peptides for a particular protein that were identified amongst most, if not all, PAB1 deletion analyses. This analysis could not be confidently done for the following proteins because of the low level of unique peptides identified across most PAB1 deletion derivatives: CBC1, CBF5, SLF1, eRF3, NOP77, and yGR250c.

Table 7 lists the intensity averages for the peptides of each protein interacting with specific PAB1 deletion derivatives. For example, of the 14 peptides of eIF4G1 that were identified in this analysis, significant less eIF4G1 peptide intensities were observed in the mass spectrometric studies with PAB1 derivatives deleted for RRM2 or RRM1 when compared to the experiments done with the other deletion derivatives. This result is consistent with the above identification of RRM1 and RRM2 as being important to the PAB1 contact made by eIF4G1 based on the average number of unique peptides identified in the mass spectrometric analysis (Table 6). Similarly, eIF4G2 displayed reduced peptide intensities in the pull-down experiments with the RRM1 and RRM2 deletion derivatives. Significantly, however, eIF4G2 did not display reduced intensities of particular peptides for the P domain deletion of PAB1, although eIF4G2 had a reduction in the average number of unique peptides identified in the P domain deletion derivative as compared to other domains deletions (Table 6). Therefore, the P domain of PAB1 is not likely to be a specific region through which eIF4G2 acts. As controls for these sets of analyses, proteins, such as XRN1, RRP5, RLR1, and yLR419w, which did not display differences in

Table 5 Proteins identified in 40 % or less of the mass spectrometric experiments conducted with the PAB1 deletion derivatives

Protein	Mol. wt. (kDa)	Unique peptides (Avg.)	PAF score	Function related to PAB1
GCN1	298	2.5	0.083	Translation
RPB1	192	0.36	0.018	Transcription
SKI2	147	0.64	0.044	mRNA degradation
RPC82	74	1.2	0.16	Transcription
UTP15	58	0.21	0.036	Nucleolar
RPC34	36	0.28	0.077	Transcription
RPB5	26	0.28	0.11	Transcription
SLX9	25	0.43	0.17	Unknown

The proteins PRP8, POL2, yER138c, TOP2, and RAT1 were detected in several of the mass spectrometric experiments but were not included in the list because they were not detected in the wild-type pull-downs when the control experiments were conducted

Table 6 Average number of unique peptides identified for proteins co-purifying with PAB1

Protein	PAB1-wt	Δ RRM1	Δ RRM2	Δ RRM3	Δ RRM4	Δ P	Δ C
PAB1	66	68	70	66	68	60	70
eIF4G1	50	20	16	46	46	42	42
eIF4G2	25	10	7	24	20	10	24
UPF1	26	8	22	21	22	18	24
CBC1	18	13	17	12	7	2	16
NAB6	14	6	10	12	20	18	17
eRF3	14	8	20	14	8	2	6
PBP2	12	14	10	11	11	7	0
SSD1	10	16	11	4	13	8	10
NOP77	10	5	13	8	6	9	10
GBP2	10	4	6	14	10	12	16
SLF1	8	2	5	4	3	3	8
CBF5	4	4	2	4	0.5	2	4
yGR250c	3	6	13	6	12	0.5	6

Mass spectrometric analysis on proteins co-purifying with individual Flag-PAB1 variants was conducted as described in the text. Only those proteins that are listed in Table 4 were compared. Values refer to the average number of unique peptides detected for each protein for the two series of experiments that were conducted. Values in bold displayed significant differences (at least two-fold differences in values as compared to the wild type)

binding PAB1 deletion derivatives based on comparing unique peptides also showed no differences when the intensities of individual peptides associating with the PAB1 deletion derivatives were compared (see legend for Table 7).

The intensity analyses for the peptides of other proteins interacting with specific domains of PAB1 confirmed that SSD1 interacted through RRM3, GBP2 through RRM1, PBP2 through the C domain, and NAB6 through the RRM1 domain (Table 7). However, for NAB6 the data also indicate that the RRM2 domain may play some role in binding it. Overall, the analysis of the intensity differences for particular peptides supports the assignment of PAB1

domains for being important in interacting with specific proteins based on the number of unique peptides observed in the mass spectrometric analyses (Table 6).

UPF1 interaction with PAB1 requires the RRM1 domain but not the C-terminal region of PAB1

Based on our mass spectrometric studies, we chose to further investigate the putative UPF1 interactions with PAB1, as mammalian studies had indicated that UPF1 controls NMD in an interaction with termination factor eRF3 that, in turn, restricts binding of PABPC1 to eRF3 (Brognia and Wen 2009). Such an interaction suggests that

Table 7 Average of individual peptide intensities for proteins associating with PAB1 deletion derivatives

Protein	PAB1	PAB1- Δ RRM1	PAB1- Δ RRM2	PAB1- Δ RRM3	PAB1- Δ RRM4	PAB1- Δ P	PAB1- Δ C
eIF4G1	100	7.4 (4.7)	3.9 (1.1)	120 (29)	110 (16)	140 (28)	160 (30)
eIF4G2	100	8.6 (4.7)	25 (13)	74 (26)	210 (25)	110 (50)	72 (30)
NAB6	100	3.8 (3.7)	23 (5.2)	62 (9.0)	130 (20)	100 (20)	94 (23)
PBP2	100	300 (160)	150 (31)	130 (9.0)	260 (21)	220 (60)	0 (0)
SSD1	100	110 (45)	53 (20)	22 (3.5)	170 (42)	180 (44)	190 (90)
GBP2	100	0 (0)	42 (13)	81 (28)	65 (19)	120 (18)	94 (24)

Mass spectrometric analysis was conducted as described in Table 6. The intensities for the peptides for each individual protein described in Table 6 were compared across the PAB1 deletion derivatives. Peptides that were represented in all or nearly all Flag-PAB1 deletion derivative pull-downs were considered “good” peptides for cross comparisons of peptide intensities. For several proteins no peptides were found in a particular Flag-PAB1 deletion derivative pull-down, but the peptide was retained in the “good” data set if this absence correlated with the domain that was suggested for interacting with the protein based on the results in Table 6. For eIF4G1, 14 peptides were identified as “good” peptides; for eIF4G2, there were 4 peptides; for NAB6, there were 4 peptides; for PBP2, there were 3 peptides; for SSD1, there were 4 peptides; and for GBP2, there were 3 peptides. One or no “good” peptides were identified for the other proteins listed in Table 6. The relative intensities were normalized to 100 for PAB1, wt, and the value given in the table is the average of these values for all of the peptides for each protein. Standard errors of the mean are given in parentheses where applicable. As additional controls, analysis of average intensities for “good” peptides for several proteins not listed in Table 6 but which were included in Table 4 as not associating with PAB1 through any particular domain demonstrated no differences in intensities across the various PAB1 deletion derivative pull-downs (RLR1, RRP5, yLR419w, and XRN1 were analyzed)

it is the C-terminal domain of mammalian PABPC1 that would be important to UPF1 interactions, in contrast to the RRM1 domain as suggested by our studies for yeast PAB1. To examine UPF1 and PAB1 interactions further, we chose to study them in the reverse direction. By first using an HA-tagged UPF1 protein to purify UPF1 from yeast cells, we then queried whether PAB1 or PAB1- Δ RRM1 could be co-immunoprecipitated. As displayed in Fig. 3, immunoprecipitation of HA-UPF1 was capable of immunoprecipitating Flag-PAB1 but was unable to co-immunoprecipitate Flag-PAB1- Δ RRM1 (compare lane 3–4). These results confirm the mass spectrometric analyses described above. Importantly, the truncated form of PAB1 (PAB1-T) (lane 3), which is missing both the P and C domains of PAB1 (mass spectrometric analysis of PAB1-T indicated that the truncation occurs between residues 496 and 506 of PAB1, unpublished observation), was quite able to interact with HA-UPF1. Therefore, PAB1 requires its RRM1 but not its P or C domain to interact with UPF1.

The RRM1 domain of PAB1 is required for UPF1-dependent NMD deadenylation but not decapping

If the interaction between PAB1 and UPF1 were to be physiologically important, we might expect that the RRM1 domain of PAB1 would play a role in UPF1-mediated NMD. However, a previous study indicated that deletion of PAB1 from yeast does not impair the NMD process (Mieux et al. 2008). As NMD consists of the acceleration of two separable steps in the degradation of mRNA, decapping and deadenylation (Cao and Parker 2003), it remains possible that PAB1 is not required for the major part of NMD (decapping) but plays a role in the secondary process of deadenylation. Previous results have also established that PAB1 deletion

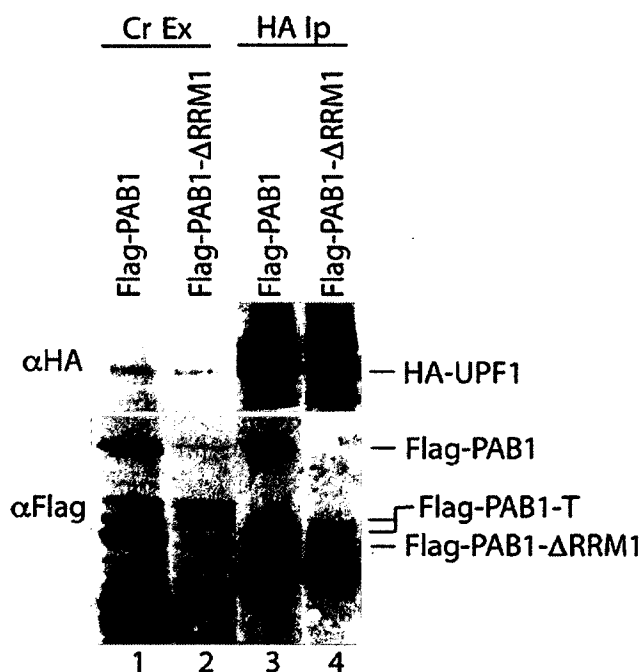


Fig. 3 UPF1 immunoprecipitates PAB1 through the PAB1 RRM1 domain. HA-UPF1 pull-downs were conducted as described in Fig. 2. Flag-PAB1 (lanes 1 and 3) and its RRM1 deletion derivative (lanes 2 and 4) were identified using antibody directed against the Flag peptide and antibody directed against the HA epitope was used to detect HA-UPF1. Lanes 1, 2 crude extracts; lanes 3, 4 HA immunoprecipitations

derivatives have no effect on general decapping (Yao et al. 2007) but that they are critical for deadenylation (Yao et al. 2007; Lee et al. 2010; Simon and Seraphin 2007).

We consequently used pulse-chase analysis to test the effect of deleting the RRM1 domain of PAB1 on nonsense-mediated decay processes. These analyses used *GALI-PGK1* mRNA

that was either wild-type or contained a nonsense mutation in residue 319 that subjects the mRNA to NMD (Cao and Parker 2003). Isogenic yeast strains carrying either Flag-PAB1 or Flag-PAB1- Δ RRM1 with either *GALI-PGK1pG* or *PGK1pG-319* were pregrown in non-galactose inducing medium and then subjected to a brief induction of the *GALI* promoter with the addition of galactose (the pulse), prior to shutting off of gene expression with glucose (the chase). Following extraction of RNA at various times after the shutoff of transcription, northern analysis was utilized to identify the *PGK1* mRNA species present as a function of time. In Fig. 4a, using wild-type PAB1 and wild-type *PGK1pG* mRNA, *PGK1pG* mRNA was deadenylated slowly in a basically distributive manner represented by the bulk of the deadenylated species moving as a relatively tight band in which it became progressively deadenylated. At about 8–12 min the 10 A's oligo(A) species that represents nearly completely deadenylated species began to become abundant and the tightness of the band became reduced, as deadenylation shifted from a primarily distributive to a processive mode (see top densitometric scan). A decapped *PGK1* mRNA fragment that was deadenylated began to be visualized over background around 4–8 min and became quite abundant at later times at 20 min (see densitometric scans), indicative of extensive decapping once the oligo(A) species was formed. These results are very similar to those obtained previously for *PGK1* mRNA (Decker and Parker 1993; Muhrad et al. 1994; Tucker et al. 2001; Cao and Parker 2003). However, it should be noted that in our experiments a small amount of decapped and nearly fully deadenylated fragment is present at the zero time point, although its abundance is very low relative to the abundance of the full-length *PGK1pG* mRNA at the same time.

As expected from previous studies (Cao and Parker 2003), in a wild-type PAB1 background the NMD target mRNA, *PGK1pG-319*, displayed much more rapid decapping and deadenylation, as evidenced in Fig. 4c. A significant abundance of deadenylated and decapped *PGK1pG-319* fragment appeared immediately and was in significant abundance as compared to that of the full-length mRNA (early time points). The increased ratio at early time points of decapped fragment to full-length mRNA for the *PGK1-319* mRNA in comparison to the ratio for the wild-type *PGK1* mRNA indicates much more rapid degradation of the *PGK1* mRNA containing the premature termination codon, as expected. Moreover, scrutiny of the early time points also indicates that a significant amount of the fragment displayed a large spread of poly(A) lengths from 70 A's to 10 A's, indicative of rapid decapping regardless of the poly(A) tail length that was present (see densitometric scans at early time points). In addition, it can be observed that the full-length *PGK1pG-319* mRNA did not uniformly decrease in poly(A) length as a tight band as it had for the *PGK1pG* mRNA (Fig. 4a). This is

consistent with a switch to primarily processive deadenylation in which full length poly(A) tails are present in the population along with completely deadenylated species.

In contrast to these results with wild-type PAB1, deleting the RRM1 domain of PAB1, blocked both normal deadenylation of *PGK1pG* and that of *PGK1pG-319* (Fig. 4b, d, respectively). In the wild-type *PGK1pG* mRNA situation, the RRM1 deletion blocked deadenylation in which no fragment accumulated (Fig. 4b). This result is consistent with deadenylation normally preceding decapping and being required for it (Decker and Parker 1993). For the *PGK1pG-319* mRNA, little apparent deadenylation of full-length *PGK1pG-319* occurred, yet the *PGK1* fragment appeared very rapidly, albeit immediately in the fully polyadenylated form. It should be noted that this fragment species did not represent the full-length mRNA species, for at later times it decreased noticeably to sizes smaller than the 0A form of the full-length mRNA version. Therefore, it corresponds to the *PGK1* fragment. In addition, both the full-length mRNA version and the fragment initially have more A's than are present in the wild-type PAB1 situation (compare Fig. 4b to that of a and Fig. 4d to that of 4c). This increased poly(A) tail length at initial times is due to the ability of the RRM1 deletion of PAB1 to block both CCR4 and PAN2 deadenylation (Yao et al. 2007) (data not shown). Blocking PAN2 deadenylation results in increased poly(A) tail lengths (Brown and Sachs 1998). These results indicate that RRM1 of PAB1 does not impair NMD-induced decapping, but it is required for the NMD acceleration of deadenylation.

Because RRM1 is required for all deadenylation processes that have been analyzed, including those that are constitutive (Yao et al. 2007) and regulated (Lee et al. 2010), it remains possible that the presumed contact of UPF1 to that of the RRM1 of PAB1 has nothing specifically to do with regulating NMD-enhanced deadenylation. To explore this possibility further, we tested the requirement for RRM1 on deadenylation in an *upf1* Δ background. Using the same pulse-chase experimental strategy described above, we first analyzed the effect of the *upf1* Δ on *PGK1* mRNA deadenylation. In this case, the mRNA became deadenylated at initial times nearly at the same rate as observed in the *UPF1* background, with the oligo(A) species becoming present at around 12 min after the transcriptional shutoff (Fig. 5a). However, it should be noted that the distribution of poly(A) tails is significantly different between the *UPF1* and the *upf1* Δ backgrounds. The poly(A) tail distribution in the *upf1* Δ background remained tighter at all time points, indicative of a primarily distributive deadenylation pattern (see densitometric scans for additional clarity). Importantly, there was no shift to the processive pattern that was apparent with the *UPF1* background at time points after 8 min as observed in Fig. 4a. This *upf1* Δ effect on the spread of poly(A) tail lengths during deadenylation is the same as previously published, albeit unremarked upon at the

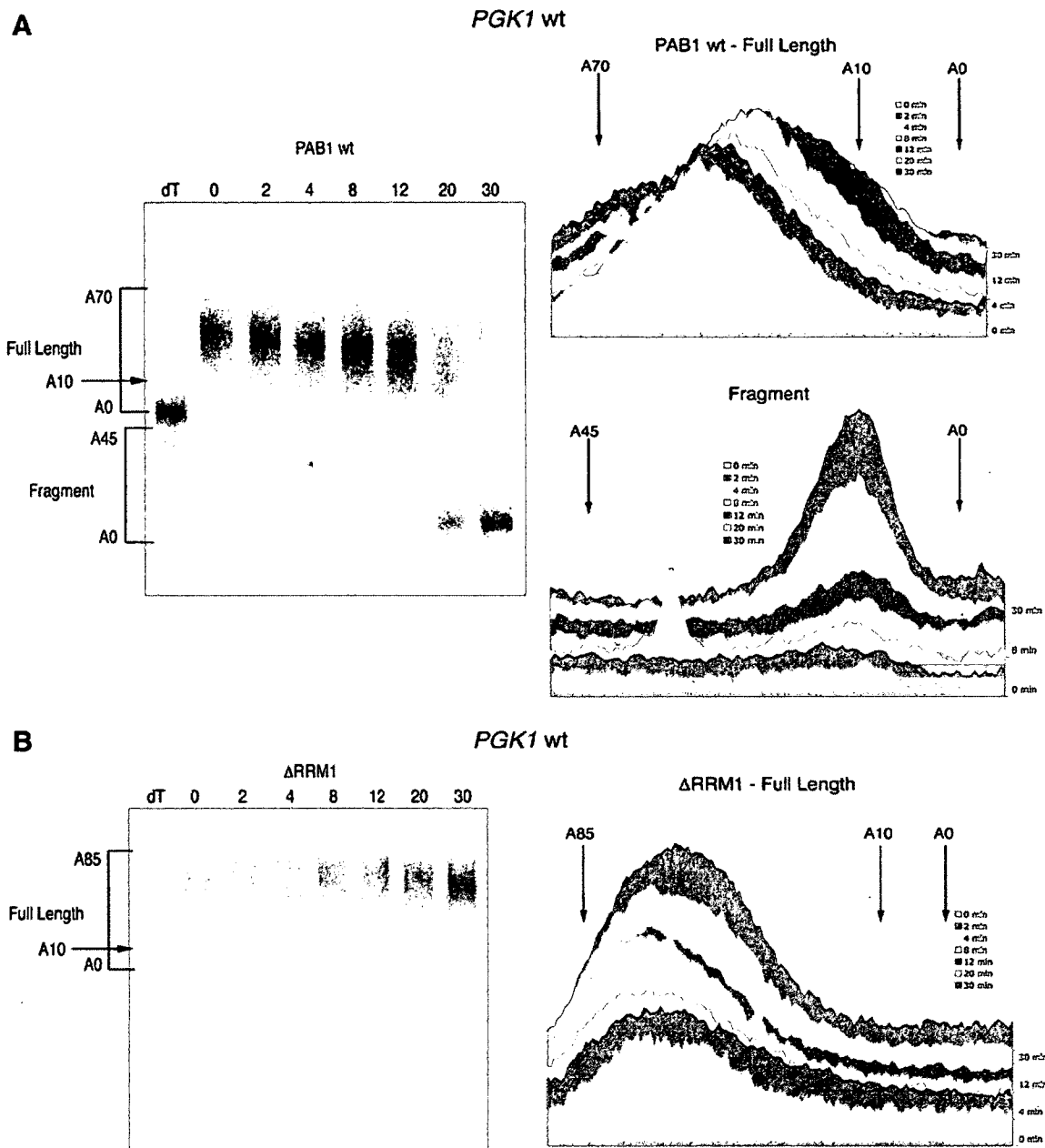


Fig. 4 Transcriptional pulse-chase analyses on *PGK1* mRNA were conducted as previously described (Lee et al. 2010). Following induction of the *GALI-PGK1* mRNA with galactose, transcription was shut off with glucose and, at the times (in min) indicated above the figure, RNA was extracted and northern analyses were conducted as described (Yao et al. 2007). dT refers to the RNA sample probed with oligo (dT) followed by RNase H digestion to remove the poly (A) tail. Equivalent amounts of RNA were loaded into each lane across a panel, as determined by A_{260} spectrophotometric analysis. **a**, **c** Strain AS319/YC504 (wild type for PAB1); **b**, **d** strain AS319/YC505 (PAB1- Δ RRM1). **a**, **b**. Strains were transformed with pRP469 carrying the *PGK1pG* wild-type gene; **c**, **d** strains were transformed

with pRP1078 carrying the *PGK1pG-319* that has a nonsense mutation at amino acid 319 (Cao and Parker 2003). Densitometric scans of the data are presented to the right of the northern. **a** Both the full-length and fragment scans are presented and in separate figures to ease identification of the species. For the full-length scan in this case, the time points are given in reverse order to clarify visualization of the latter time points. **b** Only the full-length densitometric scans are presented, as there were no identifiable fragments. **c**, **d** Both full-length and fragment densitometric scans are presented, albeit in one continuous figure. For ease of interpretation the right y axis designations skip every other time points for clarity

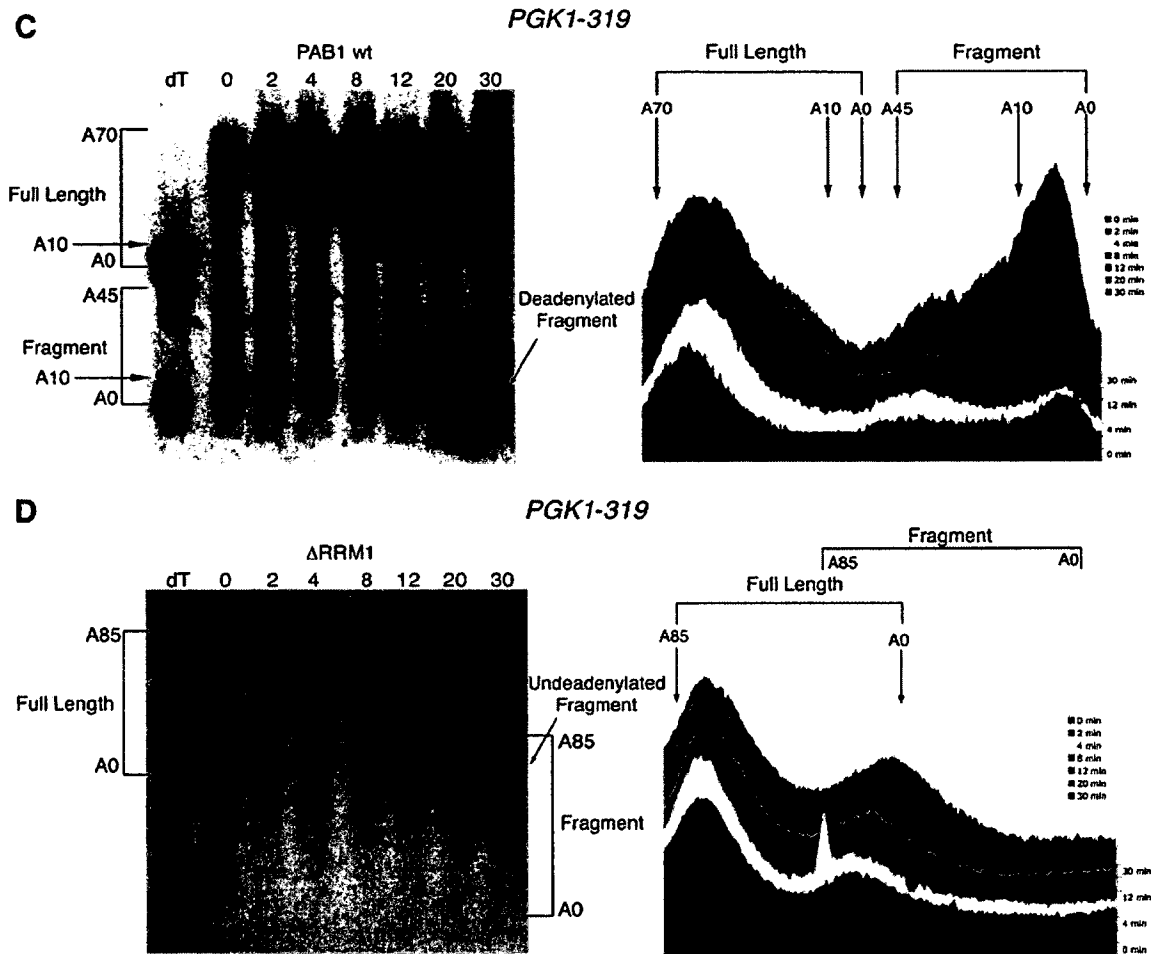


Fig. 4 continued

time (Cao and Parker 2003). These data suggest that UPF1 may play a role in the switch from distributive to processive deadenylation, a process requiring PAB1 removal from the mRNA (Tucker et al. 2002; Viswanathan et al. 2003; Yao et al. 2007). In agreement with this observation, fewer deadenylated fragments were seen in the *upf1Δ* background in Fig. 5a as compared to the *UPF1* background (Fig. 4a). This result is also the same as previously published (Cao and Parker 2003). This is consistent with fewer oligo(A) species being formed and subsequently decapped due to the reduction in processive deadenylation caused by the *upf1Δ* mutant.

In the case of NMD in a *upf1Δ* background, *PGK1-319* mRNA was deadenylated in a similar manner to that of the wild-type *PGK1* mRNA (compare Fig. 5c to a), as UPF1 is known to block NMD deadenylation. Little or no *PGK1* fragment was observed, consistent with distributive deadenylation and little or no oligo(A) species were formed due to reduction in processive deadenylation (in long exposures of Fig. 5c only a very little abundance of the fragment was detected).

In the strain background deleted for RRM1, wild-type *PGK1* mRNA did not appreciably deadenylate, as expected

(Fig. 5b). Similarly, the RRM1 deletion significantly blocked *PGK1-319* mRNA deadenylation (Fig. 5d). No *PGK1* mRNA fragments were observed in either case. These data suggest that RRM1 is required for deadenylation independent of the presence of UPF1. Other roles for the UPF1–RRM1 interaction, as in the switch from distributive to processive deadenylation, remain possible (see “Discussion”).

Discussion

Mass spectrometric identification of proteins interacting through specific PAB1 domains

We have used mass spectrometric techniques to identify a total of 55 non-ribosomal proteins that associate with PAB1 (Tables 2, 4). All but 11 of these proteins are likely components of RNA complexes or processes that involve PAB1. Many of these proteins are RNA binding factors that would be expected to interact with the mRNA and

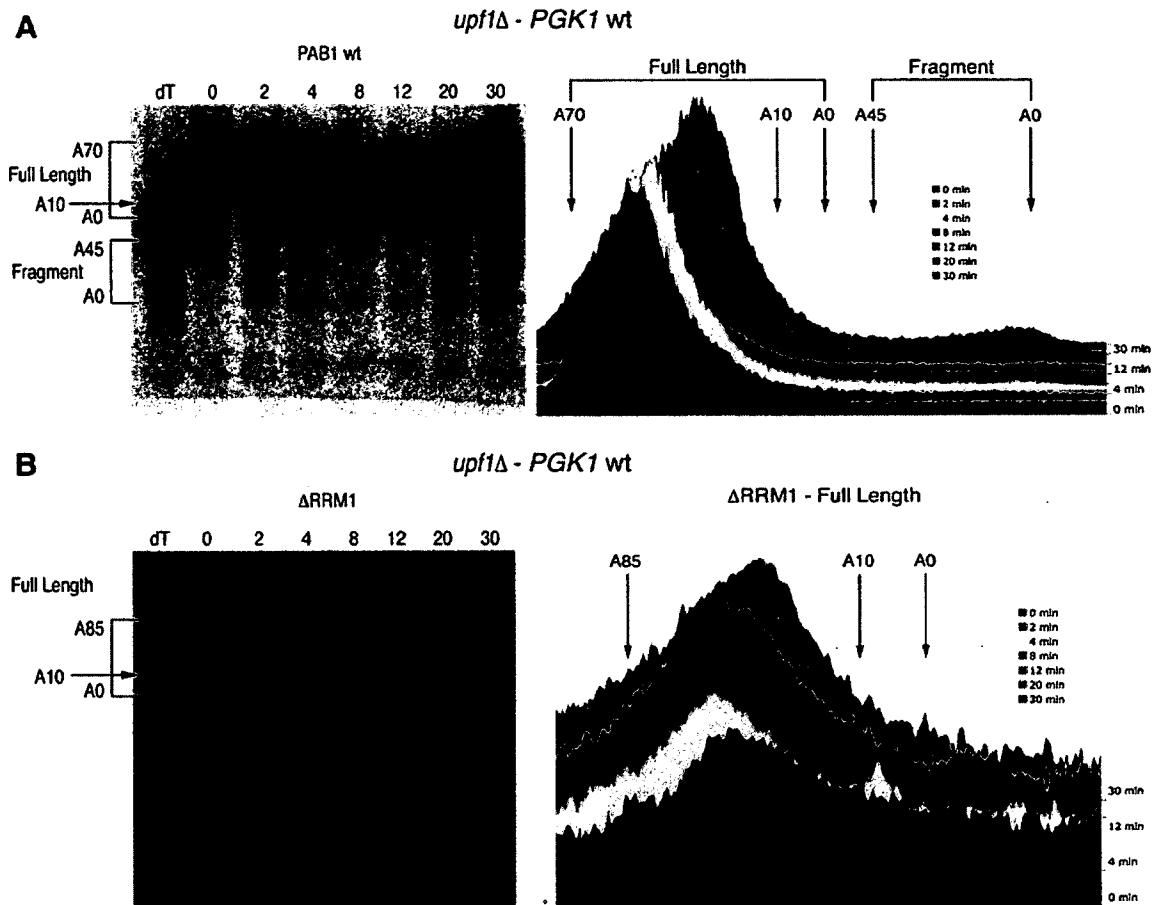


Fig. 5 Effect of *upf1Δ* on deadenylation. Pulse-chase experiments were conducted exactly as described in Fig. 4, except the following strain was used: RR27-1. **a** YC504/RP469 (*PGK1pG*); **b** YC505/

RP469; **c** YC504/RP1068 (*PGK1pG-319*); YC505/RP1068. Densitometric scans are presented as described in Fig. 4

therefore would be part of the PAB1-mRNP structure. A second large group of proteins that we found to be associating with PAB1 are nucleolar and/or involved in ribosomal biogenesis. Previous mass spectrometric studies on nucleolar components have identified PAB1, but it remains unclear as to the role that PAB1 plays in these processes (Mnaimneh et al. 2004; Staub et al. 2006; Krogan et al. 2004). There is some evidence, however, that PAB1 aids 60S assembly to form a competent translation complex (Searfoss et al. 2001). Therefore, the types of proteins we have identified as associating with PAB1 support the validity of mass spectrometric approaches in defining PAB1 interacting components. However, similar to previous mass spectrometric studies, our list of proteins may not be specific to PAB1 and may be found to associate with PAB1 through very indirect RNA interactions.

We have endeavored to surmount the above limitation attached to global mass spectrometric studies using seven different PAB1 deletion derivatives in our analyses. In this case, by comparing the effect of well-defined domain

deletions in PAB1 to each other and to wild-type PAB1, we were able to significantly shorten this list of 55 proteins associating with PAB1 to 13 factors. Of these 13 proteins, each was affected in its interaction with PAB1 for at least one of the PAB1 deletion derivatives. In validation of this methodology, we were able to identify four of the six previously known proteins that interact through specific PAB1 domains: eIF4G1, eIF4G2, PBP2, and eRF3. Our results confirmed that the eIF4G proteins contact PAB1 through the RRM1 and RRM2 domains, extended the contact region of eRF3 to PAB1 to include the P domain, and delimited the PBP2 contact to PAB1 to just the C domain. Neither PBP1 nor PAN3, the other two proteins known to contact particular regions of PAB1 (Mangus et al. 1998; Hoshino et al. 1999), were found in any of our mass spectrometric analyses. In the case of PBP1, it has been shown recently to associate in PAB1-mRNP complexes following the stress of glucose deprivation in which particular stress granules are formed (Buchan et al. 2008). Unfortunately, our Flag-PAB1 immunoprecipitations do

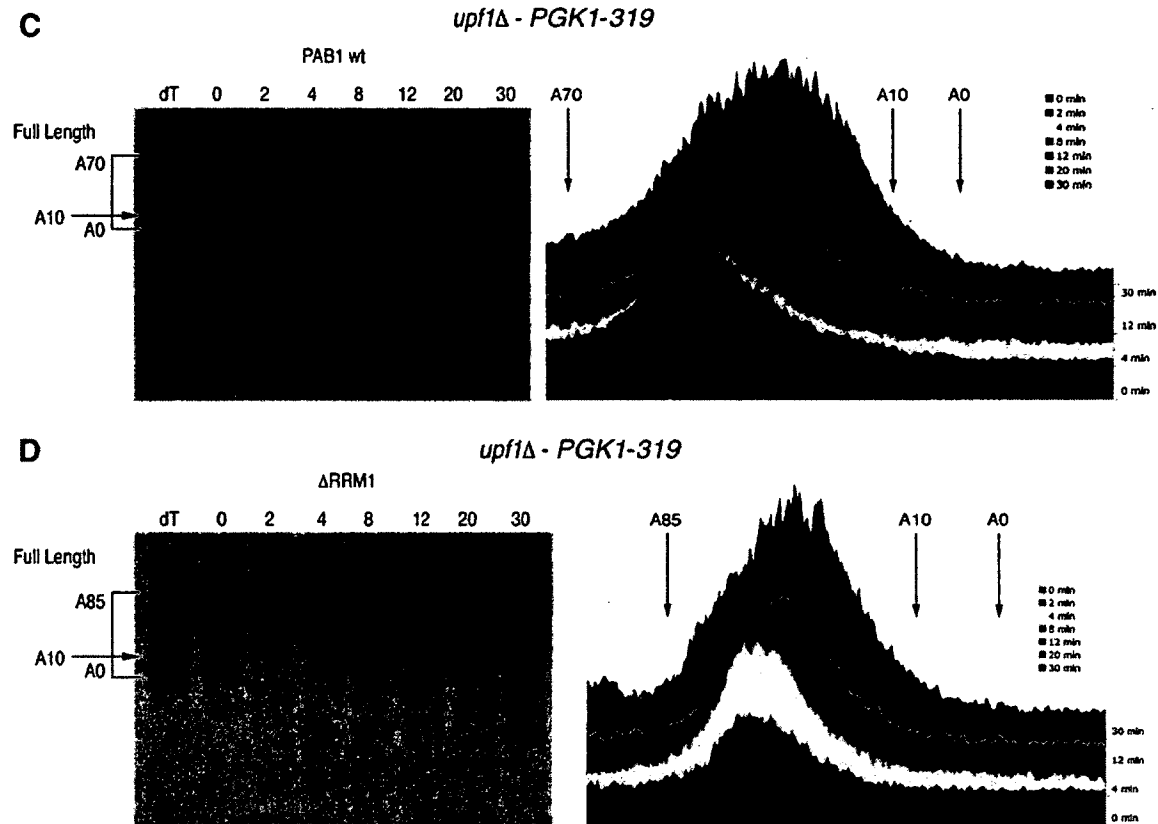


Fig. 5 continued

not detect PAB1 in yeast stress granules (unpublished observation).

For the other nine proteins found to associate with one or another of the PAB1 domains, five of them, CBC1, GBP2, NAB6, UPF1, and CBF5, have been previously found to associate with PAB1 by mass spectrometric studies (Collins et al. 2007). CBC1 is the nuclear mRNA cap-binding protein (Das et al. 2000). Because PAB1 is known to be present in the nucleus, it is possible that the nuclear mRNA configuration also involves a closed-loop structure similar to that found for cytoplasmic mRNA involving eIF4E, eIF4G, and PAB1 (Wells et al. 1998). In the case of CBC1, it may make a direct contact to the RRM4 and P domains of PAB1. This contact may not require an intermediary, as in the case of eIF4G bridging the circularization of the mRNA by eIF4E and PAB1. Because the RRM4 domain of PAB1 plays a role in mRNA transport from the nucleus (Brune et al. 2005), CBC1 contact to this region of PAB1 may play an unknown role in this process.

GBP2 has been shown to be involved in mRNA transport, translation, and stress granules (Buchan et al. 2008; Windgassen et al. 2004), all processes involving PAB1. A role for RRM1, required for GBP2 interaction, in these

processes has not been identified, although deleting RRM1 does have a significant, albeit not a large effect, on protein translation (Yao et al. 2007). Similarly, RRM1 is required for binding NAB6, an mRNA binding protein. NAB6 tends to bind mRNA involved in cell wall biogenesis (Hogan et al. 2008). Its RNA binding sites have, however, not been detected and the role of either PAB1 or its RRM1 domain in these processes is not clear. Similarly, the importance of the PAB1 RRM1 interaction with CBF5, a nucleolar protein involved in ribosomal biogenesis, is unknown. While the role of PAB1 in binding these various proteins remains to be elucidated, the observation that these proteins repeatedly are found to associate with PAB1 and to do so in a domain-specific manner, strongly suggests that they are important PAB1-associated factors.

The remaining four proteins, SSD1, SLF1, NOP77, and yGR250c, while not being previously shown to interact with PAB1, are known to be involved in translation (SSD1 and SLF1) (Sobel and Wolin 2006; Krogan et al. 2006), mRNA degradation (yGR250) (Windgassen et al. 2004), ribosomal biogenesis (NOP77) (Mnaimneh et al. 2004), or binding of eIF4E (SLF1) (Krogan et al. 2006), all pathways in which PAB1 has been directly linked. Several of these proteins deserve special comment. GBP2 and yGR250c

have been suggested to be components of yeast stress granules formed upon the stress of glucose deprivation (Buchan et al. 2008). While we have not been able to detect stress granule complexes with our Flag-PAB1, it is possible that these two proteins also associate with mRNA translational complexes prior to stress granule formation. GBP2, in fact, is known to play roles in both mRNA export and translation (Windgassen et al. 2004). SSD1 is a known mRNA binding protein and possible RNase (Uesono et al. 1997), and its sites of binding to the mRNA are very close to the 5' end of mRNA (Hogan et al. 2008; Ohyama et al. 2010). Because this location is in the vicinity where eIF4E and eIF4G would interact to form the closed-loop mRNA structure with PAB1 (Wells et al. 1998), it is possible that SSD1 associates with PAB1 and the mRNA to form a closed-loop structure. Whether there are additional contacts to other translation factors such as eIF4G in this closed-loop configuration remains to be determined. SSD1 contact to PAB1 may therefore be a means to stabilizing its interactions with both the 5' and 3' ends of the mRNA. This may further advantage those particular cell wall encoding mRNAs that it may control (Kaeberlein and Guarente 2002; Moriya and Isono 1999; Hogan et al. 2008) for optimal translation. Alternatively, SSD1 may suppress the translation of certain mRNA, such as *CLN2*, by binding to the 5' end of the mRNA (Ohyama et al. 2010; Jansen et al. 2009).

While our list of proteins interacting indirectly or directly with PAB1 includes many of the processes in which PAB1 is known to be involved, several notable proteins are missing. For example, all components of the mRNA deadenylase complex (CCR4–NOT) were absent (Tucker et al. 2001; Chen et al. 2001, 2002; Cui et al. 2008). This is most likely due to the fact that most initial deadenylation of mRNA when PAB1 occupies two to three sites on the poly(A) tail takes place in a distributive manner (Yao et al. 2007; Decker and Parker 1993). In distributive deadenylation, CCR4 would not be stably bound to the PAB1–mRNP complex. In contrast, processive deadenylation of poly(A) tails by CCR4, in which it would be more stably associated with the mRNA, requires more expansive naked poly(A) tails when PAB1 would not be expected to be present (Tucker et al. 2002; Viswanathan et al. 2003). Proteins playing roles in mRNA decapping were also uniformly missing from our mass spectrometric analyses. In this case, decapping takes place in specialized P bodies (Sheth and Parker 2007), and previous studies have indicated that PAB1 can associate with decapping proteins (Tharun and Parker 2001; Viela et al. 2000). Also, it has been reported that decapping can take place on translating ribosomes (Hu et al. 2009), in which case one would expect PAB1 to interact with decapping factors. Although PAB1 may be present in such complexes, we have no evidence

that our Flag pull downs can detect PAB1 in these complexes. Other processes in which PAB1 is involved for which we did not identify PAB1-associated proteins include that of mRNA export (Brune et al. 2005; Dunn et al. 2005; Chekanova et al. 2001) and 3' end processing (Hosoda et al. 2006; Amrani et al. 1997). Therefore, one limitation in our mass spectrometric studies is the inability to use a single bait to identify all possible protein complexes in which a particular protein is present. Moreover, any differences that we observed between the proteins associating with PAB1 and proteins previously identified by mass spectrometric procedures may be due to the bait and conditions employed for obtaining protein complexes in the respective experiments.

Role of RRM1 of PAB1 in nonsense-mediated deadenylation and decapping

Because the RRM1 domain has been shown to play a critical role in mRNA deadenylation (Yao et al. 2007; Lee et al. 2010) and UPF1 is known to control mRNA degradation by accelerating both decapping and deadenylation of mRNA containing premature codons (Cao and Parker 2003), we subjected UPF1 to further study. Our reverse immunoprecipitation analysis using UPF1 as our bait established that RRM1 of PAB1 was required for PAB1 to bind to UPF1. Also, deletion of both the P and C domains of PAB1 did not interfere with UPF1 immunoprecipitating PAB1 and neither the P nor the C domain of PAB1 was required for the ability of Flag-PAB1 to bring down UPF1. Mammalian studies have indicated that the C-terminal domains of PABPC are important to compete presumably with UPF1 for binding to translation termination factor eRF3 (Brogna and Wen 2009). No such role is likely for the combined P and C domains of PAB1 in yeast given that deletion of these two regions of PAB1 did not affect the major part of NMD (Simon and Seraphin 2007).

We further established that the RRM1 domain of PAB1 blocked NMD deadenylation processes but had no effect on the more critical NMD-induced decapping process. This result is in agreement with recent results that indicate that PAB1 in yeast is not essential for NMD decapping (Mieux et al. 2008). Yet, because we have also shown that deleting the RRM1 domain blocks deadenylation for all processes that have been analyzed, as well as for deadenylation in an *upf1*Δ background, we cannot necessarily conclude that the presumed RRM1–UPF1 interaction that we have identified has a specific role for UPF1 function in NMD.

However, one possible role for the RRM1–UPF1 interaction was suggested by our results to be in the transition from distributive to processive deadenylation by CCR4 that occurs in the process of shortening the poly(A) tail. This transition naturally occurs following PAB1 removal from

the poly(A) tail, usually when the poly(A) tail shortens to about 25 A's (Yao et al. 2007; Ohn et al. 2007; Decker and Parker 1993), the minimal size to which PAB1 binds (Deo et al. 1999). This transition is also notably enhanced and can occur on even longer poly(A) tail lengths whenever deadenylation rates become accelerated, as for the rapid deadenylation of normal mRNA (e.g., *MFA2*), the PUF3 induction of increased deadenylation of *COX17* (Decker and Parker 1993; Olivas and Parker 2000; Lee et al. 2010), the general augmented rate of deadenylation caused by translation initiation defects (Schwartz and Parker 1999), and the NMD-induced acceleration of deadenylation mediated by UPF1 (Cao and Parker 2003).

Three observations support the RRM1–UPF1 interaction as possibly important to this distributive to processive transition. First, deleting *UPF1* resulted in a shift to distributive deadenylation for the *PGK1* mRNA. Second, removal of PAB1 is a prerequisite for this shift to processive deadenylation and deleting the RRM1 domain interferes with PAB1 being removed from the mRNA (Yao et al. 2007). Third, under NMD, UPF1 is required for the very rapid processive deadenylation that occurs. These observations suggest the model that UPF1 accelerates deadenylation during NMD by particularly interacting with the RRM1 domain of PAB1 and hastening removal of PAB1 from the poly(A) tail. They also suggest that UPF1 plays a role in normal mRNA degradation, as previously reported (He and Jacobson 2001; Sheth and Parker 2006), by aiding this transition from distributive to processive deadenylation. Because the factors important to this transition have remained unknown, future studies will be required to resolve this particular process and the special role of UPF1 in this process.

Our identification of the likely domains of PAB1 to which a number of known and novel PAB1-interacting factors bind indicates that the PAB1 protein and its mRNP structure play diverse roles in the metabolism of mRNA. Clearly, it will require an in-depth analysis for each of these protein–PAB1 interactions to illuminate both the relevancy of the interaction and its biological role.

Acknowledgments We would like to thank A. Jacobson for providing HA-tagged versions of UPF1 and the *upf1*Δ-containing strain. This research was supported by NIH grants GM78087 and GM82048 to C.L.D. and from the ARRA initiative of 2009. Partial funding was provided by the New Hampshire Agricultural Experiment Station to C.L.D. This is Scientific Contribution Number 2450.

References

Altmann M, Sonnenberg N, Trachsel H (1989) Translation in *Saccharomyces cerevisiae*: initiation factor 4E-dependent cell-free system. *Mol Cell Biol* 9:4467–4672

- Amrani N, Minet M, Le Gouar M, Lacroute F, Wyers F (1997) Yeast Pab1 interacts with Rna15 and participates in the control of the poly(A) tail length in vitro. *Mol Cell Biol* 17:3694–3701
- Andersen JS, Lyon CE, Fox AH, Leung AK, Lam YW, Steen H, Mann M, Lamond AI (2002) Directed proteomic analysis of the nucleolus. *Curr Biol* 12:1–11
- Brogna S, Wen J (2009) Nonsense-mediated mRNA decay (NMD) mechanisms. *Nat Struct Mol Biol* 16:107–113
- Brown CE, Sachs AB (1998) Poly(A) tail length control in *Saccharomyces cerevisiae* occurs by message-specific deadenylation. *Mol Cell Biol* 18:6548–6559
- Brown CE, Tarun SZ Jr, Boeck R, Sachs AB (1996) PAN3 encodes a subunit of the Pab1p-dependent poly(A) nuclease in *Saccharomyces cerevisiae*. *Mol Cell Biol* 16:5744–5753
- Brune C, Munchel SE, Fischer N, Podtelejnikov AV, Weis K (2005) Yeast poly(A)-binding protein Pab1 shuttles between the nucleus and the cytoplasm and functions in mRNA export. *RNA* 11:517–531
- Buchan JR, Muhrad D, Parker R (2008) P bodies promote stress granule assembly in *Saccharomyces cerevisiae*. *J Cell Biol* 183:441–455
- Cao D, Parker R (2003) Computational modeling and experimental analysis of nonsense-mediated decay in yeast. *Cell* 113:533–545
- Chekanova JA, Shaw RJ, Belostotsky DA (2001) Analysis of an essential requirement for the poly(A) binding protein function using cross-species complementation. *Curr Biol* 11:1207–1214
- Chen J, Rappsilber J, Chiang Y-C, Russell P, Mann M, Denis CL (2001) Purification and characterization of the 1.0 MDa CCR4–NOT complex identifies two novel components of the complex. *J Mol Biol* 314:683–694
- Chen J, Chiang Y-C, Denis CL (2002) CCR4, a 3′–5′ poly(A) RNA and ssDNA exonuclease, is the catalytic component of the cytoplasmic deadenylase. *EMBO J* 21:1414–1426
- Collins SR, Kemmeren P, Zhao X-C, Greenblatt JF, Spencer F, Holstege FCP, Weissman JS, Krogan NJ (2007) Toward a comprehensive atlas of the physical interactome of *Saccharomyces cerevisiae*. *Mol Cell Proteomics* 6(3):439–450
- Cui Y, Ramnarain DB, Chiang Y-C, Ding L-H, McMahon JS, Denis CL (2008) Genome wide expression analysis of the CCR4–NOT complex indicates that it consists of three modules with the NOT module controlling SAGA-responsive genes. *Mol Genet Genomics* 279:323–337
- Das B, Guo Z, Russo P, Chartrand P, Sherman F (2000) The role of nuclear cap binding protein Cbc1p of yeast in mRNA termination and degradation. *Mol Cell Biol* 20:2827–2838
- Deardorff JA, Sachs AB (1997) Differential effects of aromatic and charged residue substitutions in the RNA binding domains of the yeast poly(A)-binding protein. *J Mol Biol* 269:67–81
- Decker CJ, Parker R (1993) A turnover pathway for both stable and unstable mRNAs in yeast: evidence for a requirement for deadenylation. *Genes Dev* 7:1632–1643
- Deo RC, Bonanno JB, Sonenberg N, Burley SK (1999) Recognition of polyadenylate RNA by the poly(A)-binding protein. *Cell* 98:835–845
- Dunn EF, Hammell CM, Hodge CA, Cole CN (2005) Yeast poly(A)-binding protein, Pab1, and PAN, a poly(A) nuclease complex recruited by Pab1, connect mRNA biogenesis to export. *Genes Dev* 19:90–103
- Fleischer TC, Weaver CM, McAfee KJ, Jennings JL, Link AJ (2006) Systematic identification and functional screens of uncharacterized proteins associated with eukaryotic ribosomal complexes. *Gene Dev* 20:1292–1307
- Gavin A-C, Bosche M, Krause R, Grandi P, Marzioch M, Bauer A, Schultz J, Rick JM, Michon A-M, Cruciat C-M, Remor M, Hofert C, Schelder M, Brajenovic M, Ruffner H, Merino A, Klein K, Hudak M, Dickson D, Rudi T, Gnau V, Bauch A,

- Bastuck S, Huhse B, Leutwien C, Heurtier M-A, Copley RR, Edelmann A, Querfurth E, Rybin V, Drewes G, Raida M, Bouwmeester T, Bor P, Searphin B, Kusteer B, Neubauer G, Superti-Furga G (2002) Functional organization of the yeast proteome by systematic analysis of protein complexes. *Nature* 415:141–147
- Gorgoni B, Gray NK (2004) The roles of cytoplasmic poly(A)-binding proteins in regulating gene expression: a developmental perspective. *Brief Funct Genomic Proteomic* 3:125–141
- Gruhler A, Oslen JV, Mohammed S, Mortensen P, Faergeman NJ, Mann M, Jensen ON (2005) Quantitative phosphoproteomics applied to the yeast pheromone signaling pathway. *Mol Cell Proteomics* 4:310–327
- He F, Jacobson A (2001) Upf1p, Nmd2p, and Upf3p regulate the decapping and exonucleolytic degradation of both nonsense-containing mRNAs and wild-type mRNAs. *Mol Cell Biol* 21:1515–1530
- Ho Y, Gruhler A, Heilbut A, Bader GD, Moore L, Adams S-L, Millar A, Taylor P, Bennett K, Boutlier K, Yang L, Wolting C, Donaldson I, Schandorff S, Shewnarane J, Vo M, Taggart J, Goudreault M, Muskat B, Alfarano C, Dewar D, Lin Z, Michalickova K, Williams AR, Sassi H, Nielsen PA, Rasmussen KJ, Andersen JR, Johansen LE, Hansen LH, Jespersen H, Podtelejnikov A, Nielsen E, Crawford J, Poulsen V, Sorensen B, Matthiesen J, Hendrickson RC, Gleeson F, Pwson T, Moran MF, Durocher D, Mann Matthies J, Hendrickson RC, Gleeson F, Lawson T, Moran MF, Durocher D, Mann M, Hogue CWV, Figeys D, Tyers M (2002) Systematic identification of protein complexes in *Saccharomyces cerevisiae* by mass spectrometry. *Nature* 415:180–183
- Hogan DJ, Riordan DP, Gerber AP, Herschlag D, Brown PO (2008) Diverse RNA-binding proteins interact with functionally related sets of RNAs, suggesting an extensive regulatory system. *PLoS Biol* 6:e255
- Hoshino S, Imai M, Kobayashi T, Uchida N, Katada T (1999) The eukaryotic polypeptide chain releasing factor (eRF3/GSPT) carrying the translation termination signal to the 3'-poly(A) tail of mRNA. Direct association of eRF3/GSPT with polyadenylate-binding protein. *J Biol Chem* 274:16677–16680
- Hosoda N, Kobayashi Uchida N, Funakoshi Y, Kikuchi Y, Hoshino S, Katada T (2003) Translation termination factor eRF3 mediates mRNA decay through the regulation of deadenylation. *J Biol Chem* 278:38287–38291
- Hosoda N, Lejeune F, Maquat LE (2006) Evidence that poly(A) binding protein C1 binds nuclear pre-mRNA poly(A) tails. *Mol Cell Biol* 26:3085–3097
- Hu W, Sweet TJ, Chamnogopal S, Baker KE, Collier J (2009) Co-translational mRNA decay in *Saccharomyces cerevisiae*. *Nature* 461:225–231
- Jansen JM, Wanless AG, Seidel CW, Weiss EL (2009) Cbk1 regulation of the RNA-binding protein Ssd1 integrates cell fate with translational control. *Curr Biol* 19:2114–2120
- Kaerberlein M, Guarente L (2002) *Saccharomyces cerevisiae* MPT5 and SSD1 function in parallel pathways to promote cell wall integrity. *Genetics* 160:83–95
- Kessler SH, Sachs AB (1998) RNA recognition motif 2 of yeast Pab1p is required for its functional interaction and eukaryotic translation initiation factor 4G. *Mol Cell Biol* 18:51–57
- Kristensen AR, Schandorff S, Heyer-Hansen M, Nielsen MO, Jaattela M, Dengjel J, Andersen JS (2008) Ordered organelle degradation during starvation-induced autophagy. *Mol Cell Proteomics* 7(12):2419–2428
- Krogan NJ, Peng W-T, Cagney G, Robinson MD, Haw R, Zhong G, Guo X, Zhang X, Canadien V, Richards DP, Beattie BK, Lalev A, Zhang W, Davierwala AP, Mnaimneh S, Starostine A, Tikuisis AP, Rigull J, Datta N, Bray JE, Hughes AE, Greenblatt JF (2004) High-definition macromolecular composition of yeast RNA-processing complexes. *Mol Cell* 13:225–239
- Krogan NJ, Cagney G, Yu H, Zhong G, Guo X, Ignatchenko A, Li J, Pu S, Datta N, Tikuisis AP, Punna T, Peregrín-Alvarez JM, Shales M, Zhang X, Davey M, Robinson MD, Paccanaro A, Bray JE, Sheung A, Beattie B, Richards DP, Canadien V, Lalev A, Mena F, Wong P, Starostine A, Canete MM, Vlasblom J, Wu S, Orsi C, Collins SR, Chandran S, Haw R, Rilstone JJ, Gandi K, Thompson NJ, Musso G, St. Onge P, Ghanny S, Lam MH, Butland G, Altaf-Ul AM, Kanaya S, Shilatifard A, O'Shea E, Weissman JS, Ingles CJ, Hughes TR, Parkinson J, Gerstein M, Wodak SJ, Emili A, Greenblatt JF (2006) Global landscape of protein complexes in the yeast *Saccharomyces cerevisiae*. *Nature* 440:637–643
- Kuhn U, Pieler T (1996) *Xenopus* Poly(A) binding protein: functional domains in RNA binding and protein-protein interaction. *J Mol Biol* 256:20–30
- Kuhn U, Wahle E (2004) Structure and function of poly(A) binding proteins. *BBA* 1678:67–84
- Lee D, Ohn T, Chiang Y-C, Liu Y, Quigley G, Yao G, Denis CL (2010) PUF3 acceleration of deadenylation in vivo can operate independently of CCR4 activity, possibly involving effects on the PAB1-mRNP structure. *J Mol Biol* 399:562–575
- Liu H-Y, Badarinarayana V, Audino DC, Rappsilber J, Mann M, Denis CL (1998) The NOT proteins are part of the CCR4 transcriptional complex and affect gene expression both positively and negatively. *EMBO J* 17:1096–1106
- Mangus DA, Amrani N, Jacobson A (1998) Pbp1p, a factor interacting with *Saccharomyces cerevisiae* poly(A)-binding protein, regulates polyadenylation. *Mol Cell Biol* 18:7383–7396
- Mangus DA, Evans MC, Jacobson A (2003) Poly (A)-binding proteins: multifunctional scaffolds for the post-transcriptional control of gene expression. *Genome Biol* 4:223–246
- Mangus DA, Evans MC, Agrin NS, Smith M, Gongidi P, Jacobson A (2004) Positive and negative regulation of poly(A) nuclease. *Mol Cell Biol* 24:5521–5533
- Melo EO, Dhalia R, Martins de Sa C, Standart N, de Melo Neto OP (2003) Identification of a C-terminal poly(A)-binding protein (PABP)-PABP interaction domain. *J Biol Chem* 278:46357–46368
- Mieux X, van Hoof A, Baker KE (2008) Nonsense-mediated mRNA decay in yeast does not require PAB1 or a poly(A) tail. *Mol Cell* 29:134–140
- Mnaimneh S, Starostine A, Tikuisis AP, Rigull J, Datta N, Bray JE, Hughes AE, Greenblatt JF (2004) High-definition macromolecular composition of yeast RNA-processing complexes. *Mol Cell* 13:225–239
- Moriya H, Isono K (1999) Analysis of genetic interactions between DHH1, SSD1 and ELM1 indicates their involvement in cellular morphology determination in *Sacharomyces cerevisiae*. *Yeast* 15:481–496
- Muhlrad D, Decker CJ, Parker R (1994) Deadenylation of the unstable mRNA encoded by the yeast *MFA2* gene leads to decapping followed by 5'-3' digestion of the transcript. *Genes Dev* 8:855–866
- Mullin C, Duning K, Barnekow A, Richter D, Kremerskothen J, Mohr E (2004) Interaction of rat poly(A)-binding protein with poly(A)- and non-poly(A) sequences is preferentially mediated by RNA recognition motifs 3 + 4. *FEBS Lett* 576:437–441
- Neff C, Sachs AB (1999) Eukaryotic translation initiation factors 4G and 4A from *Saccharomyces cerevisiae* interact physically and functionally. *Mol Cell Biol* 19:5557–5564
- Ohn T, Chiang Y-C, Lee DJ, Yao G, Zhang C, Denis CL (2007) CAF1 plays an important role in mRNA deadenylation separate from its contact to CCR4. *Nucl Acids Res* 35:3002–3015

- Ohyama Y, Kasahara K, Kokubo T (2010) *Saccharomyces cerevisiae* Ssd1p promotes CLN2 expression by binding to the 5'-untranslated region of CLN2 mRNA. *Genes Cells* 15(12):1169–1188
- Olivas W, Parker R (2000) The Puf3 protein is a transcript-specific regulator of mRNA degradation in yeast. *EMBO J* 19:6602–6661
- Otero LJ, Ashe MP, Sachs AB (1999) The yeast poly (A)-binding protein Pab1p stimulates in vitro poly (A)-dependent and cap-dependent translation by distinct mechanisms. *EMBO J* 18:3153–3163
- Pause A, Methot N, Svitkin HY, Merrick WC, Sonenberg N (1994) Dominant negative mutants of mammalian translation initiation factor eIF-4A define a critical role for eIF-rF in cap-dependent and cap-independent initiation of translation. *EMBO J* 13:1205–1215
- Peng W-T, Robinson MD, Mnaimneh S, Krogan NJ, Cagney G, Morris Q, Davierwala AP, Grigull J, Yang X, Zhang W, Mitsakakis N, Ryan OW, Datta N, Jovic V, Pal C, Canadien V, Richards D, Beattie B, Wu LF, Altsuhuler SJ, Rowles S, Frey BJ, Emili A, Greenblatt JF, Hughes TR (2003) A panoramic view of yeast noncoding RNA processing. *Cell* 113:919–933
- Schwartz DC, Parker R (1999) Mutations in translation initiation factors lead to increased rates of deadenylation and decapping of mRNAs in *Saccharomyces cerevisiae*. *Mol Cell Biol* 19:5247–5256
- Searfoss A, Dever TE, Wickner R (2001) Linking the 3' poly(A) tail to the subunit joining step of translation initiation: relations of Pab1p, eukaryotic translation initiation factor 5b(Fun 12p), and Ski2p- S1h1p. *Mol Cell Biol* 21:4900–4908
- Sheth U, Parker R (2006) Targeting of aberrant mRNAs to cytoplasmic processing bodies. *Cell* 125:1095–1109
- Sheth U, Parker R (2007) P bodies and the control of mRNA translation and degradation. *Mol Cell* 25:635–646
- Siddiqui N, Mangus DA, Chang T-C, Palermi J-M, Shyu A-B, Gehring K (2007) Poly(A) nuclease interacts with the C-terminal domain of polyadenylate-binding protein domain from poly(A)-binding protein. *J Biol Chem* 282:25067–25075
- Simon E, Seraphin B (2007) A specific role for the C-terminal region of the poly(A)-binding protein in mRNA decay. *Nucl Acids Res* 35:6017–6028
- Sladic RT, Lagnado CA, Bagley CJ, Goodal GJ (2004) Human PABP binds AU-rich RNA via RNA-binding domains 3 and 4. *Eur J Biochem* 271:450–457
- Sobel SG, Wolin SL (2006) Two yeast La motif-containing proteins are RNA-binding proteins that associate with polyribosomes. *Mol Biol Cell* 10:3849–3862
- Staub E, Mackowiak S, Vingron M (2006) An inventory of yeast proteins associated with nucleolar and ribosomal components. *Genome Biol* 7:R98
- Tarun SZ Jr, Sachs AB (1996) Association of the yeast poly(A) tail binding protein with translation initiation factor eIF-4G. *EMBO J* 15:7168–7177
- Tharun S, Parker R (2001) Targeting an mRNA for decapping: displacement of translation factors and association of the Lsm1p–7p complex on deadenylated yeast mRNAs. *Mol. Cell* 8:1075–1083
- Tucker M, Valencia-Sanchez MA, Staples RR, Chen J, Denis CL, Parker R (2001) The transcription factor associated proteins, Ccr4p and Caf1p, are components of the major cytoplasmic mRNA deadenylase in *Saccharomyces cerevisiae*. *Cell* 104:377–386
- Tucker M, Staples RR, Valencia-Sanchez MA, Muhlrud D, Parker R (2002) CCR4p is the catalytic sub-unit of Ccr4p/Pop2p/Notp mRNA deadenylase ecomplex in *Saccharomyces cerevisiae*. *EMBO J* 21:1427–1436
- Uesono Y, Toh-e A, Kikuchi Y (1997) Ssd1p of *Saccharomyces cerevisiae* associates with RNA. *J Biol Chem* 272:16103–16109
- Viela C, Velasco C, Ptushkina M, McCarthy JEG (2000) The eukaryotic mRNA decapping protein DCP1 interacts physically and functionally with eIF4F translation initiation complex. *EMBO J* 19:4372–4382
- Viswanathan P, Chen J, Chiang Y-C, Denis CL (2003) Identification of multiple RNA features that influence CCR4 deadenylation activity. *J Biol Chem* 278:14949–14955
- von der Haar T, McCarthy JEG (2002) Intracellular translation initiation factor levels in *Saccharomyces cerevisiae* and their role in cap-complex function. *Mol Microbiol* 46:531–544
- Wells S, Hillner PE, Vale RD, Sachs AB (1998) Circularization of mRNA by eukaryotic translation initiation factors. *Mol Cell* 2:135–140
- Windgassen M, Sturm D, Cajigas II, Gonzalez CI, Seedorf M, Bastians H, Krebber H (2004) Yeast shuttling SR proteins Npl3p, Gbp2p, and Hrb1p are part of the translating mRNPs, and Npl3p can function as a translational repressor. *Mol Cell Biol* 24:10479–10491
- Yao G, Chiang Y-C, Zhang C, Lee D, Denis CL (2007) PAB1 self-association precludes its binding to poly (A), thereby accelerating CCR4 deadenylation in vivo. *Mol Cell Biol* 27:6243–6253
- Yoder-Hill J, Pause A, Sonenberg N, Merrick WC (1993) The p46 subunit of eukaryotic initiation factor (eIF)-4F exchanges with eIF-4A. *J Biol Chem* 268:5566–5573